

The

GERMAN MOUSE CLINIC

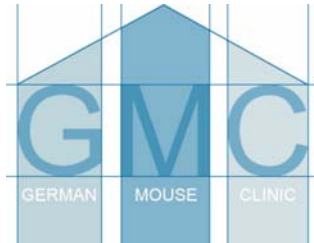
GERMAN MOUSE CLINIC

at the Helmholtz Zentrum München
German Research Center for
Environmental Health (GmbH)

Report for Eya3

Helmut Fuchs, Valérie Gailus-Durner, Christoph Lengger, Beatrix Naton, Thure Adler, Antonio Aguilar, Lore Becker, Ines Bolle, Julia Calzada-Wack, Claudia Dalke, Nicole Ehrhardt, Wolfgang Hans, Sabine M. Hölter, Gabriele Hölzlwimmer, Marion Horsch, Anahita Javaheri, Magdalena Kallnik, Eva Kling, Sandra Kunder, Holger Maier, Corinna Mörth, Ilona Moßbrugger, Ildikó Rácz, Birgit Rathkolb, Jan Rozman, Regine Schreiner, Anja Schrewe, Ralf Steinkamp, Johannes Beckers, Heidrun Behrendt, Dirk H. Busch, Jack Favor, Jochen Graw, Gerhard Heldmaier, Heinz Höfler, Boris Ivandic, Thilo Jacob, Hugo Katus, Paulus Kirchhoff, Martin Klingenspor, Thomas Klopstock, Markus Ollert, Leticia Quintanilla-Martinez, Jörg Schmidt, Holger Schulz, Eckhard Wolf, Wolfgang Wurst, Andreas Zimmer, and Martin Hrabé de Angelis

The German Mouse Clinic



The German Mouse Clinic (GMC) was founded January 2002 at the Helmholtz Zentrum München in Munich/Neuherberg to provide an open access platform for standardized mouse phenotyping. The GMC is supported by the National Genome Research Network (NGFN, <http://www.ngfn.de/>) and is a partner of the EUMORPHIA research program (<http://www.eumorphia.org/>).

In the GMC, experts from various fields of mouse genetics, physiology and pathology in close collaboration with clinicians work side by side at one location. We offer a primary phenotypic analysis of mouse mutants (more than 240 parameters/mouse) in the areas of allergy, behavior, bone and cartilage, cardiovascular diseases, clinical chemistry, energy metabolism, eye development and vision, immunology, lung function, molecular phenotyping, neurology, nociception, and pathology. Additional screens for host-pathogen interaction can be performed at the HZI Braunschweig. Secondary and tertiary screening for in depth analysis is offered by the different screens and is available on request.

Director

Prof. Dr. Martin Hrabé de Angelis
Institute of Experimental Genetics
Helmholtz Zentrum München
German Research Center for
Environmental Health (GmbH)
Ingolstädter Landstraße 1
D-85764 Neuherberg / München
Tel.: 089-3187-3302
Fax: 089-3187-3500

HelmholtzZentrum münchen
German Research Center for Environmental Health



Content

1	Summary	1
1.1	Primary Screening	1
1.1.1	Overall Assessment of the Results	1
1.1.2	Results by Screen	1
1.2	Recommendations for Secondary Screening	2
2	General Part	3
2.1	The Role of the Gene	3
2.2	Known Phenotypes	3
2.3	Suggested Human Disease Model	3
2.4	Mice	3
2.4.1	Number and kind of mice	3
2.4.2	Housing conditions	4
2.5	Workflow	4
2.5.1	Standardized workflow for the primary screen in the German Mouse Clinic	4
2.5.2	Applied screens	5
2.5.3	Quality Assurance	6
2.6	Statistical Analysis of Data	7
2.7	References	7
3	Specific part	10
3.1	Behavior Screen	10
3.1.1	Summary	10
3.1.2	Mice	10
3.1.3	Material and Methods	10
3.1.4	Results	12
3.1.5	Discussion	13
3.1.6	References	13
3.2	Dysmorphology, Bone and Cartilage	20
3.2.1	Summary	20
3.2.2	Mice	20
3.2.3	Material and Methods	20
3.2.4	Results and Discussion	21
3.2.5	References	22
3.3	Neurology Screen	28
3.3.1	Summary	28
3.3.2	Mice	28
3.3.3	Material and Methods	29
3.3.4	Parameters	31
3.3.5	Results	31
3.3.6	Discussion	32
3.3.7	References	33
3.4	Eye Screen	38
3.4.1	Summary	38
3.4.2	Mice	38
3.4.3	Materials and Methods	38
3.4.4	Parameters	39

3.4.5	Results.....	39
3.4.6	References	40
3.5	Clinical Chemistry and Hematology	42
3.5.1	Summary	42
3.5.2	Mice	42
3.5.3	Materials and Methods.....	42
3.5.4	Parameters	44
3.5.5	Results.....	44
3.5.6	Discussion	45
3.5.7	References	45
3.6	Immunology Screen	51
3.6.1	Summary	51
3.6.2	Mice	51
3.6.3	Material and Methods	51
3.6.4	Parameters	52
3.6.5	Results and Discussion.....	52
3.6.6	References	52
3.7	Allergy Screen.....	54
3.7.1	Summary	54
3.7.2	Mice	54
3.7.3	Material and Methods	54
3.7.4	Results.....	54
3.7.5	References	56
3.8	Nociceptive Screen	57
3.8.1	Summary	57
3.8.2	Mice	57
3.8.3	Material and Methods	57
3.8.4	Parameters	58
3.8.5	Results and Discussion.....	59
3.8.6	References	59
3.9	Cardiovascular Screen.....	60
3.9.1	Summary	60
3.9.2	Mice	60
3.9.3	Material and Methods	60
3.9.4	Parameters	63
3.9.5	Results.....	63
3.9.6	References	65
3.10	Lung Function Screen.....	69
3.10.1	Summary	69
3.10.2	Mice	69
3.10.3	Material and Methods	69
3.10.4	Parameters	71
3.10.5	Results and Discussion.....	71
3.10.6	References	72
3.11	Molecular Phenotyping	75
3.11.1	Introduction.....	75
3.11.2	Methods and Materials.....	75
3.11.3	Results.....	77
3.11.4	Discussion	82
3.11.5	References	85

3.12	Metabolic Screen	86
3.12.1	Summary	86
3.12.2	Mice	86
3.12.3	Material and Methods	86
3.12.4	Parameters	87
3.12.5	Results and Discussion.....	87
3.12.6	References	87
3.13	Pathology Screen.....	90
3.13.1	Summary	90
3.13.2	Mice	90
3.13.3	Materials and Methods.....	90
3.13.4	Results.....	91
3.13.5	Genotype-specific Changes.....	91
3.13.6	Secondary, not Genotype-specific Results	92
3.13.7	Discussion	94
3.13.8	References	96

1 Summary

1.1 Primary Screening

In a primary screen 49 mice (24 homozygous mutants, 25 wild-type control littermates) of the *Eya3*-KO mutant mouse line have been analyzed in the German Mouse Clinic (GMC) in the screens Behavior, Dymorphology, Neurology, Eye, Clinical Chemistry, Immunology, Allergy, Cardiovascular Function, Nociception, Lung Function, Energy Metabolism, Molecular Phenotyping and Pathology. The screening started on October 30, 2006.

1.1.1 Overall Assessment of the Results

The phenotyping at the GMC uncovered several new phenotypes which might be – at least to some extent – sex-specific and age-dependent. We recommend performing a follow-up study to analyze in-depth the age-dependency.

1.1.2 Results by Screen

Behavior: The analysis of *Eya3* mice in the mHB reveals an altered exploratory pattern in mutant mice of both sexes with males being more affected.

Dymorphology, Bone and Cartilage: In the morphological investigation via visual inspection at the age of nine weeks, we observed abnormal head morphology in 14 of 25 mutants (56%) and in 3 of 25 controls (12%). In the X-ray analysis at the age of 16 weeks, no genotype-specific differences were detectable; also the abnormal head morphology was no longer apparent. In the dual-energy X-ray absorptiometry (DXA) analysis at the age of 16 weeks, BMC (bone mineral content) was decreased in male mutants. Concurrently body length and weight were decreased in male mutants.

Neurology: The comparison of *Eya3*-mutant mice to controls revealed decreased forelimb grip force in mutant mice. All SHIRPA test parameters were without significant findings. Rotarod testing for motor coordination did not show any alterations, either.

Eye: Genotype-specific differences of unclear relevance were detected between wild-type control and mutant *Eya3* mice. Normalized axial length, but not the axial eye length itself, was reduced in mutant animals. This could be a secondary effect due to the shorter body length caused by the obviously smaller head size at this age.

Cardiovascular: The comparison of the *Eya3*-mutant to control mice in blood pressure showed no genotype-specific differences. In the ECG analysis the mutants revealed prolongations in the PQ and JT interval and decreased QRS amplitudes. The origin of the alterations is not clear, a detailed analysis would

be necessary. However, the changes are not so strong that cardiovascular function can be considered impaired.

Lung Function: Significant differences were detected for tidal and specific tidal volume at rest, mutants exhibit somewhat smaller values. However, none of the other parameters characterizing spontaneous breathing was affected by the mutation and adaptation from rest to activity was found to be normal in mutants. Therefore, it is unlikely that the mutation is associated with a pulmonary phenotype.

Molecular Phenotyping: The data analysis and various statistical methods detected several genes differentially regulated between mutant and reference tissues in heart and brain. In muscle no differences in expression levels between mutant and control mice have been detected. Several of the significantly expressed genes in spleen and thymus are associated with protein synthesis, synaptic vesicle exocytosis or they are expressed in different neuronal cell types.

Pathology: In the macroscopic examination a significantly reduced body weight could be detected in male mutants. Additionally in seven of nine mutants and in one of nine controls a mild, focal testicular tubular degeneration of unknown significance could be observed.

In the screens **Allergy, Nociception, Clinical Chemistry, Immunology, and Energy Metabolism**, no genotype-specific differences could be found.

1.2 Recommendations for Secondary Screening

Dysmorphology: For further analysis of the abnormal head morphology observed at the age of nine weeks, additional data can be generated in secondary analysis by μ CT measuring animals younger than nine weeks.

Neurology: We recommend a closer analysis of the expression in the limbs. In addition, since the head morphology defect vanishes later on and could no longer be detected by the Pathology Screen it would also be worth measuring grip force at various ages.

Please contact Valérie Gailus-Durner to discuss further steps and details.

2 General Part

2.1 The Role of the Gene

Mammalian *Eya* genes encode for transcriptional co-activator proteins and are commonly co-expressed with *Pax*, *Six* and *Dach* genes (Rebay *et al.*, 2005). Information on *Eya3* has been poorly published so far, this is the first knockout mouse for this gene.

2.2 Known Phenotypes

Despite the broad expression of *Eya3* during embryogenesis, no gross phenotype has been detected in adult mice. Even comprehensive screening for eye abnormalities (histological analysis, Slit-lamp, Funduscopy, ERG and OLC) could not uncover prominent phenotypes. However, in 50% of all cases measurement of the eye-size by OLCI-technology revealed an enlarged lens size between wild-type mice and homozygous mutants at the age of 11 and 13 weeks

All further findings which will be shown in this report we consider as new.

2.3 Suggested Human Disease Model

Human EYA3 gene is on 1p36, however, no inherited disease has been addressed to that locus so far (according to OMIM data base entry 601655).

2.4 Mice

2.4.1 Number and kind of mice

Table 1: Eya3 mice provided for analysis. Numbers in brackets indicate animals which were kept in reserve.		
Genotype / Sex	Number of Animals	
Mutant female	10	1 died
Mutant male	14	2 died
Control female	10 (+2)	1 died
Control male	15 (+1)	1 died

Two mice died for unknown reasons, three mice did not regain consciousness after anesthesia.

The knockout line was generated by gene-trapping (*German Gene Trap Consortium, GGTC, 2004*). The integration of the gene trap vector pT1 β -geo was mapped to a 16.7 kb large intronic region between exon 7 and exon 8, which lead to a null mutant.

As described by the sender, the mice analyzed were back crossed for three generations to wild-type C57BL/6J.

2.4.2 Housing conditions

In the GMC mice are housed in type II polycarbonate cages in individually ventilated caging (IVC) systems (VentiRack Bioscreen TM, Biozone, Margate, UK) on wood fiber (Altromin, Lage, Germany). The IVCs operate with positive pressure. Mice are transferred in weekly intervals to new cages with forceps in Laminar Flow Class II changing stations. Mice are fed with irradiated standard rodent high energy breeding diet (Altromin 1314) and given semidemineralized filtered (0.2 μ m) water *ad libitum*. Light is adjusted to a 12h/12h light/dark cycle; temperature and relative humidity are regulated to $22 \pm 1^\circ\text{C}$ and $55 \pm 5\%$, respectively. In specified modules husbandry conditions are adjusted according to the experiment requirements (See corresponding sections). All people attending the facility completely change their garment (jackets and trousers autoclaved) and shoes and wear caps and masks before entering the GMC (Brielmeier *et al.*, 2002).

Outbred 8-week-old male SPF Swiss mice are used as sentinels and kept on a mixture of new bedding and aliquots of soiled bedding (50:50) from all cages of the IVC rack. In addition, the sentinels were also exposed to soiled air from all “upstream” cages of the IVC rack. Health monitoring is carried out by on-site examination of the sentinel mice by certified laboratories according to FELASA recommendations (www.felasa.org).

Mice are kept according to the German laws. Tests were carried out by authority of the Regierung von Oberbayern.

2.5 Workflow

2.5.1 Standardized workflow for the primary screen in the German Mouse Clinic

Mouse mutants entering the GMC are examined in a primary screen according to the following standard workflow (Fig. 1, Gailus-Durner, Fuchs *et al.*, 2005). Analyzed parameters are listed in Table 2.

After the mice arrive at the GMC, they are acclimatized in the new environment for one week. The males then start in the Behavior Screen. There they stay for three weeks. Directly after the behavior tests, the anatomical inspection of the Dymorphology Screen is performed. In the next week, the Neurology Screen is applied. One week later the mice go through the tests of the Eye Screen. When the mice were 12 weeks old, blood is taken, and samples are distributed to the blood-based screens for Clinical Chemistry, Immunology, and Allergy. One week later, the animals are tested in the Nociceptive

Screen. One week later the mice were passed to the Cardiovascular Screen wherein the mice stay two weeks.

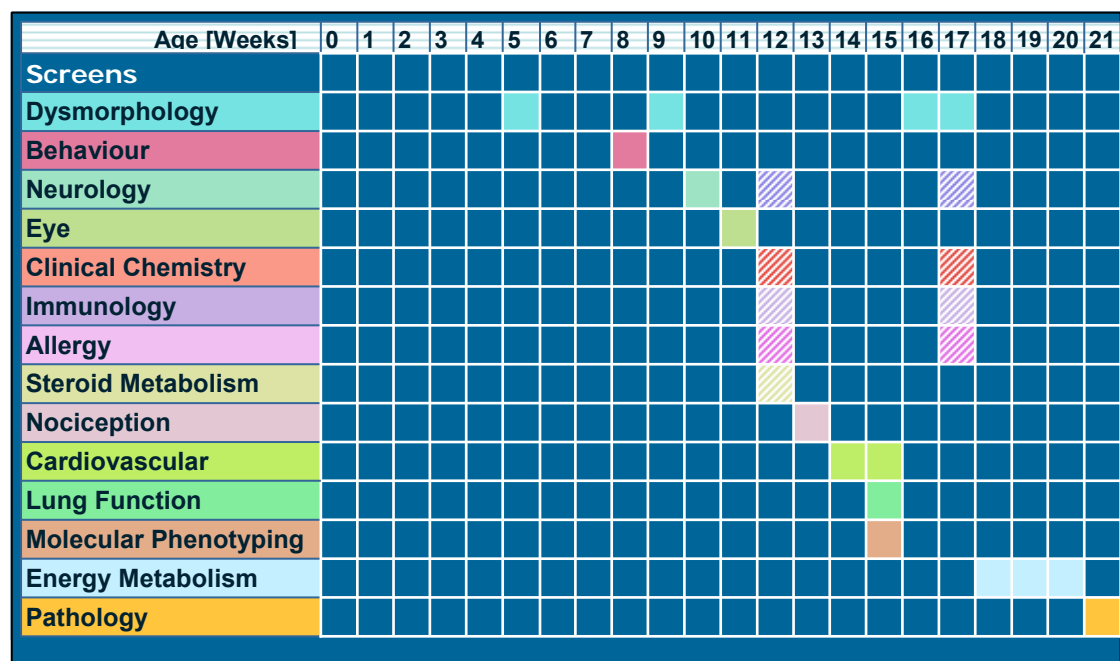



Figure 1: Workflow of the primary screen

Explanation below,  Analysis of blood-based parameters.

In parallel, 10 mutant animals (five males / five females) and 10 controls (five males / five females) leave the animal facility for the Lung Function Analysis, which for technical reasons is located elsewhere. These animals are, for hygienic reasons, not allowed to re-enter the German Mouse Clinic. The females go directly to Pathology. The males are used to freeze organs for future molecular phenotyping on request (remaining organs from those animals are analyzed by the Pathology). All other animals go through the bone and cartilage tests of the Dysmorphology Screen. Five weeks after testing of the first blood sample, a second sample is taken to confirm the findings. Then the mice stay three weeks in the Metabolic Screen. After completion of the primary screen all animals are analyzed macro- and microscopically in the Pathology.

The screening of female animals starts one week later and follows the same workflow (with the exception of Molecular Phenotyping sampling). Deviations from our Standard operation procedure (SOP) are listed below; please take the specific number of analyzed animals from the sections of the applied screen.

2.5.2 Applied screens

The GMC standard workflow for the primary screen as described above was applied to analyze the *Eya3* mice. As the demanded number of 60 animals

(15 mice per sex per genotype) could not be delivered, the workflow was adapted to the available number of animals (no female mice were available for the analysis of pulmonary function). Some parameters measured in the blood based screens could not be determined in all animals, as it was not possible to get the needed amount of blood from these animals. A few animals died during the primary screen (Table 1) and thus could not be analyzed for all parameters.

2.5.3 Quality Assurance

The Quality Assurance as part of the Quality Management at the GMC consists of the following elements: standardized analyses via Standard Operating Procedures (SOP) and validation of analysis protocols by different institutions within the EUMORPHIA program, standardized data and project management supported by the central database system MausDB and the GMC coordination tool CoordDB as well as Quality Control and continuous training of the staff.

Coordination of the GMC's operations

The GMC management team (Core Facility) coordinates the scientific issues, logistics and administration of the GMC. The coordination software tool CoordDB supports the GMC management team in handling the incoming phenotyping requests and managing the complex phenotyping workflow of the primary and secondary screening. Besides the operational business activities the management team organizes the expansion of the screening services in collaboration with its partners. Additionally, the management arranges regular training of the staff members and the clinic's quality assurance.

Standardized Operation Procedures (SOP) and Validation of Protocols

The GMC developed a set of SOPs which cover all steps from mouse import and handling to phenotyping and data analysis. These SOPs are strictly followed during the whole screening process in the GMC and all procedures are documented.

The GMC is one of the major partners of the EUMODIC consortium that emerged from the EUMORPHIA program (Brown *et al.*, 2005), a consortium for the selection, establishment, and standardization of phenotyping protocols for mice as models for human diseases and for mouse husbandry. Cross-validation of protocols by EUMORPHIA is performed by the different institutions. A collection of the protocols (EMPreSS) is posted on the EUMORPHIA web site at (<http://www.eumorphia.org/EMPreSS/>).

Central Database System

Another tool for quality assessment is the central database system which ensures full traceability of samples and documentation of all data. All mouse data is entered into the system (e.g. date of birth, sex, cage) and all screening results linked to the corresponding SOP as well as any changes of the mouse conditions are immediately put in.

Quality Control

In addition to routinely screen-specific quality control tests, control animals of selected strains (e.g. C57BL/6J and C3HeB/FeJ) are analyzed through the

standard protocol for all phenotypes at regular intervals. This data is reviewed by the coordination team.

A tissue archive has been established for the storage of tail and blood plasma samples taken from all mice that have ever been analyzed in the GMC. The tail clips can be used for post-hoc genotyping in case of doubtful genotype information. The sanitary status of every mouse completing the screening can be tested by means of these plasma samples.

Continuous Training

Regularly specific training courses are held at the GMC. Specialists are invited to give lectures and to offer practical training at special days. Staff training is documented and maintained by the management team.

2.6 Statistical Analysis of Data

If not otherwise stated, data of males and females was analyzed separately comparing mutant and control data using a Student's t-test. Sex differences within the mutant or the control group also were determined with a t-test. Tables summarizing the data will show mean \pm standard error of the mean. Significant differences are indicated stepwise from 0.05, 0.02, 0.01, 0.001 to 0.0001.

2.7 References

Brielmeier M., H. Fuchs, G. Przemeck, V. Gailus-Durner, M. Hrabé de Angelis, and J. Schmidt (2002): The GSF-Phenotype Analysis Center (German Mouse Clinic, GMC): A sentinel-based health-monitoring concept in a multi-user unit for standardized characterization of mouse mutants. In: J.-L. Guenet and C. Herweg (eds.) *Laboratory Animals Science - Basis and Strategy for Animal Experimentation Vol. 11, Proceedings of the 8th FELASA Symposium, Laboratory Animals Ltd., Aachen*, pp. 19-22.

Brown SD, Chambon P, Hrabé de Angelis M; Eumorphia Consortium. (2005): EMPReSS: standardized phenotype screens for functional annotation of the mouse genome. *Nat Genet.* 37(11): 1155

Gailus-Durner, V., Fuchs, H. *et al.* (2005): Introducing the German Mouse Clinic: open access platform for standardized phenotyping. *Nature Methods* 2: 403 - 404.

Rebay I, Silver SJ, Tootle TL (2005): New vision from Eyes absent: transcription factors as enzymes. *Trends in Genetics* 21(3): 163-171

<http://www.ncbi.nlm.nih.gov/entrez/dispomim.cgi?id=601655>

Abbreviations and Wording

Eya3	eye absent
GMC	German Mouse Clinic
IVC	individually ventilated cage
control	homozygous wild-type control, <i>Eya</i> ^{+/+}
mutant	homozygous mutant, <i>Eya</i> ^{-/-}
wt	wild-type control
KO	knockout
FELASA	Federation of E uropean L aboratory A nimal S cience A ssociations, 25 Shaftesbury Avenue, London W1D 7EG, UK, www.felasa.org

Table 2: Primary Screen at GMC

Screens	Goal	Methods
Dysmorphology, Bone and Cartilage	morphological analysis of body, skeleton, bone and cartilage	morphological observation, bone densitometry, X-ray, micro-computed tomography
Behavior	locomotor, exploratory, emotional and social behavior, object recognition memory	modified hole board
Neurology	assessment of muscle, spinocerebellar, sensory, and autonomic function	modified SHIRPA protocol
Eye	assessment of morphological alterations of the eye	funduscopy laser interference biometry slit lamp biomicroscopy histological analysis
Clinical Chemistry and Hematology	determination of clinical-chemical and hematological parameters in blood	blood autoanalyzer, ABC-animal blood counter
Immunology	analysis of peripheral blood samples for immunological parameters	flow cytometry, Multiplex Bead Array
Allergy	analysis of total plasma IgE	ELISA
Nociception	detection of altered pain response	hot plate assay
Cardiovascular	assessment of functional cardio-vascular parameters	non-invasive tail-cuff blood pressure measurement, surface limb ECG
Lung Function	assessment of alterations in breathing patterns	whole body plethysmography (Buxco®)
Molecular Phenotyping	RNA expression profiling	DNA-chip technology
Energy Metabolism	measurement of altered body weight regulation, body temperature and energy balance	bomb calorimetry
Pathology	microscopic and macroscopic examination	histology, immunochemistry

3 Specific part

3.1 Behavior Screen

3.1.1 Summary

Genetic studies in the mouse are important for the elucidation of molecular pathways underlying behavior. The goal of this endeavor is not only the identification of genes that control brain function and influence behavior, but also understanding of genetic factors involved in human psychiatric disorders (Tarrantino & Bucan, 2000; Bucan & Abel, 2002). These disorders are associated with quantitative phenotypes called “intermediate traits” or endophenotypes, some of which, in contrast to the full complex disorder, can readily be modeled in mice. These traits are risk factors which are considered to be closer to the genetic etiology than the full syndrome. Examples are anxiety in depression, prepulse inhibition and working memory deficits in schizophrenia, and social interaction deficits in autism and schizophrenia (Seong *et al.*, 2002; Gottesman & Gould, 2003; Inoue & Lupski, 2003).

In the attempt to efficiently screen for candidate endophenotypes within a limited time frame, we use the modified Hole Board (mHB) test as primary screen in the behavioral phenotyping module of the GMC. This test allows the comprehensive analysis of a range of parameters known to be indicative of behavioral dimensions such as locomotor activity, exploratory behavior, arousal, emotionality, memory and social affinity in a single short test (See Ohl *et al.*, 2001).

The analysis of *Eya3* mice in the mHB reveals an altered exploratory pattern in mutant mice of both sexes with males being more affected.

3.1.2 Mice

Mice were housed with food and water *ad libitum* under standard laboratory conditions. Animals were separated based on sex, but not genotype. They entered the laboratory at the age of six weeks, were given two weeks for acclimatization and were tested at the age of eight weeks. Three days before testing, an object (metal cube) was placed into the home cage and removed one day before testing.

In this screen, 18 female mice (nine controls, nine mutants) and 30 male mice (15 controls, 15 mutants) were available for analysis.

3.1.3 Material and Methods

The modified Hole Board test (Ohl *et al.*, 2001) was carried out as previously described (Kallnik *et al.*, 2007). The test apparatus consisted of a test arena (100 x 50 cm), in the middle of which a board (60 x 20 x 2 cm) with 23 holes (1.5 x 0.5 cm) staggered in three lines with all holes covered by movable lids was placed, thus representing the central area of the test arena as an open field. The area around the board was divided into 12 similarly sized quadrants by lines taped onto the floor of the box (See Ohl *et al.*, 2001).

Both box and board were made of dark grey PVC. All lids were closed before the start of a trial. For each trial, an unfamiliar object (a blue plastic tube lid, similar in size to the metal cube) and the familiar object (metal cube) were placed into the test arena with a distance of 2 cm between them. The illumination levels were set at approximately 150 lux in the corners and 200 lux in the middle of the test arena.

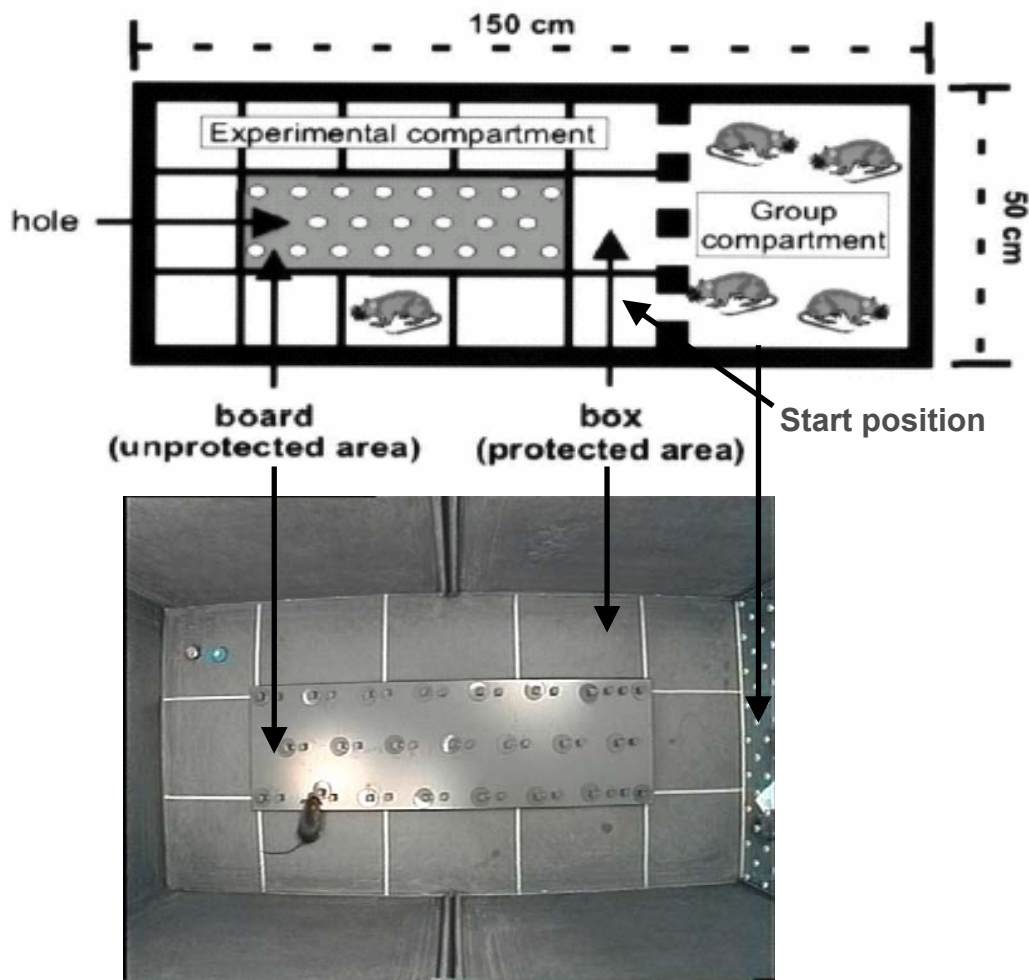


Figure 2: Test arena for modified Hole Board test.

For testing, each animal was placed individually into the test arena and allowed to explore it freely for 5 min. The animals were always placed into the test arena in the same corner next to the partition, facing the board diagonally. The two objects were placed in the corner quadrant diametrical to the starting point. During the 5 min trial, the animal's behavior was recorded by a trained observer with a hand-held computer. Data were analyzed by using the Observer 4.1 Software (Noldus, Wageningen). Additionally, a camera was mounted 1.20 m above the center of the test arena, and the animal's track was videotaped and its locomotor path analyzed with a video-tracking system (Ethovision 2.3, Noldus, Wageningen). After each trial, the test arena was cleaned carefully with a disinfectant.

Data were statistically analyzed using SPSS software (SPSS Inc, Chicago, USA). The chosen level of significance was $p < 0.05$.

3.1.4 Results

Behavioral analysis of spontaneous activity in a novel environment, as measured by the **modified Hole Board** test, revealed in respect to locomotor activity that mutants of both sexes covered less distance (total distance traveled, Table 5) and made less changes in direction of movement (turns frequency, Table 5) than controls. In addition, they moved with reduced speed as evident from reduced values for mean and maximum velocity (Table 4), although the first was a tendency only.

Concerning exploratory activity, mutants exhibited *tendentially* more rearings in the box (Table 4) and mutant males additionally reared earlier than control males (rearing in box latency, Table 4), although this was a tendency only. Regarding directed exploration as measured by hole exploration frequency (Table 4), only mutant males investigated more holes (hole exploration frequency, Table 4) than control males ($p = 0.05$), but mutants of both sexes started hole exploration earlier (hole exploration latency, Table 4).

Table 3: Evaluation of the behavioral phenotype	
Behaviors which are considered affected in mutants due to the pattern of significantly altered parameters are marked in red.	
Behavior	Measured parameters
Forward locomotor activity	Line crossings, Total distance traveled
Vertical exploratory behavior	Rearings in the box (number, latency), Rearings on the board (number)
Speed of movement	Mean and maximum velocity
Immobility	Time spent immobile
Risk assessment	Stretched attends
Anxiety-related behavior	Latency until first board entry, Time spent on board (males), Board entries
Exploratory behavior	Directed: Hole exploration (males), object exploration (obi); general: Rearings (number, Latency), activity levels
Grooming behavior	Latency to grooming, Time spent grooming, Number of groomings
Defecation	Latency to defecation, Number of boli
Social affinity	Group contacts (latency), Time spent at partition
Familiar object exploration	Latency to obj. expl., Time spent in obj. expl., Number of obj. expl.
Unfamiliar object exploration	Latency to obj. expl., Time spent in obj. expl., Number of obj. expl.

Concerning anxiety-related behavior, mutant males spent more time on board than control males (time spent on board, Table 4). In contrast, the latency to first board entry (Table 4) as well as the number of board entries (Table 4) remained unchanged.

There were no genotype effects on any other observed parameter (Table 3).

3.1.5 Discussion

The **primary behavioral observation** in the modified Hole Board demonstrated altered **forward locomotor activity** in mutants of both sexes. This interpretation is based on the observation that, firstly, in mutants total distance traveled as well as the amount of turns were declined and, secondly, they traveled with reduced speed of movement. Since the Neurological Screen reported reduced grip strength in mutants, the reduction in locomotion might be a consequence of altered muscular strength. Whether alterations in conductivity of the myocardial muscle reported by the Cardiovascular Screen (3.9.5) serve as an explanation for reduced locomotion in the mHB remains unclear, since the Cardiovascular Screen did not find any other changes that would suggest physiologically relevant alterations.

Additionally, **exploratory behavior** was changed during the test situation in mutants. This conclusion is based on the fact, that, firstly, mutants exhibited enhanced vertical exploration as measured by increased rearing frequency and, secondly, started the exploration on board (hole exploration) earlier than controls. Moreover, the observed alteration in exploratory behavior was more pronounced in male than in female mutants since only mutant males additionally started rearing behavior earlier and explored more holes, although the first did not reach significant levels.

The sex-specific alteration in **anxiety-related behavior** in male mutants which spent more time on board is likely related to their altered exploration on board.

Taken together, the analysis of *Eya3* mice in the mHB reveals an altered exploratory pattern in mutant mice of both sexes with males being more affected.

3.1.6 References

Bucan M, Abel T (2002): The mouse: genetics meets behaviour. *Nat Rev Genet* 3:114-123.

Gottesman II, Gould TD (2003): The endophenotype concept in psychiatry: Etymology and strategic intentions. *Am J Psychiatry* 160:636-645.

Inoue K, Lupski JR (2003) Genetics and genomics of behavioural and psychiatric disorders. *Curr Opin Genet Dev* 13:303-309.

Kallnik M, Elvert R, Ehrhardt N, Kissling D, Mahabir E, Welzl G, Faus-Kessler T, Hrabé de Angelis M, Wurst W, Schmidt J, Höller SM (2007): Impact of IVC housing on emotionality and fear learning in male C3HeB/FeJ and C57BL/6J mice. *Mamm Genome* 18(3): 173-186

Ohl, F., Sillaber, I., Binder, E., Keck, M.E. and Holsboer, F. (2001): Differential analysis of behavior and diazepam-induced alterations in C57BL/6N and BALB/c mice using the modified hole board test. *J. Psychiatr. Res.* 35: 147-154.

Seong E, Seasholtz AF, Burmeister M (2002): Mouse models of psychiatric disorders. *Trends Genet* 18: 643-650.

Tarantino LM, Bucan M (2000): Dissection of behaviour and psychiatric disorders using the mouse as a model. *Hum Mol Genet* 9:953-965.

Table 4: Results of behavioral observation in the modified Hole Board testData are presented as mean \pm standard error of the mean.

Yellow indicate significant alterations only in one sex

Parameter	Control		Mutant		Male + Female		ANOVA		
	Male	Female	Male	Female	Control	Mutant	sex	genotype	Interaction
	(n=15)	(n=9)	(n=15)	(n=9)	(n=24)	(n=24)			
Line crossing [frequency]	142.4 \pm 5.76	142.78 \pm 5.37	130.93 \pm 7.94	132.89 \pm 5.22	142.54 \pm 4.05	131.67 \pm 5.25	n.s.	n.s.	n.s.
Line crossing [latency]	1.43 \pm 0.42	1.38 \pm 0.3	1.72 \pm 0.48	1.73 \pm 0.42	1.41 \pm 0.28	1.73 \pm 0.33	n.s.	n.s.	n.s.
Rearings in box [frequency]	44.13 \pm 3.22	34.89 \pm 1.89	48.8 \pm 3.11	42.22 \pm 2.55	40.67 \pm 2.3	46.33 \pm 2.23	p<0.05	p=0.07	n.s.
Rearings in box [latency]	25.3 \pm 3.08	19.39 \pm 3.87	17.94 \pm 2.58	24.93 \pm 2.77	23.08 \pm 2.43	20.56 \pm 2.01	n.s.	n.s.	p=0.07
Hole exploration [frequency]	58.67 \pm 4.53	78.33 \pm 4.42	71.6 \pm 4.42	68.56 \pm 5.37	66.04 \pm 3.78	70.46 \pm 3.36	n.s.	n.s.	p<0.05
Hole exploration [latency]	14.57 \pm 3.71	13.87 \pm 3.13	8.13 \pm 1.47	8.5 \pm 1.56	14.31 \pm 2.56	8.27 \pm 1.07	n.s.	p<0.05	n.s.
Hole visit [frequency]	0 \pm 0	0 \pm 0	0 \pm 0	0 \pm 0	0 \pm 0	0 \pm 0	n.s.	n.s.	n.s.
Hole visit [latency]	300 \pm 0	300 \pm 0	300 \pm 0	300 \pm 0	300 \pm 0	300 \pm 0	n.s.	n.s.	n.s.
Board entry [frequency]	10.6 \pm 1.11	15.56 \pm 1.58	13.8 \pm 1.39	14.56 \pm 0.78	12.46 \pm 1.02	14.08 \pm 0.9	n.s.	n.s.	n.s.

Table 4: Results of behavioral observation in the modified Hole Board testData are presented as mean \pm standard error of the mean.

Yellow indicate significant alterations only in one sex

Parameter	Control		Mutant		Male + Female		ANOVA		
	Male	Female	Male	Female	Control	Mutant	sex	genotype	Interaction
	(n=15)	(n=9)	(n=15)	(n=9)	(n=24)	(n=24)			
Board entry [latency]	56.07 \pm 8.09	34.5 \pm 6.09	42.64 \pm 7.05	27.71 \pm 5.38	47.98 \pm 5.87	37.04 \pm 5	p<0.001	n.s.	n.s.
Board entry [total duration %]	9.06 \pm 0.9	13.41 \pm 1.62	13.04 \pm 1.39	11.8 \pm 1.08	10.69 \pm 0.92	12.58 \pm 0.95	n.s.	n.s.	p<0.05
Rearing on board [frequency]	0.93 \pm 0.33	1.56 \pm 0.71	1.53 \pm 0.53	1.56 \pm 0.44	1.17 \pm 0.33	1.54 \pm 0.37	n.s.	n.s.	n.s.
Rearing on board [latency]	259.46 \pm 16.16	236.06 \pm 30.36	244.81 \pm 19.29	229.36 \pm 18.95	250.68 \pm 15	239.02 \pm 13.82	n.s.	n.s.	n.s.
Risk assessment [frequency]	0 \pm 0	0 \pm 0	0 \pm 0	0 \pm 0	0 \pm 0	0 \pm 0	n.s.	n.s.	n.s.
Risk assessment [latency]	300 \pm 0	300 \pm 0	300 \pm 0	300 \pm 0	300 \pm 0	300 \pm 0	n.s.	n.s.	n.s.
Group contact [frequency]	20.27 \pm 1.12	21 \pm 1.86	19.6 \pm 1.86	19.89 \pm 2.08	20.54 \pm 0.96	19.71 \pm 1.37	n.s.	n.s.	n.s.
Group contact [latency]	15.7 \pm 1.92	14.73 \pm 3.51	13.95 \pm 2.81	18.22 \pm 3.1	15.34 \pm 1.74	15.55 \pm 2.11	n.s.	n.s.	n.s.
Group contact [total duration %]	19.76 \pm 1.74	19.91 \pm 2.37	18.13 \pm 1.53	18.74 \pm 1.76	19.82 \pm 1.38	18.36 \pm 1.14	n.s.	n.s.	n.s.

Table 4: Results of behavioral observation in the modified Hole Board testData are presented as mean \pm standard error of the mean.

Yellow indicate significant alterations only in one sex

Parameter	Control		Mutant		Male + Female		ANOVA		
	Male	Female	Male	Female	Control	Mutant	sex	genotype	Interaction
	(n=15)	(n=9)	(n=15)	(n=9)	(n=24)	(n=24)			
Grooming [frequency]	0.8 \pm 0.22	0.44 \pm 0.18	0.87 \pm 0.24	0.33 \pm 0.17	0.67 \pm 0.16	0.67 \pm 0.17	n.s.	n.s.	n.s.
Grooming [latency]	242.29 \pm 22.74	267.73 \pm 15.13	262.59 \pm 13.1	288.32 \pm 7.43	251.83 \pm 15.27	272.24 \pm 8.9	n.s.	n.s.	n.s.
Grooming [total duration %]	0.97 \pm 0.38	0.76 \pm 0.35	1.19 \pm 0.39	0.22 \pm 0.12	0.89 \pm 0.27	0.83 \pm 0.26	n.s.	n.s.	n.s.
Defecation [frequency]	0.87 \pm 0.47	0 \pm 0	1 \pm 0.39	0 \pm 0	0.54 \pm 0.3	0.63 \pm 0.26	p<0.05	n.s.	n.s.
Defecation [latency]	270.74 \pm 14.91	300 \pm 0	225.16 \pm 26.51	300 \pm 0	281.71 \pm 9.66	253.23 \pm 18.01	p<0.05	n.s.	n.s.
Unfamiliar object exploration [frequency]	6.13 \pm 0.76	8.11 \pm 0.82	7 \pm 0.59	6.33 \pm 0.65	6.88 \pm 0.59	6.75 \pm 0.44	n.s.	n.s.	n.s.
Familiar object exploration [frequency]	8.33 \pm 1.02	9.89 \pm 1.02	8.87 \pm 0.74	9.89 \pm 0.59	8.92 \pm 0.75	9.25 \pm 0.51	n.s.	n.s.	n.s.
Unfamiliar object exploration [latency]	40.5 \pm 19.64	24.7 \pm 8.22	18.43 \pm 2.56	48.58 \pm 13.67	34.58 \pm 12.57	29.73 \pm 6.01	n.s.	n.s.	n.s.

Table 4: Results of behavioral observation in the modified Hole Board testData are presented as mean \pm standard error of the mean.

Yellow indicate significant alterations only in one sex

Parameter	Control		Mutant		Male + Female		ANOVA		
	Male	Female	Male	Female	Control	Mutant	sex	genotype	Interaction
	(n=15)	(n=9)	(n=15)	(n=9)	(n=24)	(n=24)			
Familiar object exploration [latency]	40.59 \pm 19.04	18.12 \pm 3.61	20.17 \pm 2.9	13.27 \pm 2.15	32.17 \pm 12.03	17.58 \pm 2.07	n.s.	n.s.	n.s.
Unfamiliar object exploration [total duration %]	1.2 \pm 0.14	2.01 \pm 0.41	1.33 \pm 0.15	1.81 \pm 0.4	1.51 \pm 0.19	1.51 \pm 0.18	p<0.05	n.s.	n.s.
Familiar object exploration [total duration %]	1.52 \pm 0.25	1.89 \pm 0.33	1.5 \pm 0.13	1.82 \pm 0.19	1.66 \pm 0.2	1.62 \pm 0.11	n.s.	n.s.	n.s.
Object Index	-0.06 \pm 0.09	0.01 \pm 0.1	-0.07 \pm 0.05	-0.07 \pm 0.12	-0.03 \pm 0.07	-0.07 \pm 0.05	n.s.	n.s.	n.s.

Table 5: Video-tracking results regarding locomotor behavior

Data are presented as mean \pm standard error of mean.

yellow indicate significant alterations only in one sex

Parameter	Control		Mutant		Male + Female		ANOVA		
	Male	Female	Male	Female	Control	Mutant	sex	genotype	Interaction
	(n=15)	(n=9)	(n=15)	(n=9)	(n=24)	(n=24)			
Total Distance Moved [cm]	3387.22 \pm 124.93	3534.29 \pm 115.54	3086.81 \pm 126.49	3248.55 \pm 71.36	3442.37 \pm 88.88	3147.46 \pm 83.77	n.s.	p<0.05	n.s.
Mean Velocity [cm/sec]	20.67 \pm 0.51	20.93 \pm 0.5	19.49 \pm 0.6	20.1 \pm 0.45	20.77 \pm 0.36	19.72 \pm 0.41	n.s.	p=0.06	n.s.
Maximum Velocity [cm/sec]	62.85 \pm 1.92	59.79 \pm 3.2	54.97 \pm 1.87	58.22 \pm 1.86	61.7 \pm 1.68	56.19 \pm 1.37	n.s.	p<0.05	n.s.
Turns [Frequency]	1714.87 \pm 46.07	1776.78 \pm 41.72	1610.33 \pm 41.61	1688.78 \pm 39.76	1738.08 \pm 32.76	1639.75 \pm 30.46	n.s.	p<0.05	n.s.
Mean Turn Angle [degrees]	20.31 \pm 0.51	19.33 \pm 0.55	20.93 \pm 0.5	19.43 \pm 0.6	19.95 \pm 0.39	20.37 \pm 0.4	p<0.05	n.s.	n.s.
Angular Velocity [degrees/sec.]	128.37 \pm 2.55	128.42 \pm 3.79	128.11 \pm 2.28	127.3 \pm 3.64	128.39 \pm 2.08	127.81 \pm 1.93	n.s.	n.s.	n.s.
Absolute Meander [degrees/sec.]	13.66 \pm 0.39	12.81 \pm 0.41	14.27 \pm 0.41	13.04 \pm 0.43	13.34 \pm 0.3	13.81 \pm 0.32	p<0.05	n.s.	n.s.
Board entry [maximum duration. sec.]	8.59 \pm 1.12	7.78 \pm 1.04	9.52 \pm 1.43	7.3 \pm 0.77	8.29 \pm 0.79	8.69 \pm 0.95	n.s.	n.s.	n.s.
Mean distance to wall [cm]	8.87 \pm 0.17	8.22 \pm 0.1	8.46 \pm 0.16	8.49 \pm 0.24	8.62 \pm 0.13	8.47 \pm 0.13	n.s.	n.s.	n.s.
Mean distance to board [cm]	8.87 \pm 0.17	8.22 \pm 0.1	8.46 \pm 0.16	8.49 \pm 0.24	8.62 \pm 0.13	8.47 \pm 0.13	n.s.	n.s.	n.s.

3.2 Dymorphology, Bone and Cartilage

3.2.1 Summary

In the Dymorphology, Bone and Cartilage Screen of the German Mouse Clinic mice are analyzed for morphological abnormalities in different organ systems with special focus on bone and cartilage development and homeostasis. The aim of the screen is to establish mouse models for human skeletal diseases like osteoporosis (McLean & Olsen, 2001; Rosen *et al.*, 2001), scoliosis (Giampietro *et al.*, 2003), limb defects (Mariani & Martin, 2003), osteogenesis imperfecta (Rauch & Glorieux, 2004; Chipman *et al.*, 1993) or osteoarthritis (Abe *et al.*, 2006). We adapted the successful dymorphological screening protocol from the Munich ENU-Mutagenesis Screen (Hrabé de Angelis *et al.* 2000) for use in the German Mouse Clinic. The nomenclature of the parameters was adapted according to the Mammalian Phenotype Ontology wording (www.informatics.jax.org/searches/MP_form.shtml). Further tests for defects in bone development and homeostasis were taken over from human diagnosis, and were adapted for the use in mice analysis. Such tests include: X-ray analysis, bone densitometry, and, in special cases, micro computed tomography. Detailed protocols for screening for bone and cartilage phenotypes in mice are described in Fuchs *et al.* (2006).

A total of 50 animals of Eya3 mutant mouse line were analyzed in the Dymorphology, Bone and Cartilage module of the German Mouse Clinic. In the morphological investigation via visual inspection at the age of nine weeks, we observed abnormal head morphology in 14 of 25 mutants (56%) and in 3 of 25 controls (12%). In the X-ray analysis at the age of 16 weeks, no genotype-specific differences were detectable; also the abnormal head morphology was no longer apparent. In the dual-energy X-ray absorptiometry (DXA) analysis at the age of 16 weeks, BMC (bone mineral content) was decreased in male mutants. Concurrently body length and weight were decreased in male mutants. The difference in BMC is probably due to the smaller body size of the male mutants.

3.2.2 Mice

Thirty male (15 controls, 15 mutants) and 20 female (10 controls, 10 mutants) mice were analyzed by morphological inspection at the age of 9 weeks. 16-week-old mutants (19 and 20 animals for DXA and X-ray, respectively) and controls (18 and 20 animals for DXA and X-ray, respectively) entered the bone density and X-ray analysis.

3.2.3 Material and Methods

The Dymorphology, Bone and Cartilage module of the German Mouse Clinic analyzed the mice in different phases:

1. At the age of five weeks, i.e. when the mice entered the facility, the general physical condition and health were checked,
2. at the age of nine weeks, a morphological observation as a whole-body checkup was performed; and

3. at the age of 16 to 17 weeks, X-ray analysis and bone densitometry were performed.

Morphological Observation

The animals were screened using the protocol for morphological analysis from Fuchs *et al.* (2000) as adapted for the German Mouse Clinic.

Using a clickbox (supplied by the MRC Institute of Hearing Research, Nottingham, UK) we tested the mice's ability to hear a sound of 20 kHz. The reaction of the animals was classified into six categories (0=no reaction at all, 1=no Preyer reflex, 2= retarded reaction, 3= normal reaction, 4= strong reaction, 5= particularly strong reaction).

X-ray Images

Equipment: Faxitron X-ray Model MX-20 (Specimen Radiography System, Illinois, USA),

NTB Digital X-ray Scanner EZ 40 (NTB GmbH, Diepholz, Germany),

Quality control: Calibration of the system is done in monthly intervals,

Settings: Voltage 25 kV, integration time 40 ms,

Procedure: The anesthetized mouse was fixed on an X-ray-permeable plate and placed in the machine. Using iX-Pect software supplied by the manufacturer of the X-ray scanner, the image was taken and analyzed. Analysis was done qualitatively by visual inspection of the images as well as quantitatively by using the ruler tool of iX-Pect software.

Bone density analysis

Equipment: pDEXA Sabre X-ray Bone Densitometer (Norland Medical Systems. Inc., Basingstoke, Hampshire, UK; distributed by Stratec Medizintechnik GmbH, Pforzheim, Germany),

Quality control: Calibration of the system was done in daily intervals using the QC and the QA phantoms delivered by the manufacturer. Results from the quality control were recorded by the system.

Settings: Scan speed 20 mm/s, Resolution 0.5 mm x 1.0 mm, HAW 0.020

Procedure: After anesthesia, the weight and length of the mouse were recorded, and the mouse was placed in the analyzer. After a scout scan, the area of interest was optimized and the measure scan started.

Data-analysis: For analysis of the data, regions have to be defined. The standard analysis comprises a whole body analysis as well as a whole body analysis excluding the skull.

Statistical analysis of data

Analysis of quantitative data sets was carried out using StatView software package (SAS Corporation).

3.2.4 Results and Discussion

Fifty animals of Eya3 mutant mouse line were analyzed in the Dysmorphology, Bone and Cartilage module of the German Mouse Clinic. In the morpho-

logical investigation via visual inspection at the age of 9 weeks we observed abnormal head morphology (Fig. 3; Table 6) in 14 of 25 mutants (56%) and in 3 of 25 controls (12%). In mutant animals we had the impression that the neck musculature appeared to be weaker compared to controls. In the X-ray analysis at the age of 16 weeks no genotype-specific differences were detectable; the abnormal head morphology was no longer apparent either (Table 7). In the Clickbox test (Table 8) to test the hearing ability of the mice, we observed a normal reaction in mutants and controls. In the bone densitometry using DXA analysis (Table 9), only BMC was decreased in male mutants. Concurrently body length and weight were decreased in male mutants. The difference in BMC is probably due to the smaller body size of the male mutants. The sex differences we observed are common in many mouse strains, and thus are not abnormal (unpublished data).

For further analysis of the abnormal morphology of the head observed at the age of nine weeks additional data can be generated in secondary analysis by μ CT measuring animals younger than nine weeks.

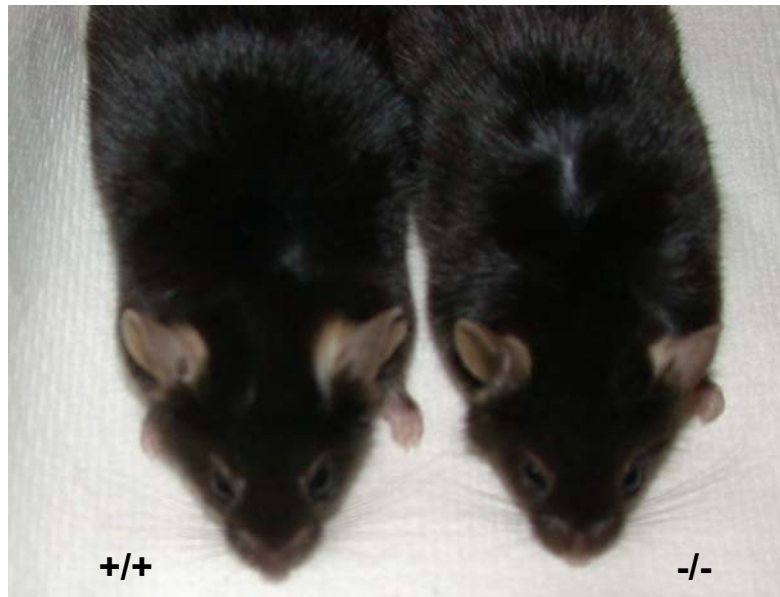


Figure 3: Abnormal head morphology

At the age of nine weeks 56% of mutants showed a smaller head compared to controls (also 12% of control animals showed a smaller head, see Table 6).

Raw data will be available on request.

3.2.5 References

Abe K., Fuchs H., Lisse T., Hans W. and Hrabé de Angelis M. (2006): New ENU induced semidominant mutation, Ali18, causes inflammatory arthritis, dermatitis, and osteoporosis in the mouse. *Mammalian Genome* 17: 915-926.

- Chipman SD, Sweet HO, McBride DJ Jr, Davisson MT, Marks SC Jr, Shuldiner AR, Wenstrup RJ, Rowe DW, Shapiro JR. (1993): Defective pro alpha 2(I) collagen synthesis in a recessive mutation in mice: a model of human osteogenesis imperfecta. *Proc Natl Acad Sci USA* 90(5): 1701-5.
- Fuchs H, Lisse T, Abe K and Hrabé de Angelis M (2006): Screening for bone and cartilage phenotypes in mice. In: *Phenotyping of the Laboratory Mouse*. Eds.: Hrabé de Angelis M., Chambon P. and Browns S. Wiley-VCH, Weinheim. pp. 35-86.
- Fuchs H, Schughart K, Wolf E, Balling R, and Hrabé de Angelis M. (2000): Screening for dysmorphological abnormalities - a powerful tool to isolate new mouse mutants. *Mammalian Genome* 11(7): 528-30.
- Giampietro PF, Blank RD, Raggio CL, Merchant S, Jacobsen FS, Faciszewski T, Shukla SK, Greenlee AR, Reynolds C, Schowalter DB. (2003): Congenital and idiopathic scoliosis: clinical and genetic aspects. *Clin Med Res* 1(2): 125-36.
- Hrabé de Angelis, M., H. Flaswinkel, H. Fuchs, B. Rathkolb, D. Soewarto, S. Marschall, S. Heffner, W. Pargent, K. Wuensch, M. Jung, A. Reis, T. Richter, F. Alessandrini, T. Jakob, E. Fuchs, H. Kolb, E. Kremmer, K. Schaeble, B. Rollinski, A. Roscher, C. Peters, T. Meitinger, T. Strom, T. Steckler, F. Holsboer, T. Klopstock, F. Gekeler, C. Schindewolf, T. Jung, K. Avraham, H. Behrendt, J. Ring, A. Zimmer, K. Schughart, K. Pfeffer, E. Wolf and R. Balling (2000): Genome-wide, large-scale production of mutant mice by ENU mutagenesis. *Nature Genetics* 25: 444-447
- Mariani FV, Martin GR (2003): Deciphering skeletal patterning: clues from the limb. *Nature* 423(6937): 319-25.
- McLean W, Olsen BR. (2001): Mouse models of abnormal skeletal development and homeostasis. *Trends Genet* (10): S38-43.
- Rauch F, Glorieux FH. (2004): Osteogenesis imperfecta. *Lancet* 363(9418): 1377-85.
- Rosen CJ, Beamer WG, Donahue LR. (2001): Defining the genetics of osteoporosis: using the mouse to understand man. *Osteoporos Int.* 12(10): 803-10.

Abbreviations

BMC	bone mineral content
BMD	bone mineral density
DXA	dual-energy X-ray absorptiometry
μCT	micro computed tomography
pQCT	peripheral quantitative computed tomography
pBMD	partial bone mineral density (excluding skull)
sBMD	specific bone mineral density

Table 6: Results from the morphological inspection (nine-week old mice)				
Parameter	Male		Female	
	Control	Mutant	Control	Mutant
Growth				
normal	15	15	10	10
Weight				
normal	15	14	10	10
fat	-	1	-	-
Body size				
normal	14	10	9	6
small	1	5	1	4
Eyes				
normal	14	15	10	10
one small	1	-	-	-
Coat hair growth				
normal	15	15	10	10
Coat hair texture				
normal	15	15	10	10
Hair follicle structure / orientation				
normal	15	15	10	10
Skin pigmentation				
normal	15	15	10	10
Skin texture / condition				
normal	15	15	10	10
Vibrissae				
normal	15	15	10	10
Limbs				
normal	15	15	10	10
Digits				
normal	15	14	9	10
syndactylism	-	1	-	-
abnormal digit	-	-	1	-
Tail				
normal	14	15	10	10
kinky tail	1	-	-	-
Teeth				
normal	15	14	10	10
long	-	1	-	-
Ear morphology				
normal	15	15	10	10
Musculature				
normal	15	15	10	10
Seizures / epilepsy				
no	15	15	10	10

Motor capabilities / coordination				
normal	15	14	10	10
trembling	-	1	-	-
Movement				
normal	15	15	10	10
Feeding / drinking behavior				
normal	15	15	10	10
Respiratory system				
normal	15	15	10	10
Reproductive system				
normal	15	15	10	10
Other abnormalities				
no	13	8	9	3
abnormal head morphology	2	7	1	7
Animals analyzed	15	15	10	10

Table 7: Results from the X-ray analysis (16-week old mice)

Parameter	Male		Female	
	Control	Mutant	Control	Mutant
Skull				
normal	10	10	10	10
Mandibles				
normal	10	10	10	10
Maxilla				
normal	10	10	10	10
Teeth				
normal	10	10	10	10
Orbit				
normal	10	10	10	10
Number of cervical vertebrae				
normal (7)	10	10	10	10
Number of thoracic vertebrae				
normal (13)	10	10	10	10
Number of lumbar vertebrae				
normal (6)	10	10	10	10
Number of sacral vertebrae				
normal (4)	10	10	10	10
Number of caudal vertebrae				
normal	10	10	10	10
Vertebrae				
normal	10	10	10	10
Ribs				
normal (26)	10	10	10	10
Scapulas				

normal	10	10	10	10
Clavicle				
normal	10	10	10	10
Pelvis				
normal	10	10	10	10
Femur				
normal	10	10	10	10
Tibia				
normal	10	10	10	10
Fibula				
normal	10	10	10	10
Humerus				
normal	10	10	10	10
Ulna				
normal	10	10	10	10
Radius				
normal	10	10	10	10
Digits				
normal (20)	10	10	10	10
Joints				
normal	10	10	10	10
Other abnormalities				
no	10	10	10	10
Animals analyzed	10	10	10	10

Table 8: Results from clickbox test (hearing test; nine-week old mice)

Phenotype	Male		Female	
	Control	Mutant	Control	Mutant
0	-	-	-	-
1	-	-	-	-
2	2	1	1	1
3	13	14	9	9
4	-	-	-	-
5	-	-	-	-
Mean Score	2.87	2.93	2.90	2.90

Kruskal-Wallis ANOVA on Ranks: n.s.

0: no reaction at all,
1: very slow reaction,
2: retarded reaction,
3: normal reaction,
4: strong reaction,
5: extremely excited

Parameter	Control (A)		Mutant (B)		A~B		ANOVA		
	Male	Female	Male	Female	Male	Female	<i>p</i> – value genotype	<i>p</i> – value sex	<i>p</i> – value interaction
	(n=9)	(n=9)	(n=10)	(n=9)	<i>p</i> – value	<i>p</i> – value			
BMD [mg/cm ²]	58 ± 2	56 ± 2	58 ± 2	58 ± 1	n.a.	n.a.	n.s.	n.s.	n.s.
pBMD [mg/cm ²]	47 ± 2	44 ± 2	46 ± 2	45 ± 1	n.a.	n.a.	n.s.	n.s.	n.s.
sBMD [10 ⁻³ x cm ⁻²]	2.12 ± 0.10	2.66 ± 0.12	2.48 ± 0.18	2.88 ± 0.16	n.a.	n.a.	n.s.	< 0.01	n.s.
BMC [mg]	557 ± 33	467 ± 21	422↓ ± 39	447 ± 33	< 0.05	n.s.	< 0.05	n.s.	n.s.
Bone Content [%]	2.04 ± 0.10	2.22 ± 0.10	1.73 ± 0.11	2.16 ± 0.10	n.a.	n.a.	n.s.	< 0.01	n.s.
Body Length [cm]	9.06 ± 0.06	8.89 ± 0.07	8.60↓ ± 0.15	8.67 ± 0.08	< 0.05	n.s.	< 0.01	n.s.	n.s.
Body Weight [g]	27.29 ± 0.63	21.05 ± 0.44	23.96↓ ± 1.12	20.57 ± 0.82	< 0.05	n.s.	< 0.05	< 0.0001	n.s.
Fat mass [units]	3.48 ± 0.63	2.11 ± 0.42	1.50 ± 0.33	2.38 ± 0.63	n.a.	n.a.	n.s.	n.s.	< 0.05
Fat Content [units x 100/g]	12.60 ± 2.21	9.96 ± 1.95	5.90 ± 1.27	10.91 ± 2.62	n.a.	n.a.	n.s.	n.s.	n.s.
Lean mass [units]	20.98 ± 0.64	16.37 ± 0.65	19.76 ± 0.76	15.54 ± 0.46	n.a.	n.a.	n.s.	< 0.0001	n.s.
Lean Content [units x 100/g]	77.04 ± 2.35	77.76 ± 2.69	82.89 ± 1.44	76.21 ± 2.94	n.a.	n.a.	n.s.	n.s.	n.s.

3.3 Neurology Screen

3.3.1 Summary

Neurological dysfunction results in a wide variety of disorders ranging from impaired movement to severe mental illness. Studying the neurobehavioral phenotype of mutant mice is a powerful tool to understand the neural basis of behavior and the pathophysiology of neurological disorders. Comparison of the mouse and human brain transcriptomes shows a good correlation for highly expressed genes in both transcript identity and abundance (Fougousse *et al.*, 2000). Therefore, screening of mice with respect to neurological disorders potentially offers an understanding of etiology and pathogenesis of the human nervous system (Hafezparast *et al.*, 2002).

The primary observation screen is a modification of the Irwin procedure (Irwin, 1968) and was proposed as a rapid, comprehensive and semi-quantitative screening method for qualitative analysis of abnormal phenotypes in a mouse strain (Rogers *et al.*, 1997). Dependant upon results of this primary screen and due to specific questions, additional tests can be carried out for further assessment of neurological functions in a hierarchical way (Schneider *et al.*, 2006).

In the primary neurological screen 25 *Eya3*-mutant mice (15 males / 10 females) and 25 control mice (15 males / 10 females) were analyzed according to our modified SHIRPA protocol where a battery of behavioral tests is carried out.

We examined the mice using designed 23 test parameters (See web page: http://www.mgu.har.mrc.ac.uk/facilities/mutagenesis/mutabase/shirpa_summary.html) to detect phenotypic differences between knockout and control mice. The test parameters contribute to an overall assessment of muscle, motor neuron, spinocerebellar, sensory and autonomic functions. The primary neurological screen is focused on investigating neurological signs to determine the neurological functioning of a mouse. We also examine forelimb grip force for the assessment of muscular function.

The comparison of *Eya3*-mutant mice to controls revealed decreased forelimb grip force in mutant mice. All SHIRPA test parameters were without significant findings. Rotarod testing for motor coordination did not show any alterations either.

3.3.2 Mice

Fifteen 10-week-old male mutant and control mice entered the neurological screen at the beginning of the 47th calendar week 2006. Ten female mutant and ten control mice entered the neurological laboratory one week later. All animals were fed *ad libitum* for a period of one week during their stay in the neurological screen.

3.3.3 Material and Methods

Primary screening 1: modified SHIRPA protocol

Assessment of each animal at age 10 weeks began with observation of undisturbed behavior (*Viewing Jar Behavior*) in a glass cylinder (11 cm in diameter). The mice were then transferred to an arena consisting of a clear Perspex box (420 x 260 x 180 mm) in which a Perspex sheet on the floor is marked with 15 squares. Locomotor activity and motor behavior within this area was observed (*Behavior recorded in the Arena*). This was followed by a sequence of manipulations testing reflexes (*Behavior recorded on or above the arena*). Measurements were completed with the recording of body weight. The last part of the primary screen also involved the analysis of righting reflex, and contact righting reflex. A glass cylinder (35 mm diameter, 135 mm length) was used for testing of the contact righting reflex. Throughout the entire procedure, abnormal behavior, biting, defecation, and vocalization were recorded. Between testing of each mouse, fecal pellets and urination were removed from the viewing jar and arena. All experimental equipment was thoroughly cleaned with Pursept-A and dried prior to testing (Schneider *et al.*, 2006).

Primary screening 2: grip strength

The grip strength meter system determines the fore limb grip strength, i.e. muscle strength of a mouse. The device exploits the tendency of a mouse to grasp a horizontal metal bar while being pulled by its tail. During the trial set-up, the mouse grasps a special adjustable grip (2 mm) mounted on a force sensor. The sensor allows measurements of up to 600 Ponds. Five trials were undertaken for each mouse within one minute. The mean value is used to represent the grip strength of a mouse.

All experimental equipment was thoroughly cleaned with Pursept-A and dried prior subsequent tests. Values were presented as means \pm standard error of mean (SEM).

Statistical analysis of the grip strength trial results. Grip strength trial results are compared between genotypes, controlling for the effects of sex and weight, by fitting linear mixed effect models (Pinheiro and Bates, 2000). A linear mixed effect model is a modified analysis of variance/covariance approach allowing for dependencies in the data. In our case, dependencies arise from repeated trials within each mouse. Genotype, sex and weight are modeled as fixed effects. Mouse-specific intercepts are modeled by including the intercept as random effect. Interaction effects are tested for and included in the model if they show a significant contribution. A serial dependency on the trial number can be tested by including the trial number as random effect with an autoregressive correlation structure. Model fitting is performed by the nlme-Package in the open-source statistical software R, a close relative of S-PLUS (The R Project for Statistical Computing, 2004). The p-value for the genotype effect within the specific model found for the data indicates the sig-

nificance of the statistical test of interest; a confidence interval for the genotype effect can also be extracted.

Secondary Screening: Rotarod test

The TSE-RotaRod 3375 apparatus (Accelerating Model, TSE, Bad Homburg) was used to measure fore limb and hind limb motor coordination, balance and motor learning ability (Jones and Roberts, 1968). The machine was set up in an environment with minimal stimuli such as noise and movement.



Figure 4: The rotarod apparatus

The rotarod device is equipped with a computer controlled motor-driven rotating rod. The unit consists of a rotating spindle and four individual lanes for each mouse (Fig. 4). The software allows pre-programming of session protocols with varying rotational speeds. Infrared beams are used to detect when a mouse falls onto the grids beneath the rotarod.

In general, the mouse is placed perpendicular to the axis of rotation, with head facing the direction of the rotation. All mice were placed on the Rotarod at an accelerating speed from 4 to 40 rpm for 300 sec with 20 min between each trial. In motor coordination testing, mice were given four trials at the accelerating speed at one day. The mean latency to fall off the Rotarod during the trials was recorded and used in subsequent analysis. Before the start of the first trial, mice were weighed.

Statistical analysis of the Rotarod performance results: The Rotarod data contain dependencies, which are more complex than the grip strength data. Repeated measurements arise from four different trials with a break in between. To compare the performance results between genotypes, linear mixed-

effect models are fitted, that allow for the dependencies of genotype and trial and for the effects of sex and weight. The latter are modeled as fixed effects. Interaction effects are considered and included in the model, if necessary.

In each model, the parameter of interest is the coefficient of the genotype effect. A significance test or a confidence interval for this coefficient can be extracted from the model fitted.

3.3.4 Parameters

Muscle/lower motor neuron function
Body position, gait, Positional passivity, tail elevation, grip strength, defecation
Spinocerebellar function
Body position, gait, righting reflex, tail elevation, grip strength
Sensory function
Transfer arousal, touch escape, gait, pinna reflex, righting reflex
Autonomic function
Palpebral closure, defecation, lacrimation
Neurological reflexes
Righting reflex (pons), contact righting reflex, pinna reflex
General appearance
Body weight, body position, transfer arousal, touch escape, vocalization, positional passivity, aggression, spontaneous activity, locomotor activity, skin color

3.3.5 Results

The primary analysis with the **modified SHIRPA** protocol did not show any significant alterations in *Eya3*-mutant mice (Tables 10-13). Lactate values measured with the AU400 analyzer of the Clinical Chemistry Screen were also devoid of particular findings (Table 14).

Comparing the **forelimb grip strength** revealed significantly reduced forelimb grip force (genotype effect $p < 0.05$; Fig. 5).

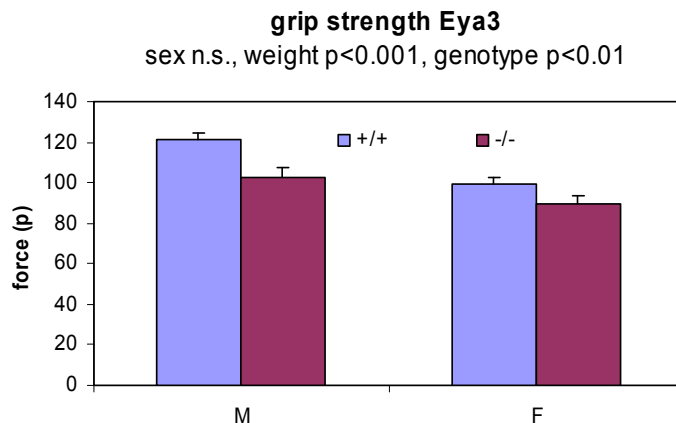


Figure 5: Results from grip strength testing

Performance of the *Eya3* mutants on the accelerating rotarod did not show significant genotype-related differences (Fig. 6).

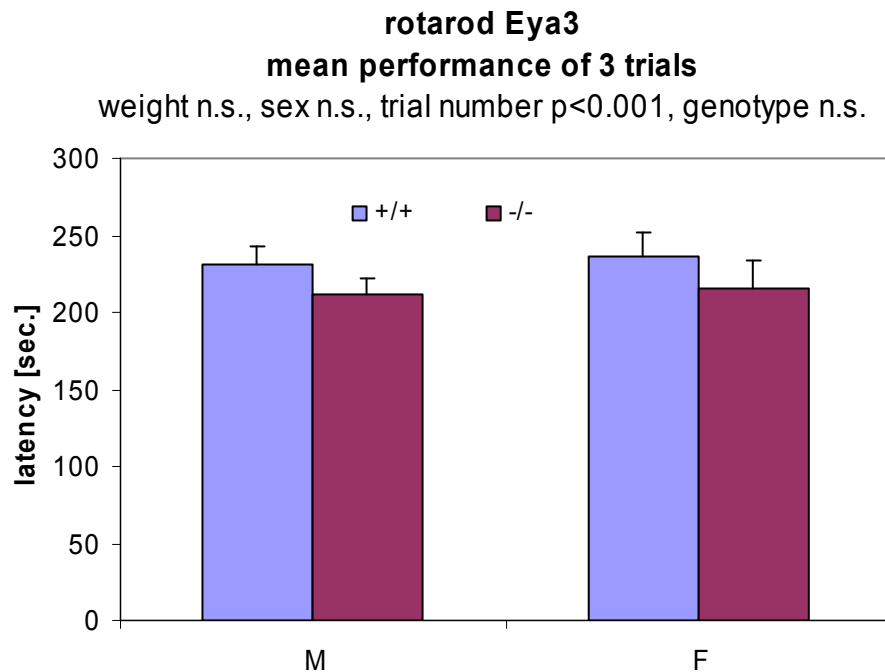


Figure 6: Results from rotarod testing

Raw data for each individual animal in Excel sheets are available on request.

3.3.6 Discussion

In our neurological screening, male and female *Eya3*-KO mice showed no clear phenotype. Basic neurological functions seem not to be affected by the mutation. Rotarod performance was only slightly impaired.

In many of the mutant animals, altered childlike head morphology was observed (pictures available on request).

The reduction in body weight has also some impact on forelimb grip force ($p < 0.001$). We often observe reduced grip strength in mutants with less body weight. However there appears also a genotype-related reduction involved as indicated by the statistical significance of the genotype effect ($p < 0.01$).

Eya genes are highly conserved and are part of the developmental regulatory cascade directed by *Pax6* and involved in tissue development especially in the eye (provider info). However, other members of the family like *Eya1* and *Eya2* are also involved in the development of muscle and connective tissue (Xu *et al.*, 1997). Expression analysis with β -Gal-staining of the *Eya3* gene-trap mutants analyzed here showed very strong signal in developing limbs. This would emphasize a role of *Eya3* in muscle or tendon development.

We recommend a closer analysis of the expression in the limbs. In addition, since the head morphology defect vanishes later on and could no longer be detected by the Pathology Screen (3.13.5), it would also be worth measuring grip force at various ages.

3.3.7 References

- Fougerousse F, Bullen P, Herasse M, Lindsay S, Richard I, Wilson D, Suel L, Durand M, Robson S, Abitbol M, Beckmann JS, Strachan T. (2000): Human-mouse differences in the embryonic expression patterns of developmental control genes and disease genes. *Hum. Mol. Genet.* 9: 165-73.
- Hafezparast M, Ahmad-Annuar A, Wood NW, Tabrizi SJ, Fisher EM. (2002): Mouse models for neurological disease. *Lancet Neurol.* 1(4): 215-24.
- Irwin S. (1968): Comprehensive observational assessment: Ia. A systematic, quantitative procedure for assessing the behavioral and physiologic state of the mouse. *Psychopharmacologia* 13(3): 222-257.
- Jones, B.J. and D.J. Roberts (1968): The quantitative measurement of motor incoordination in naive mice using an accelerating Rota-Rod. *J Pharm Pharmacol* 20: 302-304
- Pinheiro JC, Bates DM (2000): *Mixed-Effects Models in S and S-PLUS*. Springer, New York
- The R Project for Statistical Computing, 2004; <http://www.r-project.org/>
- Rogers D. C., E.M. Fisher, S.D. Brown, J. Peters, A.J. Hunter and J.E. Martin (1997): Behavioral and functional analysis of mouse phenotype: SHIRPA, a proposed protocol for comprehensive phenotype assessment. *Mamm Genome* 8(10): 711-713.
- Schneider I, Tirsch WS, Faus-Kessler T, Becker L, Kling E, Busse RL, Bender A, Feddersen B, Tritschler J, Fuchs H, Gailus-Durner V, Englmeier KH, Hrabé de Angelis M, and Klopstock T. (2006): Systematic, standardized and comprehensive neurological phenotyping of inbred mice strains in the German Mouse Clinic. *J Neurosci Methods* 157(1): 82-90
- Xu PX, Adams J, Peters H, Brown MC, Heaney S, Maas R (1999): *Eya1*-deficient mice lack ears and kidneys and show abnormal apoptosis of organ primordia. *Nature Genetics* 23: 113-117

Abbreviations

SHIRPA **S**mithKline Beecham Pharmaceuticals, **H**arwell, MRC Mouse Genome Centre and Mammalian Genetics Unit, **I**mperial College School of Medicine at St Mary's **R**oyal London Hospital, St Bartholomew's and the Royal London School of Medicine **P**henotype **A**ssessment
http://www.mgu.har.mrc.ac.uk/mutabase/shirpa_summary.html

Table 10: Recording of body weightData are presented as mean \pm standard error of mean.

Parameter	Male			Female			both
	Control (n=15)	Mutant (n=15)	<i>p</i> -value	Control (n=10)	Mutant (n=10)	<i>p</i> -value	<i>p</i> -value
Body Weight [g]	24.4 \pm 0.5	22.7 \pm 0.8	<i>n.s.</i>	19.2 \pm 0.3	18.7 \pm 0.6	<i>n.s.</i>	0.056

Table 11: Behavior recorded in viewing jarStatistical analysis: chi-squared test; significance $p < 0.05$

Parameter	Male			Female			both
	Control (n=15)	Mutant (n=15)	<i>p</i> -value	Control (n=10)	Mutant (n=10)	<i>p</i> -value	<i>p</i> -value
Body Position							
Inactive	0	0		0	0		
Active	15	15		10	10		
Excessive Activity	0	0	<i>n.s.</i>	0	0	<i>n.s.</i>	<i>n.s.</i>
Tremor							
Absent	15	15		10	10		
Present	0	0	<i>n.s.</i>	0	0	<i>n.s.</i>	<i>n.s.</i>
Palpebral closure							
Eyes open	15	15		10	10		
Eyes closed	0	0	<i>n.s.</i>	0	0	<i>n.s.</i>	<i>n.s.</i>
Coat Appearance							
Tidy and well groomed	15	15		10	10		
Irregularities	0	0	<i>n.s.</i>	0	0	<i>n.s.</i>	<i>n.s.</i>
Whiskers							
Present	15	15		10	10		
Absent	0	0	<i>n.s.</i>	0	0	<i>n.s.</i>	<i>n.s.</i>
Lacrimation							
Absent	15	15		10	10		
Present	0	0	<i>n.s.</i>	0	0	<i>n.s.</i>	<i>n.s.</i>
Defecation							
Present	15	15		10	10		
Absent	0	0	<i>n.s.</i>	0	0	<i>n.s.</i>	<i>n.s.</i>

Table 12: Recording of locomotor activity and behavior in the arena

Statistical analysis: chi-squared test; significance $p < 0.05$. Locomotor activity data are shown as mean (\pm SEM)

Parameter	Male			Female			both
	Control (n=15)	Mutant (n=15)	<i>p</i> -value	Control (n=10)	Mutant (n=10)	<i>p</i> -value	<i>p</i> -value
Transfer arousal							
Extended freeze	0	1		0	0		
Brief freeze	4	8		0	1		
Immediate movement	11	6	<i>n.s.</i>	10	9	<i>n.s.</i>	<i>n.s.</i>
Locomotor activity	26.7 \pm 2.5	26.5 \pm 2.0	<i>n.s.</i>	26.7 \pm 2.7	26.0 \pm 2.4	<i>n.s.</i>	<i>n.s.</i>
Gait							
Fluid movement	15	15		10	10		
Lack Fluidity	0	0	<i>n.s.</i>	0	0	<i>n.s.</i>	<i>n.s.</i>
Tail Elevation							
Dragging							
Horizontally extension	0	0		0	0		
	15	15		10	10		
Elevated/Straub tail	0	0	<i>n.s.</i>	0	0	<i>n.s.</i>	<i>n.s.</i>
Touch Escape							
No response	0	0		0	0		
Response to touch	15	15		10	10		
Flees prior to touch	0	0	<i>n.s.</i>	0	0	<i>n.s.</i>	<i>n.s.</i>
Positional Passivity							
Struggles when held by tail	15	15		10	10		
No struggle	0	0	<i>n.s.</i>	0	0	<i>n.s.</i>	<i>n.s.</i>

Table 13: Behavior recorded in or above the arena							
Statistical analysis: chi-squared test; significance $p < 0.05$							
Parameter	Male			Female			both
	Control (n=15)	Mutant (n=15)	<i>p-value</i>	Control (n=10)	Mutant (n=10)	<i>p-value</i>	<i>p-value</i>
Skin color							
Blanched	0	0		0	0		
Pink	15	15		10	10		
Bright deep red	0	0	<i>n.s.</i>	0	0	<i>n.s.</i>	<i>n.s.</i>
Trunk curl							
Absent	0	0		0	0		
Present	15	15	<i>n.s.</i>	10	10	<i>n.s.</i>	<i>n.s.</i>
Limb Grasping							
Absent	15	15		10	10		
Present	0	0	<i>n.s.</i>	0	0	<i>n.s.</i>	<i>n.s.</i>
Pinna Reflex							
Present	15	15		10	10		
Absent	0	0	<i>n.s.</i>	0	0	<i>n.s.</i>	<i>n.s.</i>
Corneal Reflex							
Present	15	15		10	10		
Absent	0	0	<i>n.s.</i>	0	0	<i>n.s.</i>	<i>n.s.</i>
Righting Reflex							
Rights itself	15	15		10	10		
Fails to right when released	0	0	<i>n.s.</i>	0	0	<i>n.s.</i>	<i>n.s.</i>
Contact Righting							
Present	15	14		10	10		
Absent	0	1	<i>n.s.</i>	0	0	<i>n.s.</i>	<i>n.s.</i>
Evidence of biting							
None	13	15		10	10		
Biting in response to handling	2	0	<i>n.s.</i>	0	0	<i>n.s.</i>	<i>n.s.</i>
Vocalization							
None	7	6		3	4		
Vocal	8	9	<i>n.s.</i>	7	6	<i>n.s.</i>	<i>n.s.</i>

Table 14: Lactate levelsData shown represent the results of the mean blood lactate concentrations, value (\pm SEM)

	Male			Female			both
	Control (n=15)	Mutant (n=15)	<i>p</i> - <i>value</i>	Control (n=10)	Mutant (n=10)	<i>p</i> - <i>value</i>	<i>p</i> - <i>value</i>
Lactate (mmol/l)	6.9 \pm 0.3	6.9 \pm 0.3	<i>n.s.</i>	10.9 \pm 0.4	10.3 \pm 0.4	<i>n.s.</i>	<i>n.s.</i>

3.4 Eye Screen

3.4.1 Summary

In the primary screen, different methods were employed to analyze the eyes of mutant mouse line in comparison to their control littermates. Mice were examined for anterior segment abnormalities by slit lamp biomicroscopy (Favor, 1983), as well as for posterior segment abnormalities by funduscopy. The axial eye length was measured by laser interference biometry (LIB; Puk *et al.*, 2006). If required, the retinal function can be tested with a high throughput electroretinography (ERG; Dalke *et al.*, 2004) in a secondary screen.

In humans blindness is caused by several different ocular diseases. Among these, the cataracts are responsible for half of all cases (Johnson and Foster, 2003). The retinal disorders cover a broad variety of clinical symptoms and many different genes are involved in the corresponding pathological conditions in humans. The two most important groups are retinitis pigmentosa (RP) and age-related-macular-degeneration (ARMD; for recent reviews, see Rivolta *et al.*, 2002 and Stone *et al.*, 2001). Mouse models are appropriate tools to understand the genetic and biochemical mechanisms of ocular disorders. There is a rapid increasing number of mouse mutants available suffering from various types of eye diseases (for recent reviews see Graw, 2003 and Dalke & Graw, 2005).

Genotype-specific differences of unclear relevance were detected between wild-type control and mutant *Eya3* mice.

3.4.2 Mice

Twenty-five *Eya3*-control (15 male, 10 female) and 25 *Eya3*-mutant mice (15 male, 10 female) entered the Eye Screen at the age of 11 weeks. Mice were first examined by slitlamp biomicroscopy and funduscopy, on the following day the laser interference biometry was performed. Mice were kept under standard laboratory conditions with food and water *ad libitum*. When the mice were killed for pathological examinations the eyes of some mice were fixed for histological analysis in the Eye Screen.

3.4.3 Materials and Methods

Funduscopy (Ophthalmoscopy): The posterior parts of both eyes were examined by funduscopy. After pupil dilation with one drop of atropine (1%), the mouse is grasped firmly in one hand and clinically evaluated using a head-worn indirect ophthalmoscope (Sigma 150 K, Heine Optotechnik, Herrsching, Germany) in conjunction with a condensing lens (90D lens, Volk, Mentor, OH, USA) mounted between the ophthalmoscope and the eye.

Slit Lamp Biomicroscopy: Mice were examined biomicroscopically for eye abnormalities as previously described (Favor, 1983). Briefly, pupils were dilated with a 1% atropine solution applied to the eyes at least 10 min prior to examination. Both eyes of the mice were examined by slit lamp biomicroscopy (Zeiss SLM30) at 48x magnification with a narrow beam slit lamp illumination

at 25-30°angle from the direction of observation. Observed phenotypic variants of the eyes were carefully documented.

Laser Interference Biometry (LIB) was performed using the “AC Master” (Meditec, Carl Zeiss, Jena, Germany) equipped with a new technique, optical low coherence interferometry (OLCI), adapted for short measurement distances (Schmucker and Schaeffel, 2004). Mice were anaesthetized with 137 mg Ketamine and 6.6 mg Xylazine per kg body weight and placed in front of the ACMaster.

Histology: Eyes were fixed 24 hours in Davidson solution, dehydrated and embedded in plastic medium. Transverse 2-µm sections were cut with an ultramicrotome, stained with methylene blue and basic fuchsin and evaluated with a light microscope.

Statistical Analysis: Laser interference biometry data were statistically analyzed using MS-Excel. Differences between mouse groups were evaluated with the Student’s t-test. Statistical significance was set at $p < 0.05$. Data are presented as mean values \pm standard error of the mean (SEM).

3.4.4 Parameters

Funduscopy
(qualitative) abnormalities of the retinal fundus and optic disc, vessel alterations and development disorders
Slit lamp biomicroscopy
(qualitative) abnormalities of lens and cornea like opacity and development disorders
Laser Interference Biometry (LIB)
axial eye length abnormalities
Histology
(qualitative) retinal lamination and morphology of cell layers and lens
Morphology
(qualitative) like size and degree of closure

3.4.5 Results

Laser Interference Biometry data were recorded from the groups of control and *Eya3*-mutant mice. A comparison of the axial eye length of left and right eye was performed for each group. Since no differences were observed between the left and right eye, data of both eyes were averaged for further evaluation. The mean value and standard error was calculated for each group of mice, male and female, wild-type control and mutant (Table 15). The comparison of the normalized axial lengths (axial eye length / body length) between males and females revealed sex-specific differences in the control and the mutant group. Exceptionally, the females have a larger axial length than the males in both groups. Comparing *Eya3*-mutant mice with their littermate controls, significant differences were only found for the normalized axial length,

but not for the axial eye length itself. This could be a secondary effect due to the shorter body length caused by the obviously smaller head size at this age.

All *Eya3* mice were examined by **funduscopy**. In single mice, unilateral abnormalities were observed in the retinal fundus (Table 16). However, no abnormalities associated with the *Eya3* mutation were detected.

A total of 50 mice were examined ophthalmologically by **slit lamp biomicroscopy** (Table 17). No anterior segment phenotype was shown to be associated with the *Eya3* mutation. All animals (both sexes and both genotypes) had minor fleck opacities, which are often seen in strain C57BL/6.

To conclude, no distinct genotype-specific differences between wild-type control and mutant *Eya3* mice were detected in the eye screen.

3.4.6 References

- Dalke C., J. Löster, H. Fuchs, V. Gailus-Durner, D. Soewarto, J. Favor, A. Neuhäuser-Klaus, W. Pretsch, F. Gekeler, K. Shinoda, E. Zrenner, T. Meitinger, M. Hrabé de Angelis and J. Graw (2004): Electroretinography as a screening method for mutations causing retinal dysfunction in mice. *IOVS* 45: 601-609.
- Dalke C. and Graw J. (2005): Mouse mutants as models for congenital retinal disorders. *Exp. Eye Res.* 81:503-512.
- Favor, J. (1983): A comparison of the dominant cataract and recessive specific-locus mutation rates induced by treatment of male mice with ethylnitrosourea. *Mutation Research* 110: 367-382.
- Graw J. (2003): The genetic and molecular basis of congenital eye defects. *Nat. Rev. Genet.* 4: 876-888.
- Johnson G.J. and A. Foster (2003): Prevalence, incidence and distribution of visual impairment. In: G.J. Johnson, D.C. Minassian, R.A. Weale, S.K. West (eds.): *The epidemiology of the eye disease*. Arnold, London, UK, pp. 3-28.
- Puk O., Dalke C., Favor J., Hrabé de Angelis M. and J. Graw (2006): Variations of eye size parameters among different strains of mice. *Mamm. Genome* 17: 851-857.
- Rivolta C., D. Sharon, M. Hrabé de Angelis and T.P. Dryja (2002): Retinitis pigmentosa and allied diseases: numerous diseases, genes, and inheritance patterns. *Hum. Mol. Genet.* 11: 1219-1227.
- Schmucker C., F. Schaeffel (2004): In vivo biometry in the mouse eye with low coherence interferometry. *Vision Res.* 44, 2445-2456.
- Stone E.M., V.C. Sheffield and G.S. Hageman (2001): Molecular genetics of age-related macular degeneration. *Hum. Mol. Genet.* 10: 2285-2292.

Abbreviations

n.s.	not significant
NAD	no abnormality detected

Table 15: Axial eye lengthMean \pm standard error

Parameter	Control (A)			Mutant (B)			A-B	A-B
	Male	Female		Male	Female		Male	Female
	(n=15)	(n=10)	<i>p</i> -value	(n=14)	(n=10)	<i>p</i> -value	<i>p</i> -value	<i>p</i> -value
Axial length [mm]	3.476 \pm 0.013	3.494 \pm 0.012	n.s.	3.480 \pm 0.011	3.519 \pm 0.007	<0.01	n.s.	n.s.
Axial length / body length	0.039 \pm 0.0003	0.041 \pm 0.0001	<0.001	0.040 \pm 0.0005	0.043 \pm 0.0002	<0.001	<0.01	<0.001

Table 16: Results from Funduscopy

Genotype	NAD	few white dots or streaks (unilateral)	less vessels (unilateral)	microphthalmia / anophthalmia (unilateral)	enlarged optic disc (unilateral)
male +/+ (n=15)	13	1	-	1	-
female +/+ (n=10)	10	-	-	-	-
male -/- (n=15)	11	2	1	-	1
female -/- (n=10)	10	-	-	-	-

Table 17: Results from Slit Lamp Biomicroscopy

Genotype	NAD	iris abnormality (unilateral)	zonular opacity (bilateral)	microphthalmia / anophthalmia (unilateral)
male +/+ (n=15)	14	1	-	1
female +/+ (n=10)	9	-	-	-
male -/- (n=15)	14	1	-	1
female -/- (n=10)	10	-	-	-

3.5 Clinical Chemistry and Hematology

3.5.1 Summary

The aim of the Clinical-Chemical Screen is the detection of hematological changes, defects of various organ systems, and changes in metabolic pathways and electrolyte homeostasis by means of suitable laboratory diagnostic tools. Since most inherited metabolic disorders are known to lead directly or indirectly, via altered organ functions, to changes in the parameters investigated, this screening process provides a comprehensive investigation of clinical phenotypes with counterparts in humans and animal species (Rathkolb *et al.*, 2000). The methods used are routine procedures, allowing the appropriate screen of large numbers of mice for a broad spectrum of clinical-chemical and hematological parameters (Champy *et al.*, 2004; Hough *et al.*, 2002).

In the primary clinical chemical screen, 24 (14 males/ 10 females) control mice and 24 (14 males/ 10 females) *Eya3*-mutant mice were analyzed. Twenty different clinical-chemical parameters were measured including various enzyme activities, as well as plasma concentrations of specific substrates and electrolytes. Additionally, we measured ten basic hematological parameters.

We only detected the normal sex-related differences, but no genotype effect on clinical chemical or hematological parameters. Therefore we can state that the mutation does not seem to have major effects on the metabolic pathways and organ functions investigated or the regulation of hematopoiesis.

3.5.2 Mice

Fourteen 12-week-old wild-type control males and 14 mutant males entered the clinical-chemical screen at the beginning of the 49th calendar week 2006. Ten 13-week-old control females and 10 mutant females entered the clinical-chemical screen one week later.

3.5.3 Materials and Methods

Blood Withdrawal and Storage

The Clinical-Chemical Screen of the German Mouse Clinic analyzed the mice at 13 weeks of age. A blood sample was taken from an isoflurane-anesthetized mouse by puncturing the retro-orbital sinus with a non-heparinized capillary (0.8 mm in diameter; Laborteam K&K; Munich, Germany; Art.No. 1.28.13.1.2). The time for sample taking was recorded in a work list. Blood was collected in a heparinized tube (Li-heparin, KABE; Nümbrecht, Germany; Art.No. 078028). An additional smaller sample was collected (using the same capillary) in an EDTA-coated tube (KABE, Art.No 078035). Each tube was immediately inverted five times to achieve a homogeneous distribution of the anticoagulant.

The Li-heparin-coated tubes were stored in a rack at room temperature for two hours. Afterwards, cells and plasma were separated by a centrifugation step (10 min, 4656 x g; Biofuge, Heraeus; Hanau, Germany). Plasma was distributed between the Immunology Screen (30 µl), the Allergy Screen

(30 µl), the Clinical Chemical Screen (130 µl) and the Steroid Screen (residual), while the cell pellet was given to the Immunology Screen for FACS-analysis. The plasma sample for the clinical chemical analysis was transferred into an Eppendorf tube and diluted 1:2 with aqua dest. The solution was mixed for a few seconds (Vortex genie, Scientific Industries; New York, USA) to prevent clotting and then centrifuged again for 10 min at 4656 x g. Additionally, the Clinical Chemical Screen received the EDTA-blood sample for hematological investigations.

Clinical Chemistry

The screen was performed using an Olympus AU 400 autoanalyzer and adapted reagents from Olympus (Hamburg, Germany) and Roche (Mannheim, Germany). In the primary screen, 20 different parameters were measured including various enzyme activities, as well as plasma concentrations of specific substrates and electrolytes.

Hematology

A volume of 50 µl EDTA-blood was used to measure basic hematological parameters with a blood analyzer, which has been carefully validated for the analysis of mouse blood (ABC-Blutbild-Analyzer, Scil Animal Care Company GmbH; Viernheim, Germany). Number and size of red blood cells, white blood cells, and platelets are measured by electrical impedance and hemoglobin by spectrophotometry. Mean corpuscular volume (MCV), mean platelet volume (MPV) and red blood cell distribution width (RDW) are calculated directly from the cell volume measurements. The hematocrit (HCT) is assessed by multiplying the MCV with the red blood cell count. Mean corpuscular hemoglobin (MCH) and mean corpuscular hemoglobin concentrations (MCHC) are calculated from hemoglobin/ red blood cells count (MCH) and hemoglobin/ hematocrit (MCHC), respectively.

Second sample analysis

In a second sample, collected from a subgroup of the previously tested mice at the age of 18 weeks iron metabolism related plasma parameters as well as the hematological parameter-set was retested to check the reproducibility of findings in the white and red blood cell count obtained from the first blood sample.

Analysis of Data

Data were statistically analyzed using Excel and Sigma Stat 2.0 with the level of significance set at $p < 0.05$, by an ANOVA test on the influence of genotype and sex and subsequent pair-wise comparisons of the means by T-test.

3.5.4 Parameters

Proteins and plasma enzyme activities
Alkaline phosphatase (EC 3.1.3.1), α -Amylase (EC 3.2.1.1), Creatine kinase (EC 2.7.3.2), Aspartate-aminotransferase (AST/GOT; EC 2.6.1.1), Alanine-aminotransferase (ALT/GPT; EC 2.6.1.2), Ferritin, Transferrin, Lipase (EC 3.1.1.3), Total protein
Plasma concentrations of specific substrates
Glucose, Cholesterol, Triglycerides, Uric acid, Urea, Creatinine
Plasma concentrations of electrolytes
Potassium, Sodium, Chloride, Calcium, Inorganic phosphate
Basic hematology
White blood cell count (WBC), Red blood cell count (RBC) Hematocrit (HCT), Hemoglobin (HGB), Mean corpuscular volume (MCV), Mean corpuscular hemoglobin (MCH), Mean corpuscular hemoglobin concentration (MCHC), Red blood cell distribution width (RDW), Platelet count (PLT) and Mean platelet volume (MPV)

3.5.5 Results

Clinical Chemistry

ANOVA revealed a significant influence of the genotype on α -amylase activity with decreased levels in mutant animals (Table 18). However, the values measured were still within the physiological range of normal C57BL/6 mice. In a second test a genotype effect on transferrin levels could be observed (Table 19). However, these findings were not longer associated with changes in the red blood cell count. Sex-related differences were detected for many parameters

Hematology

The red blood cell count (RBC) was significantly decreased in mutant animals. In male mutants the platelet count (PLT) was significantly decreased whereas the mean corpuscular hemoglobin content (MCH) was increased. The hemoglobin concentration was significantly decreased in female mutants (Table 20). None of these findings could be confirmed in a second blood sample (Table 21).

Raw data for each individual are available on request in Excel sheets.

3.5.6 Discussion

Clinical Chemistry

Sex-related differences were detected for many parameters, reflecting the physiological differences, often observed in various mouse strains. Since the difference detected in α -amylase activity was quite small, the difference found in transferrin levels in the second sample was not seen in the first test, and all obtained values were situated within ranges normally found in C57BL/6 mice, we conclude that these findings are most likely findings by chance due to biological variation. An influence of the *Eya3* mutation on metabolic pathways and organ functions investigated seems to be very unlikely.

Hematology

Since none of the findings in the first test was reproducible in a second one and all obtained values were situated within ranges normally found in C57BL/6 mice, these are most likely findings by chance due to biological variation. Therefore, an influence of the *Eya3*-mutation on the regulation of hematopoiesis seems to be unlikely.

Comparison to baseline data

Almost all values for the different parameters were situated within the range normally found in C57BL/6 mice with sodium-, alkaline phosphatase- and transferrin-levels in the lower region of the physiological range (Hough *et al.*, 2002; Quimby & Loeb, 1999; Kile *et al.*, 2003; own published data). However, this might be a substrain-specific feature of the genetic background.

Increased values for CK activity are most likely an effect of the blood collection procedure, since CK activities are well known to react very sensitive to differences in mouse handling. High glucose values in some of the mice can be due to the genetic background, C57BL/6 mice have a disposition to develop diabetes.

A secondary screen is not recommended.

3.5.7 References

- Champy, M.-F., M. Selloum, L. Piard, V. Zeitler, C. Caradec, P. Chambon and J. Auwerx (2004): Mouse functional genomics requires standardization of mouse handling and housing conditions. *Mammalian Genome* 15: 768-783
- Hough T.A., P. Nolan, V. Tsipouri, A. Toye, I. Gray, M. Goldsworthy, L. Moir, R. Cox, S. Clements, P. Glenister, J. Wood, R. Selley, M. Strivens, L. Vizer, S. McCormack, J. Peters, E. Fisher, N. Spurr, S. Rastan, J. Martin, S. Brown and A. Hunter (2002): Novel phenotypes identified by plasma biochemical screening in the mouse. *Mammalian Genome* 13: 595-602

- Kile B., C.L. Mason-Garrison and M.J. Justice (2003): Sex and strain-related differences in the peripheral blood cell values of inbred mouse strains. *Mammalian Genome* 14: 81 – 85
- Klempt M, Rathkolb B, Fuchs E, Hrabé de Angelis M, Wolf E, and B. Aigner (2006): Genotype-specific environmental impact on the variance of blood values in inbred and F1 hybrid mice. *Mamm. Genome* 17(2): 93-102.
- Quimby, F. (1999): The Mouse. In: *The clinical chemistry of laboratory animals*, ed. by W. F. Loeb and F. W. Quimby. Taylor and Francis, New York, pp. 3-31
- Rathkolb B., T. Decker, E. Fuchs, D. Soewarto, C. Fella, S. Heffner, W. Pargent, R. Wanke, R. Balling, M. Hrabé de Angelis, H. J. Kolb and E. Wolf (2000): The clinical-chemical screen in the Munich ENU Mouse Mutagenesis Project: screening for clinically relevant phenotypes. *Mammalian Genome* 11: 543-546

Table 18: Clinical-chemical parameters at the age of 13 weeks.

Data are presented as mean \pm standard error of mean.

Parameter	Control (A)			Mutant (B)			A~B	A~B	A~B
	Male	Female		Male	Female		Male	Female	All
	(n=14)	(n=10)	<i>p</i> -value	(n=14)	(n=10)	<i>p</i> -value	<i>p</i> -value	<i>p</i> -value	<i>p</i> -value
Sodium [mmol/l]	151.6 \pm 0.64	145.6 \pm 0.5	p<0.001	151.7 \pm 0.35	145 \pm 0.8	p<0.001	n.s.	n.s.	n.s.
Potassium [mmol/l]	4.21 \pm 0.05	4.12 \pm 0.05	n.s.	4.34 \pm 0.04	4.22 \pm 0.05	n.s.	n.s.	n.s.	n.s.
Calcium [mmol/l]	2.4 \pm 0	2.24 \pm 0.04	p<0.01	2.4 \pm 0	2.26 \pm 0.03	p<0.01	n.s.	n.s.	n.s.
Chloride [mmol/l]	110.5 \pm 0.54	107.8 \pm 0.41	p<0.001	110.7 \pm 0.33	108.2 \pm 0.55	p<0.01	n.s.	n.s.	n.s.
Inorganic Phosphate [mmol/l]	1.56 \pm 0.06	1.5 \pm 0.04	n.s.	1.56 \pm 0.07	1.5 \pm 0.08	n.s.	n.s.	n.s.	n.s.
Total Protein [g/dl]	5.89 \pm 0.05	4.74 \pm 0.06	p<0.001	5.96 \pm 0.09	4.94 \pm 0.1	p<0.001	n.s.	n.s.	n.s.
Creatinine [mg/dl]	0.388 \pm 0.008	0.396 \pm 0.008	n.s.	0.381 \pm 0.006	0.398 \pm 0.005	n.s.	n.s.	n.s.	n.s.
Urea [mg/dl]	72.9 \pm 2.42	72.8 \pm 3.47	n.s.	68.7 \pm 2.27	70.7 \pm 2.57	n.s.	n.s.	n.s.	n.s.
Uric acid [mg/dl]	2.47 \pm 0.14	1.39 \pm 0.1	p<0.001	2.5 \pm 0.18	1.31 \pm 0.11	p<0.001	n.s.	n.s.	n.s.
Cholesterol [mg/dl]	87.3 \pm 3.26	64 \pm 3.02	p<0.001	80.5 \pm 2.46	68.6 \pm 3.47	p<0.05	n.s.	n.s.	n.s.
Triglyceride [mg/dl]	123 \pm 9.2	87 \pm 7.8	p<0.01	111 \pm 7.2	107 \pm 6.8	n.s.	n.s.	n.s.	n.s.
Creatine Kinase [U/l]	224.1 \pm 34.64	302 \pm 86.5	n.s.	329 \pm 131.75	407.4 \pm 179.21	n.s.	n.s.	n.s.	n.s.
Alanine-Amino-transferase (ALT) [U/l]	41.7 \pm 4.66	32 \pm 3.44	n.s.	45.1 \pm 5.67	39.2 \pm 8.16	n.s.	n.s.	n.s.	n.s.
Aspartate-Aminotransferase (AST) [U/l]	63.9 \pm 3.96	68.3 \pm 6.4	n.s.	69.1 \pm 9.54	78.5 \pm 14.98	n.s.	n.s.	n.s.	n.s.
Alkaline Phosphatase [U/l]	114.9 \pm 4.18	150.6 \pm 5.65	p<0.001	124.4 \pm 4.25	147.4 \pm 6.05	p<0.01	n.s.	n.s.	n.s.
α -Amylase [U/l]	2501 \pm 66.3	2298 \pm 142.9	n.s.	2320 \pm 69.1	2084 \pm 52.3	p<0.05	n.s.	n.s.	p<0.05
Glucose [mg/dl]	162.5 \pm 8.3	172.2 \pm 9	n.s.	167.3 \pm 11.3	174.4 \pm 9.9	n.s.	n.s.	n.s.	n.s.
Ferritin [ng/ml]	20.9 \pm 0.85	27.9 \pm 2.37	p<0.05	22.2 \pm 1.46	32.6 \pm 1.8	p<0.001	n.s.	n.s.	n.s.
Transferrin [mg/dl]	154.6 \pm 0.94	147.5 \pm 1.49	p<0.001	151.7 \pm 1.32	149.8 \pm 1.79	n.s.	n.s.	n.s.	n.s.
Lipase [U/l]	97.7 \pm 2.3	137.7 \pm 27.7	n.s.	99.8 \pm 5.56	103.7 \pm 11.62	n.s.	n.s.	n.s.	n.s.

Table 19: Clinical-chemical parameters at the age of 18 weeks.									
Data are presented as mean \pm standard error of mean.									
Parameter	Control (A)			Mutant (B)			A~B	A~B	A~B
	Male	Female		Male	Female		Male	Female	All
	(n=9)	(n=9)	<i>p- value</i>	(n=10)	(n=9)	<i>p-value</i>	<i>p-value</i>	<i>p-value</i>	<i>p-value</i>
Ferritin [ng/ml]	27.6 \pm 1.54	25.7 \pm 2.3	n.s.	28.9 \pm 1.2	25.2 \pm 1.53	n.s.	n.s.	n.s.	n.s.
Transferrin [mg/dl]	120.3 \pm 1.88	117.3 \pm 1.45	n.s.	113.6 \pm 1.55	115.8 \pm 1.8	n.s.	p<0.05	n.s.	p=0.02

Table 20: Hematological parameters at the age of 13 weeks.Data are presented as mean \pm standard error of mean.

Parameter	Control (A)			Mutant (B)			A~B	A~B	A~B
	Male	Female		Male	Female		Male	Female	All
	(n=14)	(n=10)	<i>p</i> -value	(n=14)	(n=10)	<i>p</i> -value	<i>p</i> -value	<i>p</i> -value	<i>p</i> -value
White blood cell count [10 ³ /μl]	8.9 \pm 0.5	6.9 \pm 0.42	p<0.01	9.2 \pm 0.51	6.4 \pm 0.29	p<0.001	n.s.	n.s.	n.s.
Red blood cell count [10 ³ /μl]	10.1 \pm 0.15	10.1 \pm 0.11	n.s.	9.7 \pm 0.2	9.7 \pm 0.14	n.s.	n.s.	p<0.05	p<0.05
Platelet count [10 ³ /μl]	931 \pm 24.1	851 \pm 33.4	n.s.	843 \pm 34.5	849 \pm 43.4	n.s.	p<0.05	n.s.	n.s.
Hemoglobin [g/dl]	15.2 \pm 0.24	15.2 \pm 0.18	n.s.	14.9 \pm 0.27	14.6 \pm 0.15	n.s.	n.s.	p<0.05	n.s.
Hematocrit [%]	48.5 \pm 0.73	48.5 \pm 0.6	n.s.	47.3 \pm 1	46.8 \pm 0.62	n.s.	n.s.	n.s.	n.s.
Mean corpuscular volume [fl]	48 \pm 0.26	48 \pm 0.37	n.s.	48.9 \pm 0.35	48.4 \pm 0.27	n.s.	n.s.	n.s.	n.s.
Mean corpuscular hemoglobin [pg]	15.1 \pm 0.1	15.1 \pm 0.13	n.s.	15.4 \pm 0.14	15.1 \pm 0.11	n.s.	p<0.05	n.s.	n.s.
Mean corpuscular hemoglobin concentration [g/dl]	31.4 \pm 0.14	31.3 \pm 0.18	n.s.	31.6 \pm 0.18	31.2 \pm 0.13	n.s.	n.s.	n.s.	n.s.
Red blood cell distribution width [% of MCV]	14.2 \pm 0.1	13.9 \pm 0.18	n.s.	14.1 \pm 0.15	14.1 \pm 0.13	n.s.	n.s.	n.s.	n.s.
Mean Platelet Volume [fl]	5.37 \pm 0.05	5.36 \pm 0.05	n.s.	5.28 \pm 0.06	5.4 \pm 0.05	n.s.	n.s.	n.s.	n.s.

Table 21: Hematological parameters at the age of 18 weeks.Data are presented as mean \pm standard error of mean.

Parameter	Control (A)			Mutant (B)			A~B	A~B	A~B
	Male	Female		Male	Female		Male	Female	All
	(n=9)	(n=9)	<i>p</i> -value	(n=10)	(n=9)	<i>p</i> -value	<i>p</i> -value	<i>p</i> -value	<i>p</i> -value
White blood cell count [10 ³ /μl]	11.7 \pm 0.77	7.5 \pm 0.43	p<0.001	11.7 \pm 0.77	8.7 \pm 0.52	p<0.01	n.s.	n.s.	n.s.
Red blood cell count [10 ³ /μl]	10.2 \pm 0.12	10.2 \pm 0.1	n.s.	10.2 \pm 0.12	10.1 \pm 0.18	n.s.	n.s.	n.s.	n.s.
Platelet count [10 ³ /μl]	870 \pm 70.6	877 \pm 33.3	n.s.	870 \pm 70.6	915 \pm 21.6	n.s.	n.s.	n.s.	n.s.
Hemoglobin [g/dl]	15.3 \pm 0.24	15.2 \pm 0.09	n.s.	15.3 \pm 0.24	14.9 \pm 0.23	n.s.	n.s.	n.s.	n.s.
Hematocrit [%]	49.6 \pm 0.82	49 \pm 0.32	n.s.	49.6 \pm 0.82	47.9 \pm 0.8	n.s.	n.s.	n.s.	n.s.
Mean corpuscular volume [fl]	48.4 \pm 0.5	47.9 \pm 0.35	n.s.	48.4 \pm 0.5	47.7 \pm 0.24	n.s.	n.s.	n.s.	n.s.
Mean corpuscular hemoglobin [pg]	15 \pm 0.15	14.8 \pm 0.11	n.s.	15 \pm 0.15	14.8 \pm 0.1	n.s.	n.s.	n.s.	n.s.
Mean corpuscular hemoglobin concentration [g/dl]	30.9 \pm 0.1	30.9 \pm 0.11	n.s.	30.9 \pm 0.1	31 \pm 0.11	n.s.	n.s.	n.s.	n.s.
Red blood cell distribution width [% of MCV]	14.6 \pm 0.17	14.6 \pm 0.19	n.s.	14.6 \pm 0.17	15 \pm 0.1	n.s.	n.s.	n.s.	n.s.
Mean Platelet Volume [fl]	5.34 \pm 0.09	5.47 \pm 0.08	n.s.	5.34 \pm 0.09	5.44 \pm 0.07	n.s.	n.s.	n.s.	n.s.

3.6 Immunology Screen

3.6.1 Summary

Mouse models have been a primary source of information for understanding the intricate mechanisms of the immune system (Blüethmann and Ohashi, 1994; Mak *et al.*, 2001; Fischer 2002; Rogner and Avner, 2003). The Immunology Screen at the GMC was set up to conduct a broad immunological phenotyping of mouse mutant lines with the intention of identifying distinct gene functions, which play key roles in the immune defenses of the organism through a complex network of cellular and soluble components (Janeway *et al.*, 2004).

Under the baseline conditions of the primary immunology screen, no significant differences between the *Eya3* mutants and their littermate controls could be revealed.

3.6.2 Mice

We analyzed 22 *Eya3*-mutant animals (10 females and 12 males) and twenty-one (10 females and 11 males) of age- and sex-matched littermate controls.

3.6.3 Material and Methods

Peripheral blood leukocytes (PBLs) were isolated from 500 μ l blood by erythrocyte lysis with NH_4Cl (0.17M) - Tris buffer (pH 7.45) directly in 96-well microtiter plates. After subsequent washing with FACS staining buffer (PBS, 0.5% BSA, 0.02% sodium azide, pH 7.45), PBLs were incubated for 20 min with Fc block (clone 2.4G2, PharMingen, San Diego, USA). Cells were then stained with fluorescence-conjugated monoclonal antibodies (PharMingen). After the antibody incubation, propidium iodide was added for the identification of dead cells.

The following main cell populations were analyzed: B cells (CD19⁺ clone 1D3), B1 B cells (CD19⁺CD5⁺, clone 53-7.3), B2 B cells (CD19⁺CD5⁻), T cells (CD3⁺, clone 145-2C11), CD4⁺ T cells (clone RM4-5), CD8⁺ T cells (CD8 α , clone 53-6.7; CD8 β , clone H35-17.2), γ/δ T cells (clone GL3), granulocytes (Gr-1⁺, clone RB6-8C5), and NK cells (CD49b⁺, clone DX5). We also analyzed additional subpopulations based on the following *Eya3* antigens: IgD (clone 11-26c.2a), B220 (clone RA3-6B2), CD11b (clone M1/70), CD103 (clone 2E7), CD25 (clone PC61), CD62L (clone MEL-14), CD45RA (clone 14.8), Ly-6C (clone AL-21), and CD44 (clone IM7). Data were acquired on a Cyan flow cytometer (DakoCytomation, USA) and were analyzed using FlowJo software (TreeStar Inc, USA). All samples were acquired until a total number of 25,000 cells was reached.

The plasma levels of IgM, IgG₁, IgG_{2a}, IgG_{2b}, IgG₃, and IgA were determined simultaneously in the same sample using a bead-based assay with monoclonal anti-mouse antibodies conjugated to beads of different color regions (Biorad, USA), and acquired on a Bioplex reader (Biorad). The presence of rheumatoid factor and anti-DNA antibodies was evaluated by indirect ELISA with rabbit IgG (Sigma-Aldrich, Steinheim, Germany) and calf thymus

DNA (Sigma-Aldrich), respectively, as antigens and AP-conjugated goat anti-mouse secondary antibody (Sigma-Aldrich). Serum samples from MRL/MpJ-Tnfrsf6^{lpr} mice (Jackson Laboratory, Bar Harbor, USA) were used as positive controls in the autoantibody assays.

3.6.4 Parameters

Flow cytometry
B cells (CD19 ⁺), B1 B cells (CD19 ⁺ CD5 ⁺), B2 B cells (CD19 ⁺ CD5 ⁻), T cells (CD3 ⁺), CD4 ⁺ T cells, CD8 ⁺ T cells, γ/δ T cells, granulocytes (Gr-1 ⁺), and NK cells (CD49b ⁺). Furthermore, all potential subpopulations which can be identified by co-staining for other surface markers (IgD, B220, CD11b, MHC II, I-A ^k , CD25, CD8 β , CD62L, CD45RA, Ly-6C, CD44) using 6 parameter/5 color flow cytometry were analyzed.
ELISA
IgM, IgG ₁ , IgG _{2a} , IgG _{2b} , IgG ₃ , IgA; anti-DNA antibodies, rheumatoid factor

3.6.5 Results and Discussion

The analysis of Eya3 mice in the primary Immunology Screen did not reveal any genotype-specific differences between mutants and their littermate controls under baseline conditions (Table 22).

3.6.6 References

- Bluethmann, H., and P. S. Ohashi (eds.) (1994): Transgenesis and targeted mutagenesis in immunology. Academic Press, San Diego.
- Fischer, A. (2002): Natural mutants of the immune system: a lot to learn! Eur J Immunol 32: 1519-1523.
- Janeway C, Travers P, Walport M, Shlomchik M and M.J. Shlomchik (2004): Immunobiology: The Immune System in Health and Disease. 6th edition, Garland Publishing, London.
- Mak, T. W., J. M. Penninger and P. S. Ohashi (2001): Knockout mice: a paradigm shift in modern immunology. Nat Rev Immunol 1: 11-19.
- Rogner, U. C., and P. Avner (2003): Congenic mice: cutting tools for complex immune disorders. Nat Rev Immunol 3: 243-252.

Table 22: Basic parameters analyzed in the Immunology Screen.Data are presented as mean \pm standard error of mean.

Parameter	Control (A)			Mutant (B)			A ~ B	
	Male	Female		Male	Female		Male	Female
	(n=11)	(n=10)	<i>p</i> - value	(n=12)	(n=10)	<i>p</i> - value	<i>p</i> - value	<i>p</i> - value
CD19⁺ [%]	57.1 \pm 1.62	51.7 \pm 1.37	p<0.05	54.7 \pm 1.7	53.2 \pm 1.35	n.s.	n.s.	n.s.
CD19⁺CD5⁻ [%]	0.82 \pm 0.08	1.03 \pm 0.11	n.s.	0.92 \pm 0.06	0.99 \pm 0.08	n.s.	n.s.	n.s.
CD11b⁺Gr1⁺⁺ [%]	5.58 \pm 0.41	6.61 \pm 0.66	n.s.	5.88 \pm 0.51	5.63 \pm 0.93	n.s.	n.s.	n.s.
CD4⁺ [%]	11.91 \pm 0.76	10.18 \pm 1.14	n.s.	14.76 \pm 0.56	14.01 \pm 0.69	n.s.	n.s.	n.s.
CD8a⁺ [%]	10.7 \pm 0.44	9.69 \pm 0.91	n.s.	12.98 \pm 0.48	12.01 \pm 0.55	n.s.	n.s.	n.s.
γ/δ TCR⁺ [%]	0.39 \pm 0.03	0.73 \pm 0.08	p<0.01	0.38 \pm 0.05	0.59 \pm 0.07	p<0.05	n.s.	n.s.
IgG₁ [μ g/ml]	383 \pm 40.1	383 \pm 41.9	n.s.	611 \pm 245.1	337 \pm 30	n.s.	n.s.	n.s.
IgG_{2a} [μ g/ml]	245.5 \pm 45.21	117 \pm 15.15	p<0.05	229.7 \pm 23.82	112.9 \pm 24.28	p<0.01	n.s.	n.s.
IgG_{2b} [μ g/ml]	831.8 \pm 61.3	338.3 \pm 28.03	p<0.001	989.5 \pm 229.97	314.2 \pm 17.68	p<0.05	n.s.	n.s.
IgG₃ [μ g/ml]	280.6 \pm 33.75	215.1 \pm 43	n.s.	310.3 \pm 40.75	243.5 \pm 27.66	n.s.	n.s.	n.s.
IgM [μ g/ml]	579.3 \pm 44.56	495 \pm 82.93	n.s.	577.7 \pm 78.28	356.5 \pm 23.5	p<0.05	n.s.	n.s.
IgA [μ g/ml]	669 \pm 90.5	459 \pm 47.8	n.s.	752 \pm 93.7	407 \pm 30.8	p<0.01	n.s.	n.s.
Anti-DNA Ab [%]	0.3 \pm 0	0.4 \pm 0	p<0.05	0.3 \pm 0	0.4 \pm 0	n.s.	n.s.	n.s.
Rheumatoid factor [%]	0.1 \pm 0.01	0.2 \pm 0.02	n.s.	0.1 \pm 0.02	0.1 \pm 0.01	n.s.	n.s.	n.s.

Raw data will be available on request.

3.7 Allergy Screen

3.7.1 Summary

The goal of the Allergy screen within the German Mouse Clinic (GMC) is to search for IgE mutants in order to establish mouse models for allergic diseases and to find new strategies for antiallergic therapy. The increased production of IgE in response to common environmental antigens is the hallmark of atopic diseases in man (Hamelmann *et al.* 1999). Mouse mutants with phenotypic alterations in IgE production represent a valuable tool to study and characterize the molecular mechanisms of IgE-mediated allergic hypersensitivity (Zhang *et al.* 1997).

In the primary allergy screen of *Eya3* mice, 24 controls and 24 mutant animals at the age of 13 weeks have been screened. Additionally, a second blood sample of 18-week-old mice has been scored. The analysis did not reveal any profound differences between mutant and control mice.

3.7.2 Mice

Two age- and sex-matched groups of 24 control (14 males, 10 females) and 24 mutant mice (14 males, 10 female) aged 13 weeks has been analyzed. Five weeks a second blood sample was taken from 18 control (nine males, nine females) and 19 mutant mice (ten males, nine female).

3.7.3 Material and Methods

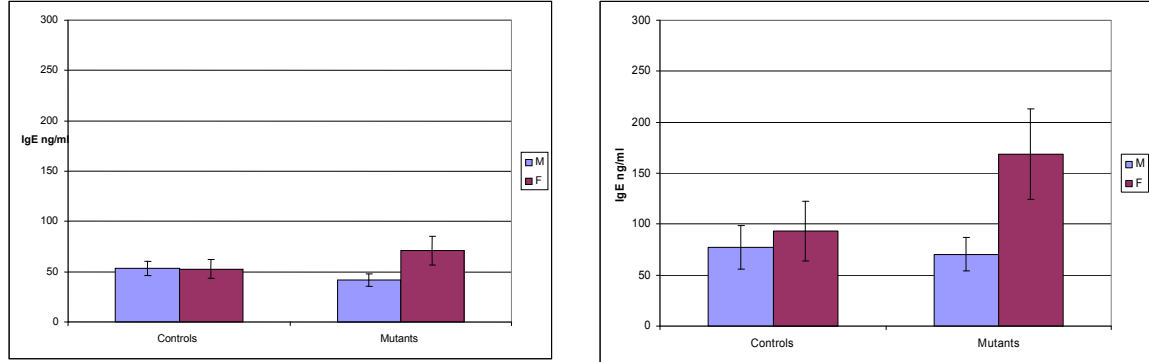
Thirteen-week-old male and female mice were screened for alterations in plasma total IgE concentrations. Blood samples were taken from animals by puncturing the retroorbital plexus under isoflurane anesthesia.

Plasma was analyzed for total IgE, using a classical immunoassay isotype-specific sandwich ELISA. In brief, microtiter plates (96-well) were coated with 10 µg/ml anti-mouse-IgE rat monoclonal IgG (clone-PC284, The Binding Site) to detect total IgE. Serum samples were diluted 1:10 and standards for murine IgE (Mouse IgE, k clone C38-2 BD Pharmingen™) were appropriately diluted. As secondary antibodies, biotinylated rat anti-mouse IgE (clone R35-118, BD Pharmingen™) were used followed by incubation with BD OptEIA Reagent Set B (Cat. No. 550534 BD Pharmingen™) Plates were analyzed using a standard micro well ELISA reader at 450 nm. Total murine IgE data are reported in ng/ml, based on a standard curve of purified murine IgE (Alessandrini *et al.*, 2001).

3.7.4 Results

The analysis of total IgE levels in plasma (mean ± SE) of *Eya3* mice revealed not statistically significant differences (Table 23 and 24). We detected higher mean IgE concentrations in female mice of both groups compared to the males. This difference was statistically significant in both groups and is a common finding for many inbred strains (Alessandrini *et al.*, 2000; Corteling *et al.*, 2004; Seymour *et al.*, 2002).

Taken together, under standard screening conditions for primary allergy screen, *Eya3*-mutant mice did not show changes in total plasma IgE levels that would reveal a major allergy phenotype.



At the age of 13 weeks

At the age of 18 weeks

Figure 7: Total plasma IgE in Eya3 mice

Table 23: Total plasma IgE in Eya3 mice (13 weeks old)								
Data are presented as mean ± standard error of mean.								
	Control (A)			Mutant (B)			A~B	A~B
	Male	Female		Male	Female		Male	Female
	(n=14)	(n=10)	<i>p</i> - value	(n=14)	(n=10)	<i>p</i> - value	<i>p</i> - value	<i>p</i> - value
Total IgE [ng/ml]	53.2± 7.4	52.4± 9.3	n.s.	41.5± 6.2	71.3± 14.2	<0.05	n.s.	n.s.

Table 24: Total plasma IgE in Eya3 mice (18 weeks old)								
Data are presented as mean ± standard error of mean.								
	Control (A)			Mutant (B)			A~B	A~B
	Male	Female		Male	Female		Male	Female
	(n=9)	(n=9)	<i>p</i> - value	(n=9)	(n=9)	<i>p</i> - value	<i>p</i> - value	<i>p</i> - value
Total IgE [ng/ml]	76.9± 21	93.3± 29	n.s.	70.4± 16	168.7 44	<0.05	n.s.	n.s.

Raw data will be available on request.

3.7.5 References

- Alessandrini, F., Jakob, T., Wolf, A., Wolf, E., Balling, R., Hrabé de Angelis, M., Ring, J., and H. Behrendt (2001): ENU mouse mutagenesis: Generation of mouse mutants with aberrant plasma IgE levels. *Int Arch Allergy Immunol* 124: 25-28
- Corteling R, Trifilieff A. (2004): Gender comparison in a murine model of allergen-driven airway Inflammation and the response to budesonide treatment *BMC Pharmacol.* 4: 4.
- Hamelmann, E., K. Takeda, A. Oshiba and E.W. Gelfand (1999): Role of IgE in the development of allergic airway inflammation and airway hyperresponsiveness – a murine model. *Allergy* 54: 297-305
- Seymour BW, Friebertshauser KE, Peake JL, Pinkerton KE, Coffman RL, Gershwin LJ. (2002): Gender differences in the allergic response of mice neonatally exposed to environmental tobacco smoke. *Dev Immunol.* 9(1): 47-54.
- Zhang, Y., W.J.E. Lamm, R.K. Albert, E.Y. Chi, W.R. Henderson and D.B. Lewis (1997): Influence of the route of allergen administration and genetic background on the murine allergic pulmonary response. *Am J Respir Crit Care Med* 155: 661-669

3.8 Nociceptive Screen

3.8.1 Summary

Pain is the perception of an aversive or unpleasant sensation that originates from a specific region of the body. The highly subjective nature of pain is one of the factors that make it difficult to define and to treat clinically. Pain is more than a conspicuous sensory experience that warns of danger.

Nociceptors are activated by tissue injury but also by mechanical, thermal, or chemical stimuli. Harmful stimuli applied to the skin or to subcutaneous tissue, activate nociceptors, the peripheral endings of primary sensory neurons whose cell bodies are located in the dorsal root or in the trigeminal ganglia.

A noxious stimulus activates the nociceptor by depolarizing the membrane of the sensory ending. When peripheral tissues are damaged, the sensation of pain in response to subsequent stimuli is enhanced. This phenomenon termed hyperalgesia, may involve a lowering of threshold of the nociceptors or an increase in the magnitude of pain evoked by supra-threshold stimuli. Hyperalgesia can occur both at the site of tissue damage (primary hyperalgesia) and in the surrounding undamaged areas (secondary hyperalgesia; Wall and Melzak, 1984). By means of different inbred mouse strains it could be demonstrated that rodents display large and heritable differences in both nociceptive and analgesic sensitivity (Mogil, 1999; Mogil *et al.*, 1999)

In the Primary Screen the responsiveness of the intact somatosensory system to thermal pain was tested in the *Eya3* mutant mouse line by means of the hot plate test (nociceptive pain). We found no significant difference in pain reactivity between the wild-type control and mutant animals. We do not recommend doing further pain-related studies in *Eya3*-mutant mice.

3.8.2 Mice

Twenty-three *Eya3*-mutant mice (14 male, nine female), and 23 control animals (14 male, nine female) were tested in our first screen.

3.8.3 Material and Methods

Hot plate test

The mice were placed on a metal surface maintained at $52 \pm 0.2^\circ\text{C}$ (Hot plate system was made by TSE GMBH, Germany; Eddy and Leimbach, 1953). Locomotion of the mouse on the hot plate was constrained by 20 cm high Plexiglas wall to a circular area with a diameter of 28 cm (Fig. 8). Mice remained on the plate until they performed one of three behaviors regarded as indicative of nociception: hind paw lick (h.p. licking), hind paw shake/flutter (h.p. shaking) or jumping.

We evaluated only hind paw but not the front paw responses, because fore paw licking and lifting are components of normal grooming behavior. Each mouse was tested only once since repeated testing leads to profound changes in response latencies. The latency was recorded to the nearest 0.1 s.

To avoid tissue injury 60 s cut-off time was used. The data values are given in seconds.

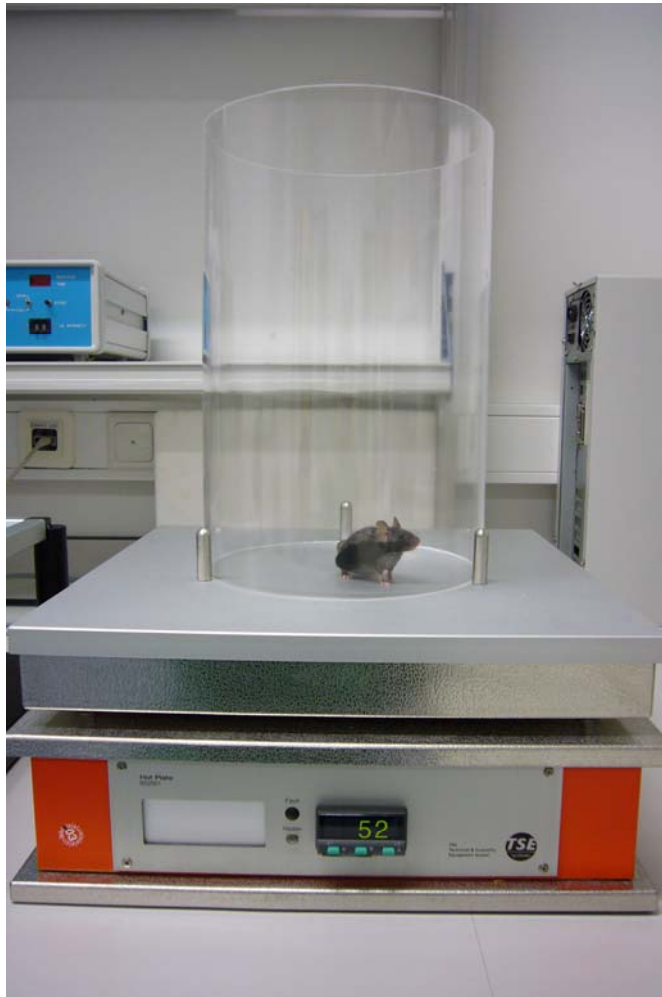


Figure 8: Hot plate system

Statistical analysis

Statistical analysis was performed using a statistical package Statgraphics® (Statistical Graphics Corporation, Rockville, MD). The differences between the groups were compared with ANOVA, LSD test was used as *post hoc*. Statistical significance was assumed at $p < 0.05$.

3.8.4 Parameters

Hind paw licking
Reaction with licking of hind paw to the thermal pain
Hind paw shaking
Reaction with shaking of hind paw to the thermal pain
Jumping
Jumping reaction to the thermal pain

3.8.5 Results and Discussion

The first nociceptive response observed in these mice was hind paw shaking, followed by hind paw licking. The latencies did not differ between mutant and control animals. The third response was jumping; again, the reaction time was not influenced by the mutation.

We do not recommend doing more pain-related studies in this mutant mouse line.

3.8.6 References

- Eddy, N.B. Leimbach, D. (1953): Synthetic analgesics II. Diethienylbutenyl and dithienylbutylamines. J. Pharmacol. Exp. Ther. 107: 385-393
- Mogil J.S. (1999): The genetic mediation of individual differences in sensitivity to pain and its inhibition. Proc. Nat. Acad. Sci. 96: 7744-7751
- Mogil J.S., S.G. Wilson, K. Bon, S.E. Lee, K. Chung, P. Raber, J.O. Pieper, H.S. Hain, J.K. Belknap, L. Hubert, G.I. Elmerl, J.M. Chung and M. Devor (1999): Heritability of nociception I: responses of 11 inbred mouse strains on 12 measures of nociception. Pain 80:67-82.
- Wall P.D. and R. Melzack (Eds.) Textbook of Pain, Churchill Livingstone, London, 1984

Abbreviations

h.p. hind paw

Table 25: Nociceptive Screen									
Data are presented as mean \pm standard error of mean.									
							ANOVA		
							genotype		sex*genotype
Parameter Latency [s]	Control (A)			Mutant (B)			A~B	A~B	ANOVA
	Male	Female		Male	Female		Male	Female	
	(n=14)	(n=9)	<i>p - value</i>	(n=14)	(n=9)	<i>p - value</i>	<i>p - value</i>	<i>p - value</i>	<i>p - value</i>
H.p. shaking	9.2 \pm 1	10.7 \pm 1.1	n.s.	12 \pm 0.9	9.9 \pm 1.1	n.s.	n.s.	n.s.	n.s.
H.p. licking	14.8 \pm 2.3	15.3 \pm 2.9	n.s.	20.1 \pm 2.3	13.2 \pm 2.9	n.s.	n.s.	n.s.	n.s.
Jumping	47.7 \pm 2.5	53.8 \pm 3.2	n.s.	45.5 \pm 2.5	50 \pm 3.2	n.s.	n.s.	n.s.	n.s.

ANOVA:

SHAKING: genotype; p = 0.340, sex; p = 0.782, genotype*sex; p = 0.085

LICKING: genotype; p = 0.569, sex p = 0.253, genotype*sex; p = 0.154

JUMPING: genotype; p = 0.304, sex p = 0.068, genotype*sex; p = 0.775

3.9 Cardiovascular Screen

3.9.1 Summary

Blood pressure (BP) analysis provides insights into functions of the vascular system including the regulation of vascular tone and left ventricular pump function. BP is strongly influenced by defects in many organ systems (heart, kidney, lung, liver) and metabolic or (neuro)endocrine pathways. Imbalances in one or, usually several organs and pathways, result in changes of this sensitive global parameter (Krege *et al.*, 1995; Lorenz, 2002; Deschepper *et al.*, 2004).

The ECG measures the electrical activity, rate and rhythm of the heart beat, supplying information about the conductive properties (function of ion channels), the excitable myocardial mass and the propagation of excitation within the heart tissue. Almost all types of cardiac pathologies will eventually cause also distinct ECG changes. Therefore, the ECG provides a comprehensive overview on cardiac function (Doevendans *et al.*, 1998; Ehmke, 2003; Royer *et al.*, 2005).

The comparison of the *Eya3*-mutant to control mice in blood pressure showed no genotype-specific differences. In the ECG analysis the mutants revealed prolongations in the PQ and JT interval and decreased QRS amplitudes. The origin of the alterations is not clear, a detailed analysis would be necessary. However, the changes are not so strong that cardiovascular function can be considered impaired.

3.9.2 Mice

The mice reached the Cardiovascular Screen at the age of 12-15 weeks, 18 female mice (nine controls, nine mutants) and 19 male mice (nine controls, ten mutants) underwent blood pressure and ECG analysis.

3.9.3 Material and Methods

Tail-cuff blood pressure measurement

Blood pressure was measured in unanesthetized mice with a non-invasive tail-cuff method using the MC4000 Blood Pressure Analysis Systems (Hatteras Instruments Inc., Cary, North Carolina, USA). Four animals were restrained on a pre-warmed metal platform in metal boxes. The tails were looped through a tail-cuff and fixed in a notch containing an optical path with a LED light and a photosensor.



Figure 9: Blood pressure set up

Platform with four measurement slots (left), mouse fixed in a tail-cuff underneath a restrainer box (right).

The blood pulse wave in the tail artery is detected as transformed into an optical pulse signal by measurement of light extinction. Pulse detection, cuff inflation and pressure evaluation are automated by the system software. After five initial inflation runs for habituation, 12 measurement runs are performed for each animal in one session. Runs with movement artifacts are excluded.

After one day of training, in which the animals are habituated to the apparatus and protocol, the measurements are performed on four consecutive days between 8:30 and 11:30 AM.

Surface limb ECG

ECG is performed in anesthetized (isoflurane/pressured air inhalation) mice by use of three metal bracelets that are put on the joints of the feet together with electrode gel. The complete setup is located in a faraday cage. The electrodes are positioned on the front-paws and the left hind-paw, resulting in the bipolar standard limb leads I, II and III and the augmented unipolar leads AVF, AVR, AVL. ECG is recorded for about seven minutes.



Figure 10: ECG-setup

Left: ECG-setup in the faraday cage; right: mouse with bracelet electrode under anesthesia.

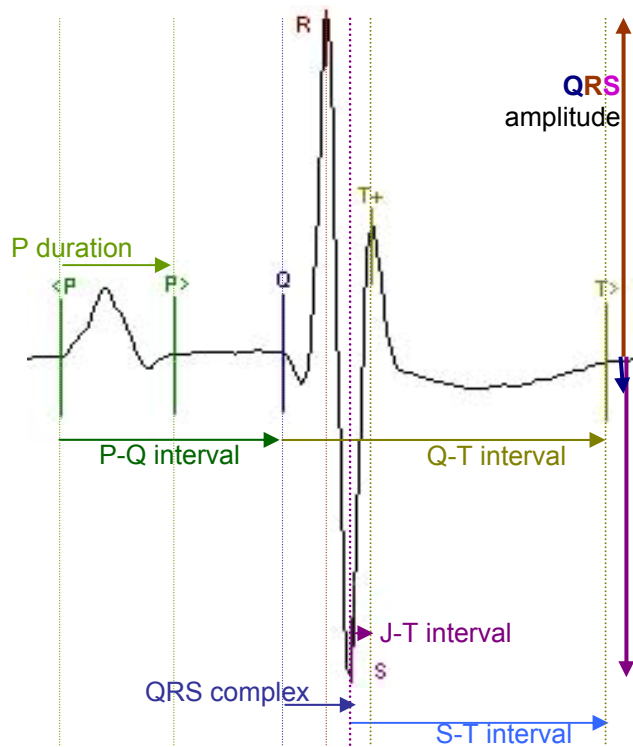


Figure 11: Example of ECG trace with analyzed parameters.

A shape analysis of the ECG traces is performed with the software ECG-auto (EMKA technologies, Paris, France). For each animal, intervals and amplitudes are evaluated from five different sets of averaged beats (usually lead II). The parameter Q-T interval is also corrected for the RR interval. In addition, the recordings are screened for arrhythmias, including supraventricular and ventricular extrasystoles and conduction blockages.

Analysis of data

For blood pressure analysis, at least 20 to 48 individual measurements are pooled to obtain a mean over the four measurement days for each animal. In the quantitative ECG analysis sets of five analyzed beats are averaged for one animal.

The data were analyzed statistically using Statistica. Analysis of variance (ANOVA) tests are used for multi-factorial analysis of sex and genotype. Post hoc analysis for multiple comparisons included a Duncan's Multiple Range Test & Critical Ranges.

3.9.4 Parameters

Blood Pressure Analysis
Systolic Pressure, Diastolic Pressure, Mean Arterial Pressure (MAP), Pulse
ECG Quantitative Analysis
PQ Interval, P-Wave Duration, QRS-Complex Duration, QT Interval, QT _{corrected} Interval, RR Interval, Heart Rate, JT Interval, ST Interval, Q Amplitude, R Amplitude, S Amplitude, QRS Amplitude
ECG Qualitative Analysis
Events of Supraventricular Extrasystoles, Ventricular Extrasystoles, AV I Blockage, AV II Blockage, AV III Blockage, AV Dissociation

3.9.5 Results

Blood pressure analysis (Table 26) revealed no genotype-specific differences between the groups.

In the **ECG** analysis (Table 27) a genotype-specific difference is found for both sexes together in the PQ interval (Fig. 12) and JT interval (Fig. 13) that are both increased in the mutants.

The **PQ interval** represents the time from onset of the electrical impulse in the sinoatrial node until conduction through the Purkinje fibers, including the depolarization of the atria. The **JT interval** reflects the transition from ventricular depolarization to ventricular repolarization.

Prolongations of these intervals can appear due to alterations in the conduction properties of the heart. Also arrhythmias such as blockages within the conduction fibers of the heart can result in a delay of electrical conduction especially of the PQ interval.

In addition, the ECG analysis revealed a decreased **QRS amplitude** of male and female mutants (Fig. 14). In humans, alterations in the QRS amplitudes can reflect a change of the electrical axis of the heart. Physiologically it occurs also with an increased vagal tone or chronic exercise training. Pathologically decreased amplitudes are found in case of adipositas or edema. However, since we perform a surface ECG, the amplitude could as well be influenced by the genotypic differences found in body size and body composition (see Dymorphology Screen, 3.2.5).

The found alterations might be of interest since mutation of the *Eya4* gene leads to dilated cardiomyopathy and heart failure (Schonberger *et al.*, 2005). Also the *Eya* genes take part in the Six-Eya-Dach regulatory network that is involved in organogenesis and muscle development (Heanue *et al.*, 1999; Li *et al.*, 2003).

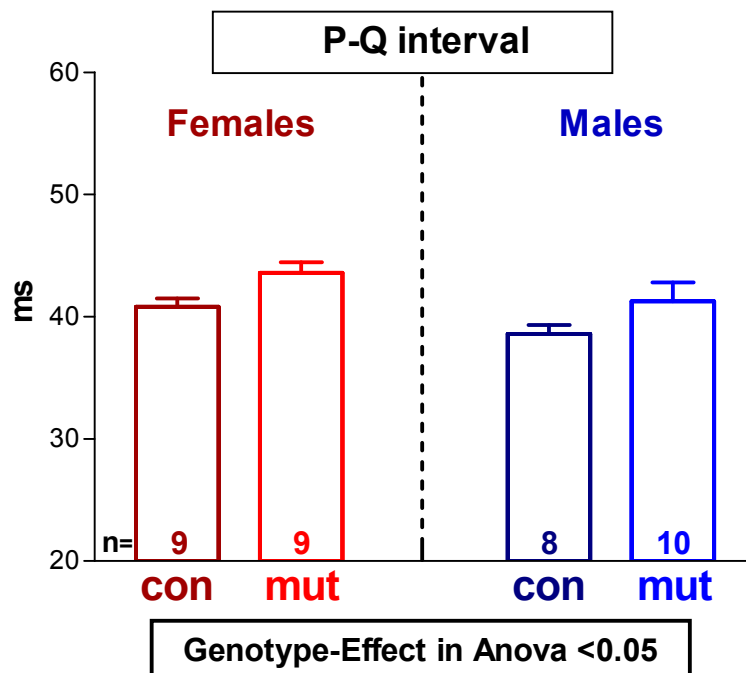


Figure 12: ECG-parameter P-Q interval

The P-Q interval was increased in the mutant mice taking both sexes together.

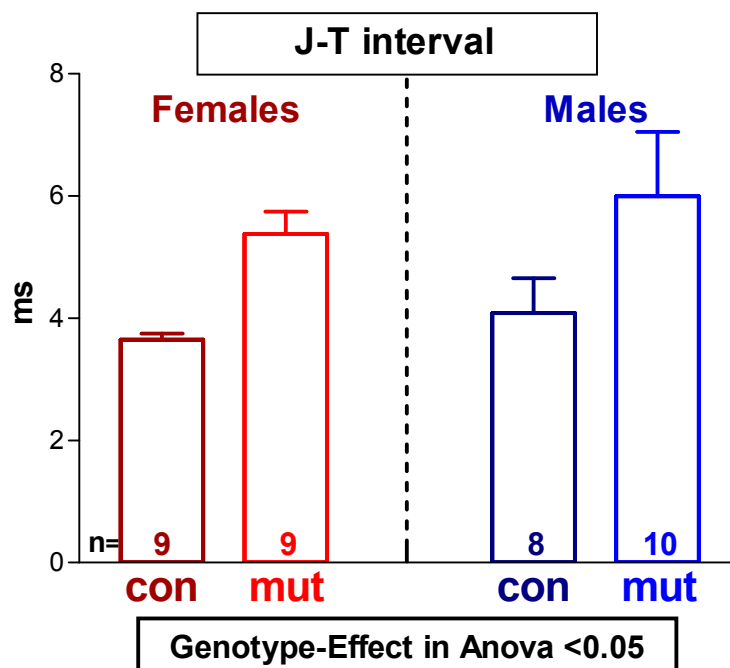


Figure 13: ECG-parameter J-T interval

The J-T interval was increased in the mutant mice taking both sexes together.

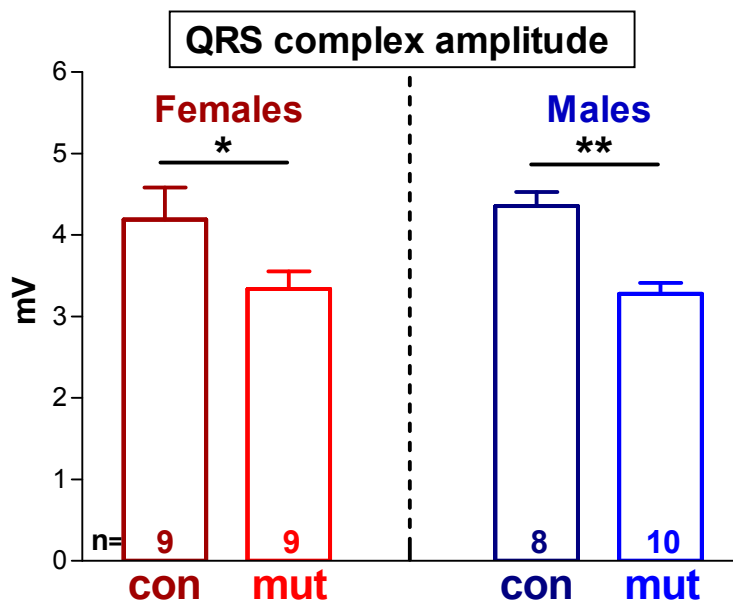


Figure 14: ECG-parameter QRS amplitude

Differences in QRS amplitude reached significance in the post hoc analysis in both sexes

In summary the mutation shows an effect on ECG parameters. The origin of the alterations is not clear, a detailed analysis would be necessary. However, the changes are not so strong that cardiovascular function can be considered impaired.

Raw data are available on request.

3.9.6 References

Deschepper CF, Olson JL, Otis M, Gallo-Payet N (2004): Characterization of blood pressure and morphological traits in cardiovascular-related organs in 13 different inbred mouse strains. *J Appl Physiol* 97:369-376.

Doevendans PA, Daemen MJ, de Muinck ED, Smits JF (1998): Cardiovascular phenotyping in mice. *Cardiovasc Res* 39:34-49.

Ehmke H (2003): Mouse gene targeting in cardiovascular physiology. *Am J Physiol Regul Integr Comp Physiol* 284:R28-30.

Heanue TA, Reshef R, Davis RJ, Mardon G, Oliver G, Tomarev S, Lassar AB, Tabin CJ (1999): Synergistic regulation of vertebrate muscle development by Dach2, Eya2, and Six1, homologs of genes required for Drosophila eye formation. *Genes Dev* 13:3231-3243.

Krege JH, Hodgin JB, Hagaman JR, Smithies O (1995): A noninvasive computerized tail-cuff system for measuring blood pressure in mice. *Hypertension* 25:1111-1115.

- Li X, Oghi KA, Zhang J, Krones A, Bush KT, Glass CK, Nigam SK, Aggarwal AK, Maas R, Rose DW, Rosenfeld MG (2003): Eya protein phosphatase activity regulates Six1-Dach-Eya transcriptional effects in mammalian organogenesis. *Nature* 426:247-254.
- Lorenz JN (2002): A practical guide to evaluating cardiovascular, renal, and pulmonary function in mice. *Am J Physiol Regul Integr Comp Physiol* 282:R1565-1582.
- Royer A, van Veen TA, Le Bouter S, Marionneau C, Griol-Charhbil V, Leoni AL, Steenman M, van Rijen HV, Demolombe S, Goddard CA, Richer C, Escoubet B, Jarry-Guichard T, Colledge WH, Gros D, de Bakker JM, Grace AA, Escande D, Charpentier F (2005): Mouse model of SCN5A-linked hereditary Lenegre's disease: age-related conduction slowing and myocardial fibrosis. *Circulation* 111:1738-1746.
- Schonberger J, Wang L, Shin JT, Kim SD, Depreux FF, Zhu H, Zon L, Pizard A, Kim JB, Macrae CA, Mungall AJ, Seidman JG, Seidman CE (2005): Mutation in the transcriptional coactivator EYA4 causes dilated cardiomyopathy and sensorineural hearing loss. *Nature Genet* 37:418-422.

Table 26: Blood Pressure Parameters

Data are presented as mean +/- standard error of mean.

Parameter	Control (A)		Mutant (B)		ANOVA			Post hoc test	
	Male	Female	Male	Female	Sex	Genotyp	Interact.	A~B Male	A~B Female
	(n = 9)	(n = 9)	(n = 10)	(n = 9)	<i>p</i> - value	<i>p</i> - value	<i>p</i> - value	<i>p</i> - value	<i>p</i> - value
Systolic pressure [mm Hg]	123.7 +/- 2.8	117.2 +/- 2.9	127.4 +/- 2.0	122.9 +/- 3.4	n.s.	n.s.	n.s.	n.a.	n.a.
Diastolic pressure [mm Hg]	109.0 +/- 2.5	102.1 +/- 3.1	107.9 +/- 3.7	105.3 +/- 3.8	n.s.	n.s.	n.s.	n.a.	n.a.
Mean arterial pressure [mm Hg]	113.5 +/- 2.5	106.8 +/- 2.9	114.1 +/- 2.9	110.9 +/- 3.6	n.s.	n.s.	n.s.	n.a.	n.a.
Pulse [bpm]	574.1 +/- 23.0	529.8 +/- 17.9	568.4 +/- 23.0	600.8 +/- 18.3	n.s.	n.s.	n.s.	n.a.	n.a.

Abbreviations

SVES **S**upra**v**entricular **E**xtrasystoles
VES **V**entricular **E**xtrasystoles

Table 27: ECG Parameters

Data are presented as mean +/- standard error of mean.

Parameter	Control (A)						Mutant (B)						ANOVA			Post hoc test	
	Male			Female			Male			Female			Sex	Genotyp	Interact.	A~B Male	A~B Female
	(n = 8)			(n = 9)			(n = 10)			(n = 9)			p - value	p - value	p - value	p - value	p - value
PQ interval [ms]	38.6 +/- 0.7			40.8 +/- 0.7			41.3 +/- 1.6			43.6 +/- 0.9			p<0.05	p<0.05	n.s.	n.s.	n.s.
P-wave duration [ms]	20.4 +/- 0.6			20.4 +/- 0.8			20.8 +/- 0.6			21.4 +/- 0.3			n.s.	n.s.	n.s.	n.a.	n.a.
QRS-complex duration [ms]	9.6 +/- 0.2			9.6 +/- 0.2			10.0 +/- 0.2			9.8 +/- 0.3			n.s.	n.s.	n.s.	n.a.	n.a.
QT interval [ms]	46.2 +/- 1.3			41.7 +/- 0.6			45.6 +/- 2.1			42.7 +/- 0.6			p<0.05	n.s.	n.s.	n.a.	n.a.
QT _{corrected} [ms]	40.6 +/- 1.4			36.5 +/- 0.5			40.1 +/- 1.5			38.2 +/- 0.7			p<0.05	n.s.	n.s.	n.a.	n.a.
RR interval [ms]	130.6 +/- 3.8			130.9 +/- 4.1			130.1 +/- 4.9			125.2 +/- 3.7			n.s.	n.s.	n.s.	n.a.	n.a.
Heart rate [bpm]	463.7 +/- 13.5			463.4 +/- 14.2			469.1 +/- 18.6			482.7 +/- 13.3			n.s.	n.s.	n.s.	n.a.	n.a.
JT interval [ms]	4.1 +/- 0.6			3.7 +/- 0.1			6.0 +/- 1.1			5.4 +/- 0.4			n.s.	p<0.05	n.s.	n.s.	n.s.
ST interval [ms]	36.6 +/- 1.5			32.1 +/- 0.6			35.6 +/- 2.1			32.9 +/- 0.6			p<0.05	n.s.	n.s.	n.a.	n.a.
Q amplitude [mV]	0.01 +/- 0.00			0.02 +/- 0.01			0.04 +/- 0.01			0.03 +/- 0.01			n.s.	p<0.01	n.s.	p<0.01	n.s.
R amplitude [mV]	3.10 +/- 0.18			3.16 +/- 0.35			2.32 +/- 0.14			2.33 +/- 0.29			n.s.	p<0.01	n.s.	p<0.05	p<0.05
S amplitude [mV]	-1.26 +/- 0.22			-1.03 +/- 0.16			-0.95 +/- 0.14			-1.01 +/- 0.16			n.s.	n.s.	n.s.	n.a.	n.a.
QRS amplitude [mV]	4.35 +/- 0.17			4.19 +/- 0.40			3.28 +/- 0.13			3.34 +/- 0.22			n.s.	p<0.001	n.s.	p<0.01	p<0.05
Arrhythmias [# of animals]	SVES	VES	other	SVES	VES	other	SVES	VES	other	SVES	VES	other					
	1	0	1	0	0	0	0	0	1	0	0	0					
Regular [# of animals]	6			9			9			9							

3.10 Lung Function Screen

3.10.1 Summary

Neural and mechanical processes that control breathing frequency have been investigated in man for a long time (Mead, 1960; Otis *et al.*, 1959), but only with the availability of mouse inbred strains the contribution of genetic determinants to differential baseline breathing patterns could be elucidated (Tankersley *et al.*, 1997; Tankersley, 1999; Reinhard *et al.*, 2002; Reinhard *et al.*, 2005). By use of genetically engineered mice, candidate genes for human developmental disorders of breathing have been identified (Katz, 2003).

Spontaneous breathing patterns during rest and activity were studied in 15-week-old male and female mutant and wild-type control mice of the Eya3-KO mouse line.

Significant differences were detected for tidal and specific tidal volume at rest, mutants exhibit somewhat smaller values. However, none of the other parameters characterizing spontaneous breathing was affected by the mutation and adaptation from rest to activity was found to be normal in mutants. Therefore, it is unlikely that the mutation is associated with a lung phenotype.

3.10.2 Mice

Due to the low number of females, only male mutant and control mice were studied at the age of 15 weeks (Table 28). There were no significant differences between mutant and control mice in body weight. Mutant males (24.9 ± 0.8 g) were only 1.3% heavier than control males (24.6 ± 0.9 g).

3.10.3 Material and Methods

Whole Body Plethysmography

A commercially available system from Buxco[®] Electronics (Sharon, Connecticut) was used to assess breathing patterns in unrestrained animals according to the principle described by Drorbaugh and Fenn (1955). It measures the pressure changes which arise from inspiratory and expiratory temperature and humidity fluctuations during breathing (Figs. 15 and 16).

Calibration of the system allows to transform these pressure swings into flow and volume signals so that automated data analysis provides tidal volumes (TV), respiratory rates (f), minute ventilation (MV), inspiratory and expiratory times (Ti, Te), as well as peak inspiratory and peak expiratory flow rates (PIF, PEF). These data were stored online as mean values at 10 s intervals.

Measurements were always performed between 8 a.m. and 11 a.m. to account for potential diurnal variations in breathing. The system was set up in a quiet room where temperature and humidity were kept constant throughout the measurements. Before each measurement, the system was calibrated and the actual barometric pressure, temperature, and humidity were supplied to warrant adequate calculations of flow rates and volumes. After placing the

animals into the chamber, data recording was immediately started and was continued for 40 min.



Figure 15: System used at GMC to assess breathing patterns.

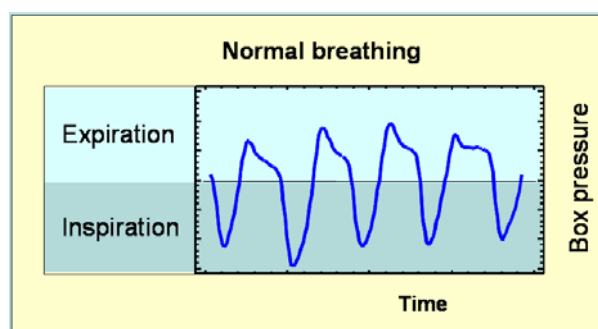


Figure 16: Recorded data used to calculate the breathing parameters.

Mice underwent typical phases during the measuring period. Primarily, the animals were stressed so that the respiratory rate was highest at the beginning. Usually after 5 min. the animals became calmer, they slightly reduced their respiratory rate, and began to explore the chamber and start cleaning themselves – *phase of activity*. Later activity was more and more interrupted by phases of rest or even short periods of snoozing – *resting phase*. Some of the animals even went to *phases of sleep*, which resulted in a further marked decrease in respiratory rate. The frequency histogram of the respiratory rates was determined for each individual, and breathing was analyzed for the above mentioned parameters during the phases of activity and rest. In addition to the directly recorded parameters, mean inspiratory and expiratory flow rates (MEF, MIF) were calculated offline from the ratio of tidal volume and the respective time interval. The relative duration of inspiration (T_i/TT) was determined from the ratio of inspiratory time to total time required for the breathing cycle. Specific tidal volumes and minute ventilations (sTV, sMV) were calculated by relating the absolute values to the body weight of the animal. Furthermore, the mean of all breathing frequencies (mean_f) measured during the 40-minute-period was calculated as a rough and ready parameter to assess whether the duration of rest and activity was similar in all mouse strains.

Statistical Analysis of Data

Statistical analyses were performed using a commercially available statistics package (Statgraphics®, Statistical Graphics Corporation, Rockville, MD). Differences between strains were evaluated by Students t-test. Statistical significance was assumed at $p < 0.05$. Data are presented as mean values \pm standard error of the mean (SEM).

3.10.4 Parameters

Directly recorded data
Tidal volumes (TV), respiratory rates (f), minute ventilation (MV), inspiratory and expiratory times (Ti, Te), as well as peak inspiratory and peak expiratory flow rates (PIF, PEF).
Calculated data
mean inspiratory flow rates (MEF), expiratory flow rates (MIF), relative duration of inspiration (Ti/TT), specific tidal volumes (sTV), minute ventilations (sMV), mean of all breathing frequencies (mean_f)

3.10.5 Results and Discussion

Tables 28 and 29 summarize the results obtained for spontaneous breathing under resting and active conditions. All parameters characterizing spontaneous breathing were similar between groups except tidal volume and specific tidal volume at rest, which were lower in mutants (see figures).

Significant differences were detected for tidal and specific tidal volume at rest. None of the other parameters characterizing spontaneous breathing was affected by the mutation and adaptation from rest to activity was found to be normal in mutants. Hence, despite the significant differences it is unlikely that the mutation is associated with a pulmonary phenotype.

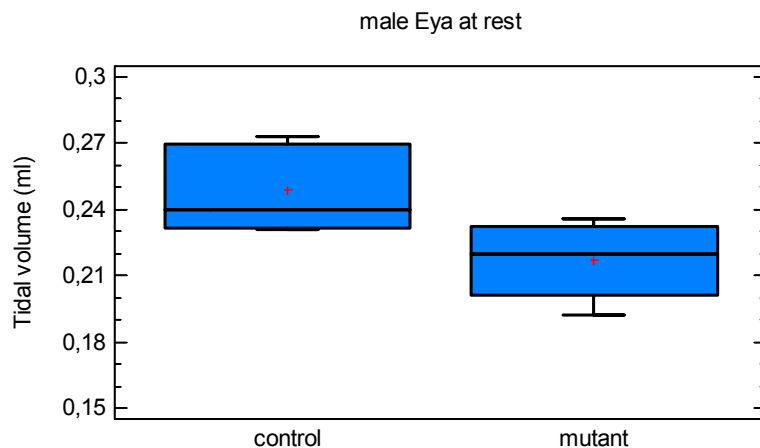


Figure 17: Tidal volume at rest

Mutant male showed a significant smaller tidal volume at rest

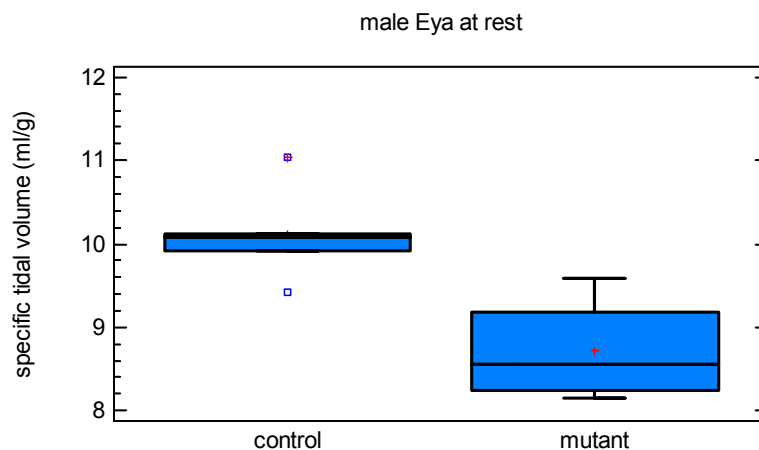


Figure 18: Specific Tidal Volume at rest

Mutant male showed a significant smaller specific tidal volume at rest

3.10.6 References

- Drorbaugh J.E. and W.O. Fenn (1955): A barometric method for measuring ventilation in newborn infants. *Pediatrics* 16: 81-87
- Katz D.M. (2003): Neuronal growth factors and development of respiratory control. *Respir. Physiol. Neurobiol.* 135: 155-165
- Mead, J. (1960): Control of respiratory frequency. *J. Appl. Physiol.* 15: 325-336
- Otis, A.B., W.O. Fenn and H. Rahn (1950): Mechanics of breathing in man. *J. Appl. Physiol.* 2: 592-607
- Reinhard C, Eder G, Fuchs H, Ziesenis A, Heyder J, Schulz H. (2002): Inbred strain variation in lung function. *Mammalian Genome* 13: 429-437
- Reinhard C, Meyer B, Fuchs H, Stoeger T, Eder G, Ruschendorf F, Heyder J, Nurnberg P, Hrabé de Angelis M, Schulz H. (2005): Genomewide linkage analysis identifies novel genetic loci for lung function in mice. *Am J Respir Crit Care Med.* 171(8): 880-8.
- Tankersley, C.G. (1999): Genetic control of ventilation: What are we learning from murine models? *Current Opinion in Pulmonary Medicine* 5: 344-348
- Tankersley, C.G., Fitzgerald R.S., Levitt R.C., Mitzner W.A., Ewart S.L. and S.R. Kleeberger (1997): Genetic control of differential baseline breathing pattern. *J. Appl. Physiol.* 82: 874-81

Abbreviations

bw	body weight (g)
mean_f	mean of all respiratory rates (1/min)
f	respiratory rate (1/min)
TV	tidal volume (ml)
sTV	specific tidal volume ($\mu\text{l/g}$)
MV	minute ventilation (ml/min)
sMV	specific ventilation (ml/min/g)
Ti	inspiratory time (ms)
Te	expiratory time (ms)
Ti/TT	relative duration of inspiration
PIF	peak inspiratory flow rate (ml/s)
PEF	peak expiratory flow rate (ml/s)
MIF	mean inspiratory flow rate (ml/s)
MEF	mean expiratory flow rate (ml/s).

Table 28: Characterization of studied mice

Data are presented as mean \pm standard error of mean.

Parameter	Control (A)			Mutant (B)			A~B	A~B
	Male	Female		Male	Female		Male	Female
	(n=5)	(n=0)	<i>p - value</i>	(n=4)	(n=0)	<i>p - value</i>	<i>p - value</i>	<i>p - value</i>
Bw [g]	24.6 \pm 0.9			24.9 \pm 0.8			n.s.	
Mean_f [1/min]	403.8 \pm 7.8			431.6 \pm 28.1			n.s.	

Table 29: Spontaneous breathing pattern during rest and activity of male Eya3 mice
Data are presented as mean \pm standard error of mean.

Parameter	Control (A)	Mutant (B)	<i>p</i> - value
	(n=5)	(n=4)	
Rest			
f [1/min]	302.2 \pm 9.3	342.6 \pm 19.1	n.s.
TV [ml]	0.25 \pm 0.01	0.22 \pm 0.01	< 0.05
sTV [μ l/g]	10.1 \pm 0.3	8.7 \pm 0.3	< 0.02
MV [ml/min]	72.7 \pm 3.5	71.0 \pm 1.6	n.s.
sMV [ml/min/g]	3.0 \pm 0.1	2.9 \pm 0.1	n.s.
Ti [ms]	59.9 \pm 3.0	53.8 \pm 2.5	n.s.
Te [ms]	139.4 \pm 3.3	123.0 \pm 7.7	n.s.
Ti/TT	0.30 \pm 0.01	0.30 \pm 0.01	n.s.
PIF [ml/s]	7.3 \pm 0.4	7.0 \pm 0.1	n.s.
PEF [ml/s]	3.5 \pm 0.2	3.8 \pm 0.1	n.s.
MIF [ml/s]	4.2 \pm 0.2	4.0 \pm 0.0	n.s.
MEF [ml/s]	1.8 \pm 0.1	1.8 \pm 0.1	n.s.
Activity			
f [1/min]	470.1 \pm 8.2	493.2 \pm 12.2	n.s.
TV [ml]	0.24 \pm 0.01	0.22 \pm 0.01	n.s.
sTV [μ l/g]	9.8 \pm 0.4	8.9 \pm 0.3	n.s.
MV [ml/min]	111.6 \pm 4.9	107.4 \pm 3.4	n.s.
sMV [ml/min/g]	4.5 \pm 0.2	4.3 \pm 0.2	n.s.
Ti [ms]	42.2 \pm 0.8	41.3 \pm 0.9	n.s.
Te [ms]	85.6 \pm 1.8	80.6 \pm 2.4	n.s.
Ti/TT	0.33 \pm 0.00	0.34 \pm 0.00	n.s.
PIF [ml/s]	9.5 \pm 0.5	8.9 \pm 0.2	n.s.
PEF [ml/s]	5.5 \pm 0.3	5.4 \pm 0.2	n.s.
MIF [ml/s]	5.7 \pm 0.3	5.3 \pm 0.1	n.s.
MEF [ml/s]	2.8 \pm 0.1	2.7 \pm 0.1	n.s.

3.11 Molecular Phenotyping

3.11.1 Introduction

Comparative genome-wide expression profiling is a powerful tool in the effort to annotate the mouse genome with biological function. The analysis of RNA expression data of mouse lines might support the understanding of the molecular biology of such mutants and provide new insights into mammalian gene function. We demonstrated the feasibility to detect transcriptional affected organs employing RNA expression profiling as a tool for molecular phenotyping (Seltmann *et al*, 2005).

In this report, we describe the results of using close to genome-wide 21K cDNA microarrays for the RNA expression profiling of **heart, muscle** and **brain** of four animals of the *Eya3* mutant mouse line. In total 24 chip hybridizations including biological and experimental replicates were performed.

The data analysis and various statistical methods detected several genes differentially regulated between mutant and reference tissues in heart and brain. In muscle no differences in expression levels between mutant and control mice have been detected. Several of the significantly expressed genes in spleen and thymus are associated with protein synthesis, synaptic vesicle exocytosis or they are expressed in different neuronal cell types.

3.11.2 Methods and Materials

Organ Collection

The molecular phenotyping screen archives organs of mutant mice for subsequent DNA-chip expression profiling analysis. Nine male mice of the *Eya3* mutant mouse line were provided to the molecular phenotyping screen.

Mouse ID	Strain	Sex	Genotype	Date of Collection
30053653	Eya3	m	+/+	15.12.2007
30053655	Eya3	m	-/-	15.12.2007
30053656	Eya3	m	+/+	15.12.2007
30053657	Eya3	m	-/-	15.12.2007
30053667	Eya3	m	+/+	15.12.2007
30053668	Eya3	m	+/+	15.12.2007
30053669	Eya3	m	-/-	15.12.2007
30053670	Eya3	m	+/+	15.12.2007
30053671	Eya3	m	-/-	15.12.2007

Organs were collected at the age of 81-96 days. To minimize the influence of circadian rhythm on gene expression, mice were killed between 9 am and

12 am by carbon dioxide asphyxiation. The following 10 organs were collected and archived in liquid nitrogen following our established SOPs (Standard operation protocols): spleen, kidney, testis, liver, heart, lung, thymus, skin/cartilage (outer ear), skeletal muscle and brain. Organs were immediately frozen and stored in liquid nitrogen until isolation of total RNA. The 108 organ samples collected either may be used for further expression profiling analysis in the GMC or, alternatively may be transferred to the collaborator.

Isolation of total RNA

Total RNA was isolated just before processing for expression profiling. For preparation of total RNA individual organs were thawed in buffer containing chaotropic salt (RLT buffer, Qiagen) and homogenized using a Polytron homogenizer. Total RNA from individual samples was obtained according to manufacturer's protocols using RNeasy Midi kits (Qiagen). The concentration was calculated from OD_{260/280} measurement and 2- μ g-RNA aliquots were run on a formaldehyde agarose gel to check for RNA integrity. The RNA was stored at -80°C in RNase free water (Qiagen).

Chip Hybridization

Depending on the amount of RNA available for hybridization, in general two chip hybridizations were performed with RNA from all selected organs of each individual mutant mouse. Each chip hybridization was performed against the identical pool of the same organ of reference RNAs (reference RNA pool). For each individual mutant mouse the chip experiments include a color-flip experiment (in total 10 hybridizations).

Reverse Transcription and Fluorescent Labeling

For labeling 15 μ g of total RNA were used for reverse transcription and indirectly labeled with Cy3 or Cy5 fluorescent dye according the TIGR protocol (Hegde *et al.*, 2000). Labeled cDNA was dissolved in 50 μ l hybridization buffer (6x SSC, 0.5% SDS, 5x Denhardt's solution and 50% formamide) and mixed with 50 μ l of reference cDNA solution (pool from six control animals) labeled with the second dye. This hybridization mixture was injected on a pre-hybridized microarray in a HS4800 Hybstation (Tecan) and incubated at 42°C for 16 hours. After hybridization slides were washed with 3x SSC, 1x SSC, 0.5xSSC and 0.1x SSC at room temperature. Slides were dried with nitrogen. Dried slides were scanned with a GenePix 4000A microarray scanner and the images were analyzed using the GenePix Pro6.0 image processing software (Axon Instruments, USA) (Drobyshev *et al.*, 2003; Seltmann *et al.*, 2005; Greenwood *et al.*, 2005; Mijalski *et al.*, 2005; Frey *et al.*, 2007).

Significance of Regulation

TIGR software package for Microarray analysis (TM4; Chu *et al.*, 2002, Saeed *et al.*, 2003) was used for normalization (MIDAS: Microarray Data Analysis System; Quackenbush 2002) and identification of genes with significant differential regulation (SAM, Significance Analysis of Microarrays; Tusher *et al.*, 2001). Expression data were normalized performing a total intensity normalization to transform the mean log₂ ratio to zero. To eliminate low-quality array elements several filtering methods were applied. They include: Background

checking for both channel with a signal/noise threshold of 2.0, one bad tolerance policy parameter and flip dye consistency checking (Yang *et al.*, 2002).

SAM was used to identify genes with statistically significant changes in expression. Genes were ranked according to their relative difference value $d(i)$, a score assigned to each gene on the basis of change in gene expression levels relative to the standard deviation. Genes with $d(i)$ values greater than a threshold were selected as significantly differentially expressed. The percentage of such genes identified by chance is the false discovery rate (FDR). To estimate the FDR, nonsense genes were identified by calculating permutations of the measurements. The selection of the top differentially expressed genes with reproducible up- or down-regulation includes less than 10% false positives (FDR).

BiblioSphere Pathway analysis

To select pathways relevant for the selected genes of an organ we used the BiblioSphere Pathway Edition/Genomatix (Scherf *et al.*, 2005). This software allows a view on our data, integrated in biological networks according to co-citation levels: a) Two genes are co-cited within abstracts, b) two genes are co-cited in one sentence and c) two genes are co-cited restricted to sentences with a function word. In a further analysis significant regulated genes were filtered for two categories of Gene Ontology terms (Biological Processes and Molecular Functions). A GOFilter consists of a hierarchy of terms and the corresponding annotations for the BiblioSphere analysis. A statistical analysis is also performed based on the number of observed and expected annotations of each term. The z-score of the GO-terms indicates whether a certain annotation or group of annotations is over- or underrepresented in a dataset of genes.

3.11.3 Results

Selection of Organs and RNA isolation

Heart, muscle and brain were selected as organs for expression profiling analysis. We isolated total RNA of these organs of four mutant mice and five wild-type control individuals (Table 31).

Table 31: Amount of total RNA [μg] isolated from heart, thymus, and brain			
Mouse ID	Heart	Muscle	Brain
30053653	112	147	360
30053655	145	156	347
30053656	119	174	336
30053657	123	198	404
30053667	155	175	364
30053668	101	115	223
30053669	160	97	332
30053670	118	181	372
30053671	124	266	334

Chip experiments

Eight hybridizations were performed for each selected organ (in total 24 chip experiments).

Gene regulation in Muscle

No differences in expression levels between wild-type control and mutant tissue were identified in muscle of all analyzed animals.

Gene regulation in Heart

Table 32 summarizes the results of eight chip hybridizations performed with RNA from heart.

In total 17 significantly regulated genes were identified. These top ranked genes with $d(i) > 0.5$ are reproducibly differentially expressed on all microarray experiments of four mutant individuals. The estimated number of falsely significant genes was calculated for 1000 permutations, yielding a FDR of 0% for this data set.

Table 32: Heat plots of gene expression profiles from eight DNA microarray experiments of *Eya3*-mutant out versus control mice.

One dye-flip pair represents two experimental replicates of each analyzed animal. One Array TAG ID is the unique probe identifier from the Lion Bioscience clone set. Official gene symbols are given. The scale bar encodes the log ratio of the fold induction; 0% of the elements are above the upper limit of the color range selection (red is up-regulated and green down-regulation in mutant mice).

Mean ratio	-1.0	0.0	1.0	ArrayTAG ID	Gene symbol	Comment
-3.46	655	657	659	671	MG-4-145j12	Hba-a1 Hemoglobin alpha, adult chain 1
-3.30					MG-68-14317	CR518113
-2.67					MG-14-3i19	Pgm2 Phosphoglucomutase 2
-2.64					MG-13-32i8	Rbms2 RNA binding motif, interacting protein 2
-2.59					MG-4-146i20	Clptm1 Cleft lip-associated transmembrane 1
-2.58					MG-13-32k20	Ankrd1 Ankyrin repeat domain 1
-2.57					MG-8-17b4	Tnnc1 Troponin C
-2.46					MG-8-86g2	1110017116Rik
-2.35					MG-8-64o9	Calm3 Calmodulin 3
-2.22					MG-8-42b9	H3f3a H3 histone, family 3A
-2.21					MG-4-6d16	Tap1 Transporter 1, ATP-binding cassette
-2.19					MG-4-5j21	Il6st Interleukin 6 signal transducer
-2.18					MG-8-71j2	Nup155 Nucleoporin 155
-2.16					MG-6-19n14	Abr Active BCR-related gene
-2.15					MG-3-37d17	Hspb7 Heat shock protein family, member 7
-2.15					MG-4-148e3	Hba-a1 Hemoglobin alpha, adult chain 1
-2.11					MG-47-1h17	Hbb-bh1 Hemoglobin Z, beta-like embryonic chain

Classification by molecular functions and biological processes

In a further analysis significantly regulated genes in heart are filtered for two categories of Gene Ontology Terms (Molecular Functions and Biological Processes) using the GOFilter Structure of the BiblioSphere Pathway Edition. The z-score of the GO-terms indicates whether a certain annotation or group of annotations is over- or underrepresented in the dataset of genes. No overrepresentation of the two categories was found for genes regulated in heart.

Gene regulation in Brain

Table 35 summarizes the results of eight chip hybridizations performed with RNA from brain.

In total 93 significantly regulated genes were identified. These top ranked genes with $d(i) > 0.5$ are reproducibly differentially expressed on all microarray experiments of four mutant individuals. The estimated number of falsely significant genes was calculated for 1000 permutations, yielding a FDR of 0% for this data set.

Classification by molecular functions and biological processes

In a further analysis significantly regulated genes in brain are filtered for categories of Gene Ontology Terms (Molecular Functions and Biological Processes) using the GOFilter Structure of the BiblioSphere Pathway Edition. The z-score of the GO-terms indicates whether a certain annotation or group of annotations is over- or underrepresented in the dataset of genes (Tables 33 and 34).

Table 33: Gene Ontology terms

Molecular functions overrepresented in genes differentially regulated in heart.

Term	Genes	Z-Score
structural constituent of cytoskeleton	<i>Actr3, Actg1, Krt16, Tuba1b</i>	5.79
structural constituent of ribosome	<i>Rpsa, Rpl14, Rpl4, Pps15, Uba52</i>	5.73

Table 34: Gene Ontology terms:

Biological processes overrepresented in genes differentially regulated in heart.

Term	Genes	Z-Score
macromolecule biosynthetic process	<i>Rpsa, Rpl14, Rpl4, Rps15, Uba52</i>	14.34

Table 35: Heat plots of gene expression profiles from eight DNA microarray experiments of *Eya3*-mutant versus control mice.

One dye-flip pair represents two experimental replicates of each analyzed animal. One Array TAG ID is the unique probe identifier from the Lion Bioscience clone set. Official gene symbols are given. The scale bar encodes the log ratio of the fold induction; 0% of the elements are above the upper limit of the color range selection (red is up-regulated and green down-regulation in mutant mice).

Mean ratio	-1.0 0.0 1.0				ArrayTAG ID	Gene symbol	Comment
	655	657	669	671			
3.72					MG-3-169b8	Rbm11	RNA binding motif protein 11
3.73					MG-3-52a20	Ap1gbp1	AP1 gamma subunit binding protein 1
3.99					MG-8-117f2	Commdd3	COMM domain containing 3
4.22					MG-8-1m3	Ass1	Argininosuccinate synthetase 1
4.33					MG-3-23c1	Jub	Ajuba
4.44					MG-6-29i19	Odz4	Odd Oz/ten-m homolog 4
4.49					MG-6-92i20	Ugcg11	UDP-glucose ceramide glucosyltransferase-like 1
4.62					MG-6-28n4	CR515399	
4.67					MG-8-117d3	Hdlbp	High density lipoprotein (HDL) binding protein
4.81					MG-14-129o10	BX638808	
5.07					MG-8-117j15	Pdlim4	PDZ and LIM domain 4
6.60					MG-8-117d11	Glul	glutamate-ammonia ligase
7.38					MG-8-118g23	CR522214	
-5.64					MG-4-86f7	Hb2-a2	hemoglobin alpha, adult chain 2
-4.86					MG-15-96a15	Gorasp1	golgi reassembly stacking protein 1
-4.56					MG-4-3k1	Hba-a1	Hemoglobin alpha, adult chain 1
-4.48					MG-4-148e12	Hba-2a	hemoglobin alpha, adult chain 2
-4.40					MG-3-12j20	Ubc	Ubiquitin C
-4.24					MG-13-3c23	Rbm3	RNA binding motif protein 3
-4.22					MG-3-25i14	Sparc	Secreted acidic cysteine rich glycoprotein
-4.20					MG-6-25k12	Atp2b2	ATPase, Ca++ transporting, plasma membrane 2
-4.11					MG-4-146e19	Cdca8	Cell division cycle associated 8
-4.07					MG-4-145f7	Scl43a2	solute carrier family 43, member 2
-3.96					MG-4-148e3	Hba-a1	Hemoglobin alpha, adult chain 1
-3.86					MG-6-3d7	Wdr22	WD repeat domain 22
-3.84					Fbxo32	Fbxo32	F-box only protein 32
-3.78					MG-4-4h13	Grrp1	glycine/arginine rich protein 1
-3.73					MG-8-13m24	Eef2	Eukaryotic translation elongation factor 2
-3.73					MG-8-86g2	1110017116Rik	
-3.72					MG-15-136d2	Hps6	Hermansky-Pudlak syndrome 6
-3.71					MG-15-214i1	Rhob	Ras homolog gene family, member B
-3.66					MG-8-40d4	Hba-a1	Hemoglobin alpha, adult chain 1
-3.65					MG-12-228k24	Eif3s8	Eukaryotic translation initiation factor 3, subunit 8
-3.64					MG-12-147c15	Lamr1	Laminin receptor 1
-3.61					MG-4-3k8	1300018I05Rik	
-3.61					MG-4-147o3	Hba-a1	Hemoglobin alpha, adult chain 1
-3.59					MG-4-2e20	Hba-a1	Hemoglobin alpha, adult chain 1
-3.52					MG-16-239p7	Actr3	ARP3 actin-related protein 3 homolog
-3.49					MG-11-1e9	Ttr	Transthyretin
-3.48					MG-13-4p13	Rps15	Ribosomal protein S15
-3.46					MG-14-107i21	Apg12l	Autophagy 12-like
-3.44					MG-8-51k21	Krt1-16	Keratin complex 1, acidic, gene 16
-3.43					MG-3-69i14	Mkrn1	Makorin, ring finger protein, 1
-3.42					MG-4-145i14	Actr3	ARP3 actin-related protein 3 homolog
-3.36					MG-15-131g17	Sparcl1	SPARC-like 1
-3.32					MG-6-70o16	Ncald	Neurocalcin delta

-3.31		MG-6-47j7	Kcna1	Potassium voltage-gated channel
-3.28		MG-3-136g8	Actg1	actin, gamma, cytoplasmic 1
-3.28		MG-3-45k11	H3f3b	H3 histone, family 3B
-3.26		MG-16-235h23	Sfrs5	Splicing factor, arginine/serine-rich 5
-3.25		MG-14-103c17	Crhr1	Corticotropin releasing hormone receptor 1
-3.23		Fos	Fos	FBJ osteosarcoma related oncogene
-3.20		MG-8-35o20	Rpl4	Ribosomal protein L4
-3.20		MG-4-145j12	Hba-a1	Hemoglobin alpha, adult chain 1
-3.18		MG-14-129I18	Ier3ip1	immediate early response 3 interacting protein 1
-3.18		MG-6-23e8	6720456B07Rik	
-3.18		MG-6-4f14	Uba52	Ubiquitin A-52 residue ribosomal protein product 1
-3.17		MG-26-276o2	Aldoa	Aldolase 1, A isoform
-3.17		Serpine1	Serpine1	serine peptidase inhibitor, clade E, member 1
-3.16		MG-3-102p7	Eif4a2	Eukaryotic translation initiation factor 4A2
-3.16		MG-14-29j24	Ubl5	Ubiquitin-like 5
-3.16		MG-8-118i19	Got2	Glutamate oxaloacetate transaminase 2
-3.14		Adcyap1r1	Adcyap1r1	Adenylate cyclase activating polypeptide 1
-3.13		MG-6-26k12	Slc29a1	Solute carrier family 29, member 1
-3.13		MG-16-78n13	Fkbp1a	FK506 binding protein 1a
-3.12		MG-14-39I16	Adra2a	Adrenergic receptor, alpha 2a
-3.11		MG-4-146d10	Tysnd1	Trypsin domain containing 1
-3.10		MG-3-45c6	Nsg1	Neuron specific gene family member 1
-3.07		MG-6-23g12	Vamp2	Vesicle-associated membrane protein 2
-3.07		MG-15-133g11	Pgrmc1	Progesterone receptor membrane component 1
-3.06		MG-6-30h12	Gnaq	Guanine nucleotide binding protein, alpha q
-3.04		MG-6-3o4	Fbxw7	F-box and WD-40 domain protein 7
-3.04		MG-3-92f15	BC031181	
-3.03		MG-14-62p24	Cyfp2	cytoplasmic FMR1 interacting protein 2
-3.03		MG-6-4a18	Mt3	Metallothionein 3
-3.01		MG-6-65c15	Oxct1	3-oxoacid CoA transferase 1
-3.00		MG-8-56a10	Tmem15	Transmembrane protein 15
-2.97		MG-4-146n10	BX639812	
-2.97		MG-6-2d7	Fkbp3	FK506 binding protein 3
-2.96		MG-6-49n24	Slc6a7	Solute carrier family 6, member 7
-2.96		Birc4	Birc4	Baculoviral IAP repeat-containing 4
-2.95		MG-8-68o23	Sca10	Spinocerebellar ataxia 10 homolog
-2.94		MG-6-3o20	Syt1	Synaptotagmin 1
-2.94		MG-3-14d5	Eef1a1	Eukaryotic translation elongation factor 1 alpha 1
-2.94		MG-16-41a6	Tuba2	Tubulin, alpha 2
-2.91		MG-16-113k22	Rpl14	Ribosomal protein L14
-2.91		Il7r	Il7r	interleukin 7 receptor
-2.90		MG-3-98g16	Stk35	Serine/threonine kinase 35
-2.90		MG-3-75o23	Tsc22d1	TSC22 domain family, member 1
-2.89		MG-6-71I24	Atp6ap1	ATPase, H+ transporting
-2.89		MG-8-71j2	Nup155	Nucleoporin 155
-2.88		MG-3-9d12	Arpp19	cAMP-regulated phosphoprotein 19
-2.87		MG-3-24p8	Cct8	Chaperonin subunit 8

3.11.4 Discussion

Significantly regulated genes were identified in heart and brain. No differences of gene expression levels were detected in muscle between mutant and wild type tissue. Several of the significantly expressed genes in spleen and thymus are associated with protein synthesis, synaptic vesicle exocytosis or they are expressed in different neuronal cell types.

Three genes (*1110017116Rik*, *Hba-a1*, *Nup155*) were significantly regulated in brain and heart. For both organs down-regulation was observed for all three genes. The differential expression of *Acrt3* in brain and *Hba-a1* in brain and heart were confirmed by up to six independent probes on the array. These different probes for identical genes show similar down-regulation. The fact, that two independent probes for the same gene show similar expression levels give additional confidence in these expression profiling data.

Our array contains a probe for the *Eya3* gene (MG-26-124e21) but in all analyzed organs no differential gene expression could be identified.

In brain only one GO-term for biological processes (macromolecule biosynthetic process) was overrepresented. For molecular functions in brain two terms were overrepresented which were annotated with structural constituent of cytoskeleton and structural constituent of ribosome. No overrepresentation of GO-terms could be identified in heart.

Table 36: Function of some of the differentially regulated genes in brain		
Gene ID	Description	PubMed ID
<i>Actg1</i>	plays a role in skeletal sarcomere assembly	15194427
<i>Adcyap1r1</i>	regulates neurogenesis and gliogenesis, role in neural/glial progenitor cells not only differentiation but also proliferation in the cortical astrocyte lineage via Ca ²⁺ -dependent signaling pathways	17115416
<i>Adra2a</i>	plays a prominent role in the postnatal development of the respiratory pattern; involved in the development of the central noradrenergic system and alterations in alpha2A AR expression may contribute to variations in fear and stress responses	11729878 12965240
<i>Arpp19</i>	an important link between NGF signaling and post-transcriptional control of neuronal gene expression	12221279
<i>Ass1</i>	role in preventing autotoxicity from nitric oxide overproduction	15192091
<i>Atp2b2</i>	localized to rod bipolar cells, horizontal cells, amacrine cells, and ganglion cells	12209837
<i>Atxn10</i>	interacts with O-linked N-acetylglucosamine in vivo and is modified by O-linked glycosylation in the insulinoma MIN6 cell line	16182253
<i>Crhr1</i>	required for a normal chromaffin cell structure and function and deletion of this gene is associated with a significant impairment of epinephrine biosynthesis	12399950
<i>Dolk</i>	catalyzes the CTP-mediated phosphorylation of dolichol in eu-	12213788

Table 36: Function of some of the differentially regulated genes in brain		
Gene ID	Description	PubMed ID
	karyotic cells	
<i>Eef2</i>	plays a key role in the essential process of protein synthesis by translocating tRNAs from the ribosomal A- and P-sites to the P- and E-sites	17118580
<i>Fbxw7</i>	implicated in the ubiquitin-mediated turnover of cyclin E as well as the Notch/Lin-12 family of transcriptional activators; controlling cyclin E and Notch signaling pathways	14766969
<i>Fkbp1a</i>	plays an important role in the Ca(2+) signaling of muscle contraction and relaxation	12414688
<i>Fos</i>	genetic regulator for cellular mechanisms mediating neuronal excitability and survival	11925568
<i>Jub</i>	a new cytosolic component of the IL-1 signaling pathway, influencing the assembly and activity of the aPKC/p62/TRAF6 multi-protein-signaling complex, cytosolic LIM domain-containing proteins has the potential to shuttle from sites of cell adhesion into the nucleus and thus can be candidate transducers of environmental signals	15870274
<i>Kcna1</i>	expressed strongly in the ventral cochlear nucleus (VCN) and the medial nucleus of the trapezoid body (MNTB) of the auditory pathway	14534254
<i>Mt3</i>	[Mt3]-null mice had increased expression of neurotrophins, it may influence neuronal regeneration during the recovery process.	12758064
<i>Ncald</i>	neuron-specific "EF-hand" calcium-binding protein involved in the maturation of motor end-plates	16101019
<i>Odz4</i>	performs roles in the mouse brain, heart, and embryonic patterning	15489520
<i>Rbm3</i>	a glycine-rich RNA-binding protein, enhanced under conditions of mild hypothermia, has been postulated to facilitate protein synthesis at colder temperatures; part of a homeostatic mechanism that regulates global levels of protein synthesis under normal and cold-stress conditions	15684048
<i>Rhob</i>	a small GTPase that regulates actin organization and vesicle transport; essential for apoptosis and antineoplastic activity of farnesyltransferase inhibitors;	11905808 10913192
<i>Serpine1</i>	a negative regulator of cell growth, exerting its effect on the phosphatidylinositol 3-kinase/Akt pathway and allowing controlled cell proliferation	16785241
<i>Sparc</i>	is found to regulate fibroblast migration, it appears to play an important role in the injured myocardium with regard to healing and scar formation	16416312
<i>Syt1</i>	synchronizes the rapid release of neurotransmitters after Ca2+ entry into presynaptic terminals and also appears to suppress the slower, asynchronous form of transmitter release	15240804
<i>Ttr</i>	major thyroxine-binding protein in the plasma of rodents, and the main thyroxine-binding protein in the cerebrospinal fluid of both rodents and humans	12182890
<i>Uba52</i>	ubiquitin ribosomal fusion protein, that may be relevant in the pathogenesis of diabetic nephropathy	12171997

Table 36: Function of some of the differentially regulated genes in brain		
Gene ID	Description	PubMed ID
<i>Ubl5</i>	presence and distribution of ubiquitin-like 5 in the mouse hypothalamus and pituitary	12932856
<i>Vamp2</i>	major SNARE protein of synaptic vesicles, is required for fast calcium-triggered synaptic-vesicle exocytosis	15475946

Table 37: Function of some of the differentially regulated genes in heart		
Gene ID	Description	PubMed ID
<i>Abr</i>	plays important roles during vestibular morphogenesis	11921339
<i>Ankrd1</i>	plays a unique role in therapeutic angiogenesis during wound healing	15632022
<i>Il6st</i>	needed for the normal balance of hematopoietic progenitors during fetal & adult life	12423677
<i>Tap1</i>	required for class I major histocompatibility complex (MHC-I) to bind endoplasmic reticulum-derived stabilizing peptides to achieve stability needed for alternate MHC-I processing via peptide exchange in acidic vacuolar processing compartments	12794107
<i>Tnnc1</i>	Overexpression in muscle cells is controlled by its rapid degradation	12062407

Conclusion

Using the statistical methods described above, a number of genes that are differentially expressed in heart and brain in *Eya3*-mutant mice were identified. The relevance of these genes in terms of the studied allele should be evaluated. This may be done by a detailed inspection of the functional annotations for each of these genes, as initiated here in the discussion. Please, contact us if you have questions concerning this analysis.

3.11.5 References

- Beckers, J., Herrmann, F., Rieger, S., Drobyshev, A., Horsch, M., Hrabé de Angelis, M. and Seliger, B. (2005): Identification and validation of novel *ERBB2* (*Her2*, *NEU*) targets including genes involved in angiogenesis. *Int. J. Cancer* 114: 590-597.
- Bender, A., Beckers, J., Schneider, I., Hölter, S., Haack, T., Ruthsatz, T., Vogt-Weisenhorn, D., Becker, L., Genius, J., Rujescu, D. et al. (2007). Creatine improves health and survival of mice. *Neurobiology of Aging*, in press.
- Drobyshev A., M. Hrabé de Angelis and J. Beckers (2003a): Artifacts and reliability of DNA microarrays expression profiling data. *Current Genomics* 4: 615-621
- Drobyshev A., C. Machka, M. Horsch, M. Seltmann, V. Liebscher, M. Hrabé de Angelis and J. Beckers (2003b): Specificity assessment from fractionation experiments (SAFE): a novel method to evaluate microarray probe specificity base on hybridisation stringencies. *Nucleic Acids Res.* 31(2)
- Frey, I.M., Rubio-Aliaga, I., Siewert, A., Sailer, D, Drobyshev, A., Beckers, J., Hrabé de Angelis, M., Aubert, J., Bar Hen, A., Fiehn, O., Eichinger, H.M., and Daniel, H. (2007). Profiling at mRNA, protein and metabolite level reveals alterations in renal amino acid handling and glutathione metabolism in kidney tissue of *Pept2^{-/-}* mice. *Physiol Genomics* 28: 301-310.
- Greenwood AD, Horsch M, Stengel A, Vorberg I, Lutzny G, Maas E, Schädler S, Erfle V, Beckers J, Schätzl H and Leib-Mösch C (2005): Cell Line Dependent RNA Expression Profiles of Prion-infected Mouse Neuronal Cells. *JMB* 349: 487-500
- Saeed AI, Sharov V, White J, Li J, Lioang W, Bhagabati N, Braisted J, Klapa M, Currier T, Thiagarajan M, Sturn A, Snuffin M, Rezantsev A, Popov D, Ryltsov A, Kostukovich E, Borisovsky I, Liu Z, Vinsavich A, Trush V, Quackenbush J (2003): TM⁴: a free, open-source system for microarray data management and analysis. *Biotechniques* 34 (2):374-8
- Seltmann, M., Horsch, M., Drobyshev, A., Chen, Y., Hrabé de Angelis, M. and Beckers, J. (2005): Assessment of a Systematic Expression Profiling. Approach in ENU-Induced Mouse Mutant Lines. *Mamm. Genome*, 16, 1-10.
- Tusher VG, Tibshirani R and Chu G (2001): Significance analysis of microarrays applied to the ionizing radiation response: *Proceedings of the National Academy of Sciences USA* 98: 5116-5121
- Yang YH, Dudoit S, Luu P, Lin DM, Peng V, Ngai J and Speed TP (2002): Normalization for cDNA microarray data: a robust composite method addressing single and multiple slide systematic variation. *Nuc Acid Research* 30(4): e15

3.12 Metabolic Screen

3.12.1 Summary

The metabolic screening provides a comparative analysis of bioenergetic parameters in mice. Mechanisms which lead to disturbances in body weight regulation and energy metabolism are determined. Hence, the basal energetic demands are monitored during *ad libitum* feeding and under food restricted conditions. In humans unbalanced energy uptake and energy expenditure cause the development of obesity (Spiegelman and Flier, 2001) or anorexia nervosa with severe weight loss (Hebebrand *et al.*, 2003). Some rodent and other species tend to increase activity upon food restriction leading to weight loss when given access to an activity wheel (Exner *et al.*, 2000). Several studies described that fasting in mice results in transient depression of metabolic rate, heart rate, body temperature and locomotor activity (Duffy *et al.*, 1990; Williams *et al.*, 2002). Therefore the primary Metabolic Screening focuses on the determination of food and energy uptake under *ad libitum* conditions and metabolic adaptations during food restriction and serves as the origin for further investigations in the Secondary and Tertiary screening which go into details of energy expenditure and energy storage.

In the primary metabolic screen 12 animals (six males / six females) of the *Eya3* mutant mouse line were analyzed. Thirteen control mice (six males / seven females) were available. They were fed under *ad libitum* conditions for two weeks followed by two days of acute fasting. The primary metabolic screen focuses on investigation of metabolic demands of mice determining daily body weight, energy uptake, metabolizable energy and body temperature. The analysis for genotype specific differences revealed no significant results in any of the recorded metabolic parameters.

3.12.2 Mice

Six adult control males and six adult *Eya3*-mutant males entered the Metabolic Screen at the beginning of calendar week 3 in 2007. The females (seven controls and six mutants) entered the metabolic laboratory one week later. The mice were single caged on grid panels (0.5°cm grid hole diameter). They were fed *ad libitum* for a period of 14 days, followed by two days of acute fasting to analyze adaptive responses of metabolism.

3.12.3 Material and Methods

Recorded Data

During the different feeding regimes body weight, food consumption (F_{con}), rectal temperature (T_{re}), daily feces production (Fec), energy uptake (E_{up}), energy content of the feces (E_{fec}), metabolizable energy (E_{met}) and the food assimilation coefficient (F_{ass}) were recorded.

Analysis of Feces

The separation of mice in single cages allowed collection of feces in three day intervals. Samples of lab chow and feces (~1 g) were dried at 60°C for two days, homogenized in a coffee grinder and squeezed to a pill for determination of energy content in a bomb calorimeter (IKA Calorimeter C7000) based on dry measurement principle. Energy uptake is determined as the product of food consumed and the caloric value of the food. To obtain metabolizable energy (E_{met}) the energy content of feces and urine (2% of E_{up} ; Drozd 1975) were subtracted from energy uptake.

Statistical Analysis

All values are presented as means \pm SEM. Two-way-ANOVA (SigmaStat, Jandel Scientific) was used to test for effects of the factors strain and sex (ANCOVA with body mass as covariate). The Fisher test was applied for post hoc multiple comparisons. The Mann-Whitney-Test for paired samples was used to analyze the effect of nutritional status on parameters of energy metabolism.

3.12.4 Parameters

Recorded Data during the different feeding regimes
--

body weight, food consumption (F_{con}), rectal temperature (T_{re}), daily feces production (Fec), energy uptake (E_{up}), energy content of the feces (E_{fec}), metabolizable energy (E_{met}), food assimilation coefficient (F_{ass})
--

3.12.5 Results and Discussion

The analysis for genotype specific differences revealed no statistically significant effect of the mutation. None of the parameters was changed in mutant mice (Table 38). The only significant difference was detected in assimilation efficiency that was higher in mutant females. The relevance of this result remains unclear.

Other common sex-specific differences in body mass and rectal body temperature were detected.

Prior to the metabolic screening no metabolic phenotype was known in *Eya3*-mutant mice. Body mass and energy metabolism were seemingly not affected by the mutation.

Raw data for each individual are available on request in Excel sheets.

3.12.6 References

Drozd A. (1975): Food habits and food assimilation in mammals. In: Methods for Ecological Bioenergetics, edited by W. Grodzinski, R.Z. Klekowski and A Duncan. Oxford, UK: Blackwell, p: 23-47

- Duffy, P.H., R. J. Feuers and R. W. Hart (1990): Effect of chronic caloric restriction on the circadian regulation of physiological and behavioral variables in old male B6C3F1 mice. *Chronobiol Int* 7: 291-303
- Exner, C., J. Hebebrand, H. Remschmidt, C. Wewetzer, A. Ziegler, S. Herpertz, U. Schweiger, W. F. Blum, G. Preibisch, G. Heldmaier and M. Klingenspor (2000): Leptin suppresses semi-starvation induced hyperactivity in rats: implications for anorexia nervosa. *Mol Psychiatry* 5: 476-481.
- Hebebrand J., C. Exner, K. Hebebrand, C. Holtcamp, R.C. Casper, H. Remschmidt, B. Herpertz-Dahlmann, and M. Klingenspor (2003): Hyperactivity in patients with anorexia nervosa and in semistarved rats: Evidence for a pivotal role of hypoleptinemia. *Physiology and Behavior* 79: 25-37
- Spiegelman B.M. and J.S. Flier (2001): Obesity and the regulation of energy balance. *Cell* 104: 531-543
- Williams T. D., J.B. Chambers, R.P. Henderson, M.E. Rashotte and J.M. Overton (2002): Cardiovascular responses to caloric restriction and thermoneutrality in C57BL/6J mice. *Am J Physiol Regul Integr Comp Physiol* 282: R1459-67

Abbreviations

F_{con}	Food consumption
T_{re}	rectal temperature
Fec	daily feces production
E_{up}	energy uptake
E_{fec}	energy content of the feces
E_{met}	metabolizable energy
F_{ass}	food assimilation coefficient

Table 38: Metabolic parameters recorded in the primary screen											
Data are presented as mean \pm standard error of mean.											
Parameter	Control				Mutant				2 – Way - ANOVA		
	<i>ad libitum</i>		<i>2 days acute fasting</i>		<i>ad libitum</i>		<i>2 days acute fasting</i>		<i>p</i> <i>genotype</i>	<i>p</i> <i>sex</i>	<i>p</i> <i>interaction</i>
	male (n=6)	female (n=7)	male (n=6)	female (n=7)	male (n=6)	female (n=6)	male (n=6)	female (n=6)	<i>ad libitum</i> <i>food reduced</i>	<i>ad libitum</i> <i>food reduced</i>	
Body weight [g]	26.2 \pm 0.7	20.9 \pm 0.6	21.3 \pm 0.6	16.6 \pm 0.6	24.6 \pm 0.8	20.1 \pm 0.6	19.8 \pm 0.6	16.1 \pm 0.5	n.s. n.s.	<0.001 <0.001	n.s. n.s.
Rectal body temperature [°C]	36.6 \pm 0.2	37.2 \pm 0.1	35.2 \pm 0.4	31.6 \pm 0.4	36.8 \pm 0.1	37.3 \pm 0.1	32.8 \pm 0.9	33.1 \pm 0.8	n.s. n.s.	<0.001 <0.05	n.s.
Food consumption [g day ⁻¹]	2.9 \pm 0.1	2.9 \pm 0.1	no food for two days		3.1 \pm <0.1	2.9 \pm 0.1	no food for two days		n.s.	n.s.	n.s.
Energy uptake [kJ day ⁻¹]	49.86 \pm 2.48	48.81 \pm 1.72			52.01 \pm 0.66	48.35 \pm 1.23			n.a.	n.a.	n.a.
Energy uptake BW ⁻¹ [kJ g ⁻¹ day ⁻¹]	1.91 \pm 0.09	2.34 \pm 0.07			2.13 \pm 0.07	2.41 \pm 0.07			n.a.	n.a.	n.a.
Feces production [g day ⁻¹]	0.65 \pm 0.03	0.68 \pm 0.03			0.69 \pm 0.01	0.61 \pm 0.03			n.a.	n.a.	n.a.
Energy content feces [kJ g ⁻¹]	14.86 \pm 0.06	15.26 \pm 0.05			14.80 \pm 0.04	15.33 \pm 0.07			n.s.	<0.001	n.s.
Metabolized energy [kJ day ⁻¹]	39.34 \pm 2.08	37.65 \pm 1.21			40.94 \pm 0.50	38.16 \pm 0.86			n.s.	n.s.	n.s.
Metabolized energy [kJ g ⁻¹ day ⁻¹]	1.50 \pm 0.08	1.80 \pm 0.05			1.67 \pm 0.05	1.90 \pm 0.05			n.a.	n.a.	n.a.
Food assimilation coefficient [%]	78.8 \pm 0.4	77.2 \pm 0.4			78.7 \pm 0.3	79.0 \pm 0.4			<0.05	n.s.	<0.05

3.13 Pathology Screen

3.13.1 Summary

The Pathology screen performed a complete morphological analysis with standard stains. In the macroscopic examination a significantly reduced body weight could be detected in the male mutants. Additionally in seven of nine mutants and in one of nine controls a mild, focal testicular tubular degeneration of unknown significance could be observed.

3.13.2 Mice

A total of 36 mice, 18 *Eya3* homozygous mutant mice (nine females, nine males) and 18 control mice (nine females, nine males) were analyzed macroscopically. Histological analysis was performed in 36 mice. Due to the workflow in the GMC, mice of different ages were received from different screens (Table 39). Two mice died because of blood retrieval before they entered the Pathology Screen.

Table 39: <i>Eya3</i> -mutant mice and their control littermates analyzed.						
Origin	Control		Mutant		Number of Animals	Age [weeks]
	Female	Male	Female	Male		
Dysmorphology Screen	2	3	3	3	11	19-23
Metabolic Screen	7	6	6	6	25	20-23
Total Number of Animals	9	9	9	9	36	

3.13.3 Materials and Methods

Mice received in the laboratory of pathology were sacrificed with CO₂. The animals were analyzed macroscopically and weighed (www.eulep.org/Necropsy_of_the_Mouse/index_2004.php). The thymus and left lobe of the liver were measured. Blood samples were taken, centrifuged and the serum was saved at -20°C. Tails were preserved at -70°C for further genetic analysis. Following a complete dissection, an x-ray of the complete bone structure was taken, when indicated (Hewlett Packard, Cabinet X-Ray System Faxitron Series). All organs were fixed in 4% buffered formalin and embedded in paraffin for histological examination. Two-µm-thick sections from skin, heart, muscle, lung, brain, cerebellum, thymus, spleen, cervical lymph nodes, thyroid, parathyroid, adrenal gland, stomach, intestine, liver, pancreas, kidney, reproductive organs, and urinary bladder were cut and stained with haematoxylin and eosin (H&E). Prussian's Blue staining was performed when indicated.

3.13.4 Results Overview

Table 40: Genotype-specific alterations of <i>Eya3</i> -mutant mice:			
Analyzed:	Alteration	Analyzed:	Alteration
Bodyweight	Yes, males	Pancreas	No
Skin	No	Cervical lymph node	No
Musculoskeletal system	No	Thymus	No
Eyes	No	Spleen	No
Cerebrum	No	Thyroid	No
Cerebellum	No	Parathyroid	No
Heart	No	Adrenal gland	No
Trachea	No	Kidneys	No
Lung	No	Urinary bladder	No
Teeth	No	Testes	Yes??
Salivary gland	No	Epididymis	No
Esophagus	No	Funiculus spermaticus	No
Stomach	No	Ovaries	No
Small intestine	No	Uterus	No
Large intestine	No	Vagina	No
Liver	No	Mamma	No

Only in male *Eya3* mutant mice significant differences could be detected. Female *Eya3* mutant mice showed no genotype-specific morphological phenotype. However secondary results (not genotype-specific) were observed in both sexes.

3.13.5 Genotype-specific Changes Body Weight

The body weight of the male but not the female *Eya3* mutant mice did significantly differ ($p < 0.05$) from the body weight of their control littermates (Table 41).

Table 41: Mean absolute body weight \pm standard deviation of <i>Eya3</i> mutant mice and their control littermates.					
Origin	Control		Mutant		Age [weeks]
	Female	Male	Female	Male	
Dysmorphology Screen/ Metabolic Screen	22.2 \pm 1.6	26.9 \pm 1.4	22.3 \pm 2.1	24.3 \pm 2.1	19-23

Testicular tubular degeneration

In seven of nine *Eya3* mutants and in one of nine controls, a very mild and focal testicular tubular degeneration of single tubules could be detected (Fisher's Exact Test: $p=0.02$). These degenerative changes consisted of scattered degenerated (vacuolated or with cytoplasmatic protein clumping) and/or necrotic spermatogenic cells. The number of germinal cells was reduced to absent in the affected tubuli (Fig. 19). In some tubuli only Sertoli cells were present.

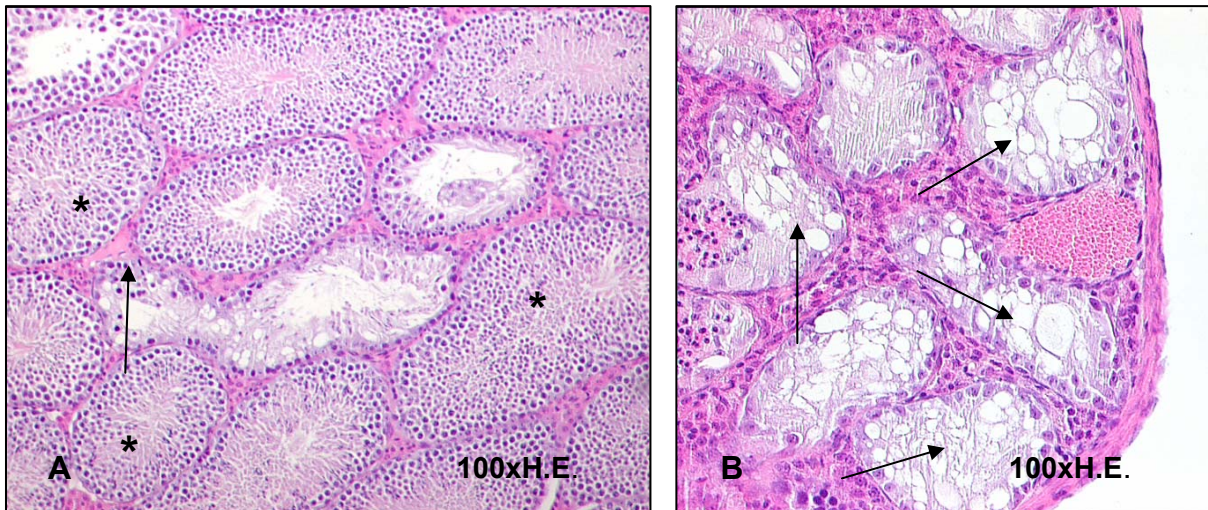


Figure 19: Degenerated seminiferous tubuli

A: Degenerated seminiferous tubuli (arrow) of a control mouse. Note the normal seminiferous tubuli (asterix) with germ cells of a variable majority. **B:** Degenerated seminiferous tubuli of an *Eya3*-mutant mouse. Note the vacuolated spermatogenic cells and the marked depletion of germ cells (H.E., original magnification 100x)

3.13.6 Secondary, not Genotype-specific Results

Inflammatory changes

Eleven mice (eight controls and seven mutants, 30.6%) showed microgranulomas and lymphocytic infiltrates in the liver. In Twenty-two (13 mutants and nine controls, 61.1%) nonspecific infiltrates were present in the kidney. In nine mice (six controls and three mutants, 25%) pneumonia could be detected (Fig. 20).

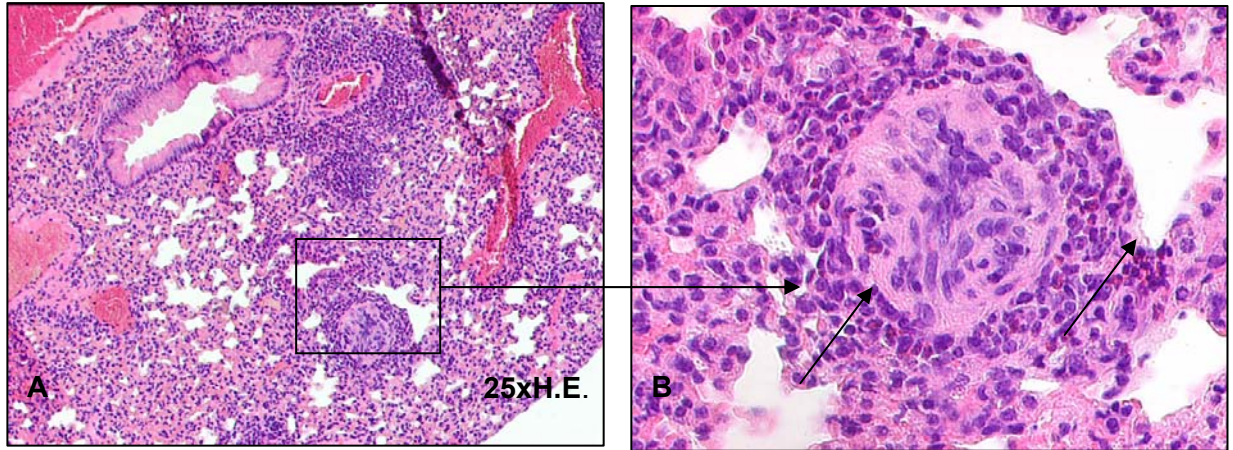


Figure 20: Pneumonia

A: Severe interstitial and granulomatous pneumonia in a control mouse (H.E., original magnification 25x). **B:** Higher magnification: note the strong infiltration (arrows) of granulocytes that demarcates a granuloma (H.E., original magnification 400x)

Kidney

Uni- or bilateral hydronephrosis was found in four of 36 mice (11.1%). The altered kidneys showed a dilation of the renal pelvis with a secondary flattening of the papilla depending on the severity of the pathological changes (Fig. 21).

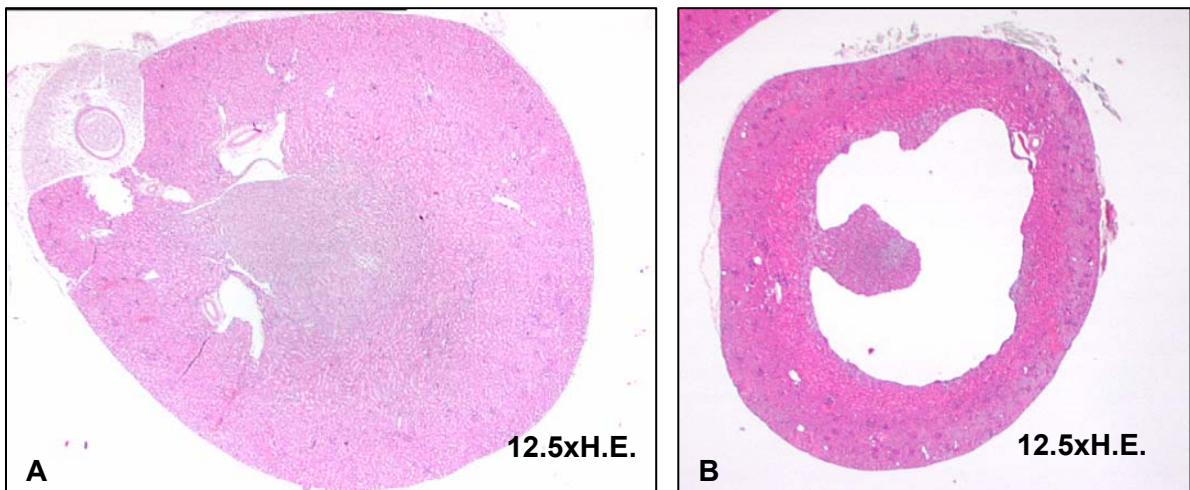


Figure 21: Hydronephrosis

A: Kidney of an *Eya3*-deficient mouse without pathological alteration (H.E., original magnification 12.5x). **B:** Kidney with hydronephrosis (H.E., original magnification 12.5x).

3.13.7 Discussion

Eya3 mutant mice have not been described so far. The *Eya3* gene is an ortholog of the gene *eyes absent (eya)* in *Drosophila melanogaster*. A knock out of this gene results in progenitor cell death with the consequence of missing of compounds of the eyes in *D. melanogaster* (Bonini *et al.*, 1993). Mammalian *Eya* genes are often coexpressed with PAX, SIX and DACH genes and there is an assumption that *Eya* genes are a part of a highly regulated network with PAX on the top (Xu *et al.*, 1999; Rebay *et al.*, 2005). As a consequence of this, *Eya* genes can be involved in the development of many tissues (e.g. eye, gonad, muscle and ear; kidney; skeleton; Rebay *et al.*, 2005; Xu *et al.*, 1999; Li *et al.*, 2003). *Eya1* haploinsufficiency induces the branchio-oto-renal (BOR) or branchio-oto syndrome in humans. In patients with BOR branchial cysts, ear malformations, hearing loss and renal abnormalities can be found (Abdelhak *et al.*, 1997). Knockout phenotypes were described for the *Eya1* gene (Xu *et al.*, 1999) but not for *Eya2*, *Eya3* and *Eya4*. Thus, all organs were of special interest.

Mice of this batch show two genotype-specific differences mainly affecting the males. A **focal testicular tubular degeneration** in seven of nine mutants was observed. Although the Fisher's Exact Test was significant, the relevance of this finding remains unknown. In 18 month old BDF1 mice, it is described that degenerated tubuli occupy 2.2% and in 33 month old mice 63% of the testis (Tanemura *et al.*, 1993). However, since the controls did not show these focal changes, we conclude that the testicular changes observed are genotype-specific. At the beginning tubular degeneration is often accompanied with the appearance of scattered degenerated (vacuolated or with cytoplasmic protein clumping) or necrotic spermatogenic cells. In advanced cases germ cells are markedly reduced and only flattened Sertoli cells and few spermatogonia are left. This reduced number of germ cells is the best hallmark for a tubular degeneration. The tubular degeneration of the *Eya3*-mutant mice was very mild and focal and a high number of intact tubuli with a normal amount of germ cells were left so that fertility of the mice should not be compromised, at least at this early stages. Furthermore in the epididymis a normal amount of mature sperms could be detected and the number of immature cells was not significantly increased. Thus the relevance of this finding for the *Eya3* mutation remains to be clarified.

Lymphocyte infiltrates, especially around blood vessels, are common in mice without having any pathological relevance. Several bacteria including *Proteus mirabilis*, *Corynebacterium kutcherii*, *Pseudomonas aeruginosa* and *Staphylococcus aureus* can cause inflammatory changes in the kidney (Montgomery, 1986; Burek *et al.*, 1988).

Focal granuloma is a frequent incidental finding in the liver of aging mice and it is more prevalent in females than in males (Harada *et al.*, 1996). Focal necrosis of hepatocytes could be the reason for these granulomas. Additionally focal accumulations of mononuclear, polymorphonuclear and/or histiocytic cells are also often observed in aging mice. These focal lesions vary in size and distribution. The cause is unknown, but it may be due to infections with viruses and bacteria (Hall *et al.*, 1992). *Helicobacter sp.*, that is

the causative agent inducing chronic active hepatitis in mice, may cause focal hepatic granulomas in resistant strains like C57BL/6Ncr and B6C3F1 mice (Ward *et al.*, 1994a, Ward *et al.*, 1994b). Another reason for the infiltration of inflammatory cells could be an infection with mouse hepatitis virus. This virus can not be excluded as causative agent because it was found in 22 of 25 mice in the last health check (see health report). The infiltrates in the liver and the kidney of the Eya3 mice can be accounted as secondary finding because mutants and controls were nearly equally affected.

Interstitial pneumonia which was found in nine mice is an inflammatory change of the lung. Within the scope of this kind of pneumonia the inflammatory infiltrate spreads in the interstitium. Acute interstitial pneumonia can be caused by viruses (Schuhmacher, 1969; Ferlinz, 1974), *Rickettsia* (Ferlinz, 1974), *Mycoplasma spp.* (Spencer, 1977) and/or *Chlamydia* (Ferlinz, 1974). In most of the cases a progressive interstitial fibrosis will develop. Regardless the specific cause, the earliest manifestation is an alveolitis (Chan-Yeung and Muller, 1997) and in the scope of this an accumulation of leucocytes within the alveolar walls and spaces. The result is a distortion of the normal lung tissue. As a consequence of a release of mediators parenchymal cells can be injured followed by fibrosis. A beginning fibrosis could be detected only in some of the mice examined and the infiltrates were composed mainly of granulocytes. Pathogens described to cause inflammatory changes in the lung of mice are: Sendai virus (Parker and Richter, 1982), *Mycoplasma pulmonis* (Saito *et al.*, 1981; Lai *et al.*, 1993), *Corynebacterium kutcheri* (Jacoby and Fox, 1984); *Pasteurella pneumotropica* (Needham and Cooper, 1975), Cilia-Associated Respiratory Bacillus (Griffith *et al.*, 1988) and *Pneumocystis carinii* (Walzer *et al.*, 1989). Sendai virus, *Mycoplasma pulmonis*, *Pasteurella pneumotropica* and *Corynebacterium kutcheri* can be excluded as causing pathogens because the sentinel mice investigated during the health check procedure were negative concerning these pathogens. Cilia-Associated Respiratory Bacillus and *Pneumocystis carinii* have not been checked in the examination but they can nearly be ruled out because the pathological alterations found in the mice were different from those described for these two pathogens. Cilia-Associated Respiratory Bacillus causes bronchiectasis, bronchiolectasis, abscessation and atelectasis in affected mice and the characteristic feature of a *Pneumocystis carinii* infection is an accumulation of homogenous, eosinophilic, foamy material in the distended alveoli (Maronpot, 1999). Furthermore other reasons for an interstitial pneumonia can be foreign bodies, chemicals, radiation etc. Due to the fact that the initial stimuli for an interstitial pneumonia are heterogeneous, the cause can not be figured out. But as the mutants and the controls were equally affected this pneumonia can be assumed as a finding by chance.

In four mice a **hydronephrosis** of unknown etiology was found. Uni- or bilateral hydronephrosis can appear in both sexes. Hydronephrosis can also be a developmental defect. In addition it can be secondary caused by pyelonephritis, urinary tract obstruction or papillary necrosis associated with amyloidosis. Pyelonephritis most often result from ascending infections. Such infections are often a result of bite wounds to the genital region in male mice caged together (Tuffery, 1966; Geistfeld *et al.*, 1998). Histologically hydronephrosis can be characterized by a dilation of the renal pelvis with a secondary flattening of the renal papilla depending on the severity of the lesion.

In severe cases the whole papilla can be destroyed and the renal cortex can be reduced in size because of the continuous increasing pressure due to the accumulated urine. Certain strains such as C3H, C57BL/6 and DDD have a high incidence (Hsu, 1986), and in C57BL/6 mice an autosomal recessive and progressive hydronephrosis has been reported (Horton *et al.*, 1988). Furthermore hydronephrosis can be recognized as consequence of chemical administration (Gage and Sulik, 1991; Bryant *et al.*, 1997; Yang *et al.*, 1986) or the presence of uroliths or neoplasms. Due to the fact that only a few mice and mainly the controls showed a hydronephrosis, this alteration can be accounted as secondary finding for this mouse batch.

3.13.8 References

- Abdelhak S, Kalatzis V, Heilig R, Compain S, Samson D, Vincent C, Levi-Acobas F, Cruaud C, Le Merrer M, Mathieu M, König R, Vigneron J, Weissenbach J, Petit C, Weil D (1997): Clustering of mutations responsible for branchio-oto-renal (BOR) syndrome in the eyes absent homologous region (*eyaHR*) of *EYA1*. *Human molecular genetics* 6(13): 2247-55
- Bonini NM, Leiserson WM, Benzer S (1993): The eyes absent gene: genetic control of cell survival and differentiation in the developing *Drosophila* eye. *Cell* 72 (3): 379-95
- Bryant, P.L., Clark, G.C., Probst, M.R. and Abbott, B.D. (1997): Effects of TCDD on Ah receptor, ARNT, EGF and TGF-alpha expression in embryonic mouse urinary tract. *Teratology* 55: 326-337
- Burek, J.D., Duprat, P., Owen, R., Peter, C.P. and Zwieter M.J. (1988): Spontaneous renal disease in laboratory animals. *International Review of experimental Pathology. Kidney Disease*. Richter G.W. and Solez K. (eds). Academic Press Inc., San Diego.; 231-319
- Chan-Yeung M and Muller NL (1997): Cryptogenic fibrosing alveolitis. *Lancet* 350: 651-656
- Ferlinz R (1974): Lungen- und Bronchialerkrankungen, Ein Lehrbuch der Pneumologie. Thieme, Stuttgart
- Gage, J.C. and Sulik, K.K. (1991): Pathogenesis of ethanol-induced hydronephrosis and hydroureter as demonstrated following in vivo exposure of mouse embryos. *Teratology* 44: 299-312
- Geistfeld, J.G., Weisbroth, S.H., Jansen, E.A. and Kumpfmiller, D., (1998): Epizootic of group B streptococcus agalactiae serotype V in DBA/2 mice. *Lab. Anim. Sci*, 48, 29-33
- Griffith JW, White WJ, Danneman PJ and Lang CM (1988): Cilia associated respiratory (CAR) bacillus infection of obese mice. *Vet Pathol*, 25:72-76
- Hall, W.C., Ganaway, J.R., Rao, G.N., Peters, R.L., Allen, A.M., Luczak, J.W., Sandberg, E.M. and Quigley, B.H. (1992): Histopathologic observations in weanling B6C3F1 mice and F344/N rats and their adult parental strains. *Toxicol. Pathol.*: 20; 46-54
- Harada, T., Maronpot, R.R., Enomoto, A., Tamano, S and Ward, J.M. (1996): Changes in the liver and gallbladder. In: *Pathobiology of the Aging Mouse*, Vol. 2. Mohr, U., Dungworth, D.L., Capen, C.C., Carlton, W.W.,

- Sundberg, J.P. and Ward, J.M. (eds) ILSI Press, Washington DC., pp. 207-241
- Horton, C.E., Davisson, M.T., Jacobs, J.B., Bernstein, G.T., Retik, A.B. and Mandell, J. (1988): Congenital progressive hydronephrosis in mice: a new recessive mutation. *J. Urol.*: 140; 1310-1315
- Hsu, H.H. (1986): Hereditary hydronephrosis, mouse. In: *Urinary system*. Jones, T.C., Mohr, U. and Hunt, R.D. (eds). Springer-Verlag, Berlin. pp. 273-275
- Jacoby RO and Fox JG (1984): biology and disease of mice In: *Laboratory Animal Medicine*. Fox JG, Cohen BJ and Loew Franklin M (eds). Academic Press Inc., New York. pp. 31-89
- Lai WC, Linton G, Bennet M and Pakes SP (1993): Genetic control of resistance to *Mycoplasma pulmonis* infection in mice. *Infect Immun.* 61: 4615-4621
- Li X, Oghi KA, Zhang J, Krones A, Bush KT, Glass CK, Nigam SK, Aggarwal AK, Maas R, Rose DW, Rosenfeld MG (2003): Eya protein phosphatase activity regulates Six1–Dach–Eya transcriptional effects in mammalian organogenesis. *Nature* 426: 247-265
- Maronpot RR. (1999): *Pathology of the mouse*; eds. RR Maronpot; GA Boorman; BW Gaul, Cache River Press, USA
- Montgomery C.A. (1986): Interstitial nephritis mouse. In: *Urinary System*. Jones TC, Mohr, U and Hunt, R.D. (eds) Springer Verlag, Berlin, pp. 210-215
- Needham JR and Cooper JE (1975): An eye infection in laboratory mice associated with *pasteurella pneumotropica*. *Lab Anim.* 9: 197-200
- Parker JC and Richter CB (1982): Virla diseases of the respiratory system. In: *The Mouse in Biomedical research, Vol. II; Diseases*. Foster HL, Small JD and Fox JG (eds). Academic press, New York., pp. 107-152
- Rebay I, Silver SJ, Tootle TL (2005): New vision from Eyes absent: transcription factors as enzymes. *Trends in Genetics* 21(3): 163-171.
- Saito M, Nakagawa M, Suzuki E, Kinoshita K and Imaizumi K (1981): Synergistic effect of sendai virus on *Mycoplasma pulmonis* infection in mice. *Jpn j Vet Sci.* 43: 43-50
- Schuhmacher H (1969): Ätiologie der akuten Atemwegsinfektion des Säuglings. *Virologische und serologische Untersuchungen. Z. Kinderheilk.* 107: 191-201
- Spencer H (1977): *Pathology of the lung*. 3rd Edn., Pergamon Press, Oxford New York Toronto Sydney Paris Frankfurt
- Tanemura K, Kurohmaru M, Kuramoto K and Hayashi Y (1993): Age-related morphological changes in the testis of BDF1 mouse. *J Vet Med Sci.* 55: 703-710
- Tuffery, A.A. (1966): Urogenital lesions in laboratory mice. *J. Pathol. Bacteriol.* 91: 301-309
- Walzer PD, Kim CK, Linke J, Pogue CL, Huerkamp MJ, Chrisp CE, Lerro AV, Wixson SK, Hall E and Shultz LD (1989): Outbreaks of *Pneumocystis carinii* pneumonia in colonies of immunodeficient mice. *Infect Immun* 57: 62-70
- Ward, J.M., Anver, M.R., Haines, D.C. and Benveniste R.E. (1994a): Chronic active hepatitis in mice caused by *Helicobacter hepaticus*. *Am. J. Pathol.* 145: 959-968

- Ward, J.M., Fox, J.G., Anver, M.R., Haines, D.C., George, C.V., Collins, M.J. Jr, Gorelick; P.L., Nagashima, K., Gonda, M.A. Gilden. R.V., Tully, J.G., Russel, R.J., Benveniste, R.E., Paster, B.J., Dewhirst, F.E., Donovan, J.C., Anderson, L.M. and Rice, J.M. (1994b): Chronic active hepatitis and associated liver tumors in mice caused by a persistent bacterial infection with a novel *Helicobacter* species. *J. Natl. Cancer Inst.* 86: 1222-1227
- Xu PX, Adams J, Peters H, Brown MC, Heaney S, Maas R (1999): *Eya1*-deficient mice lack ears and kidneys and show abnormal apoptosis of organ primordia. *Nature Genetics* 23: 113-117
- Yang, R.S.H., Huff, J.E., Boorman, G.A., Haseman, J.K., Kornreich, M. and Stookey, J.L. (1986): Chronic toxicity and carcinogenesis studies of telone II by gavage in Fischer-344 rats and B6C3F1 mice. *J. Toxicol. Environ. Health* 18: 377-392

www.eulep.org/Necropsy_of_the_Mouse/index_2004.php
<http://www.geocities.com/virtualbiology/>

Acknowledgements

A large team consisting of scientists, technicians and animal caretakers all contribute to the success of the German Mouse Clinic. We want to thank Reinhard Seeliger, Elfi Holupirek, Susanne Axtner, Miriam Backs, Christine Fürmann, Tamara Halex, Sabine Holthaus, Nadine Kink, Claudia Kloss, Regina Kneuttinger, Kerstin Kutzner, Maria Kugler, Jacqueline Müller, Elenore Samson, Sandra Schädler, Ann-Elisabeth Schwarz, Bettina Sperling, Susanne Wittich, and Claudia Zeller for expert technical help and Daniela Kißling, Manuela Huber, Petra Thalmeier, Sabine Schwarz, and Anica Miedl for the care of the mice.

Appendix: Tables

Table	1: Eya3 mice provided for analysis.	3
Table	2: Primary Screen at GMC	9
Table	3: Evaluation of the behavioral phenotype	12
Table	4: Results of behavioral observation in the modified Hole Board test	15
Table	5: Video-tracking results regarding locomotor behavior	19
Table	6: Results from the morphological inspection (nine-week old mice).....	24
Table	7: Results from the X-ray analysis (16-week old mice)	25
Table	8: Results from clickbox test (hearing test; nine-week old mice).....	26
Table	9: Bone- and weight-related quantitative parameters (15-18-week old mice)	27
Table	10: Recording of body weight.....	34
Table	11: Behavior recorded in viewing jar	34
Table	12: Recording of locomotor activity and behavior in the arena.....	35
Table	13: Behavior recorded in or above the arena	36
Table	14: Lactate levels	37
Table	15: Axial eye length.....	41
Table	16: Results from Funduscopy	41
Table	17: Results from Slit Lamp Biomicroscopy.....	41
Table	18: Clinical-chemical parameters at the age of 13 weeks.	47
Table	19: Clinical-chemical parameters at the age of 18 weeks.	48
Table	20: Hematological parameters at the age of 13 weeks.	49
Table	21: Hematological parameters at the age of 18 weeks.	50
Table	22: Basic parameters analyzed in the Immunology Screen.	53
Table	23: Total plasma IgE in Eya3 mice (13 weeks old)	55
Table	24: Total plasma IgE in Eya3 mice (18 weeks old)	55
Table	25: Nociceptive Screen	59
Table	26: Blood Pressure Parameters	Fehler! Textmarke nicht definiert.
Table	27: ECG Parameters.....	68
Table	28: Characterization of studied mice	73
Table	29: Spontaneous breathing pattern during rest and activity of male Eya3 mice	74
Table	30: Mutant and control mice stored for expression profiling	75
Table	31: Amount of total RNA [µg] isolated from heart, thymus, and brain	77
Table	32: Heat plots of gene expression profiles from eight DNA microarray experiments of <i>Eya3</i> -mutant out <i>versus</i> control mice.	78
Table	33: Gene Ontology terms	79
Table	34: Gene Ontology terms:.....	79
Table	35: Heat plots of gene expression profiles from eight DNA microarray experiments of <i>Eya3</i> -mutant <i>versus</i> control mice.	80
Table	36: Function of some of the differentially regulated genes in brain	82
Table	37: Function of some of the differentially regulated genes in heart	84
Table	38: Metabolic parameters recorded in the primary screen	89
Table	39: <i>Eya3</i> -mutant mice and their control littermates analyzed.....	90
Table	40: Genotype-specific alterations of <i>Eya3</i> -mutant mice:	91
Table	41: Mean absolute body weight ± standard deviation of <i>Eya3</i> mutant mice and their control littermates.....	91

Figures

Figure 1:	Workflow of the primary screen.....	5
Figure 2:	Test arena for modified Hole Board test.....	11
Figure 3:	Abnormal head morphology	22
Figure 4:	The rotarod apparatus	30
Figure 5:	Results from grip strength testing	31
Figure 6:	Results from rotarod testing	32
Figure 7:	Total plasma IgE in Eya3 mice.....	55
Figure 8:	Hot plate system	58
Figure 9:	Blood pressure set up	61
Figure 10:	ECG-setup	61
Figure 11:	Example of ECG trace with analyzed parameters.....	62
Figure 12:	ECG-parameter P-Q interval.....	64
Figure 13:	ECG-parameter J-T interval	64
Figure 14:	ECG-parameter QRS amplitude	65
Figure 15:	System used at GMC to assess breathing patterns.	70
Figure 16:	Recorded data used to calculate the breathing parameters.....	70
Figure 17:	Tidal volume at rest.....	71
Figure 18:	Specific Tidal Volume at rest.....	72
Figure 19:	Degenerated seminiferous tubuli	92
Figure 20:	Pneumonia.....	93
Figure 21:	Hydronephrosis.....	93

Addresses of screeners and modules

Coordinators

Dr. Valérie Gailus-Durner
Dr. Helmut Fuchs
Barbara Ferwagner
Dr. Christoph Lengger
Dr. Beatrix Naton
Prof. Dr. Martin Hrabé de Angelis
Institute of Experimental Genetics
Helmholtz Zentrum München
German Research Center for Environ-
mental Health (GmbH)
Ingolstädter Landstraße 1
D-85764 Neuherberg
Tel.: 089-3187-3613
Fax: 089-3187-3500
Email: gailus@helmholtz-muenchen.de

Behavior Screen

Dr. Sabine M. Hölter
Magdalena Kallnik
Institute of Developmental Genetics
Helmholtz Zentrum München
German Research Center for Environ-
mental Health (GmbH)
Ingolstädter Landstraße 1
D-85764 Neuherberg
Tel.: 089-3187-3674
Fax: 089-3187-3099
Email: hoelter@helmholtz-muenchen.de

Dysmorphology Screen,

Dr. Helmut Fuchs
Dr. Wolfgang Hans
Prof. Dr. Martin Hrabé de Angelis
Institute of Experimental Genetics
Helmholtz Zentrum München
German Research Center for Environ-
mental Health (GmbH)
Ingolstädter Landstraße 1
D-85764 Neuherberg
Tel.: 089-3187-3151
Fax: 089-3187-3500
Email: hfuchs@helmholtz-muenchen.de

Neurology Screen

Dr. Lore Becker
Eva Kling
German Mouse Clinic (GMC)/Neurology
Institute of Experimental Genetics
Helmholtz Zentrum München
German Research Center for Environ-
mental Health (GmbH)
Ingolstädter Landstraße 1
D-85764 Neuherberg
Tel.: 089-3187-3654
Fax: 089-3187-3500
Email: lore.becker@helmholtz-muenchen.de

PD Dr. Thomas Klopstock
Friedrich-Baur-Institut,
Neurologische Klinik
Ludwig-Maximilians-Universität München
Ziemssenstraße 1a
D-80336 München
Tel: 089-5160-7474
FAX: 089-5160-7402
Email:
Thomas.Klopstock@nro.med.uni-muenchen.de

Eye Screen

Dr. Claudia Dalke
Institute of Developmental Genetics
Helmholtz Zentrum München
German Research Center for Environ-
mental Health (GmbH)
Ingolstädter Landstraße 1
D-85764 Neuherberg
Tel.: 089-3187-2910
Fax: 089-3187-2210
Email: dalke@helmholtz-muenchen.de

Clinical-Chemical Screen

Dr. Birgit Rathkolb
Dr. Corinna Mörth
GMC - German Mouse Clinic
Clinical-Chemical Screen
Institute of Experimental Genetics
Helmholtz Zentrum München
German Research Center for Environ-
mental Health (GmbH)
Ingolstädter Landstraße 1
D-85764 Neuherberg
Tel.: 089-3187-3282
Email: birgit.rathkolb@helmholtz-muenchen.de

Prof. Dr. Eckhard Wolf
Institute of Molecular Animal Breeding
and Biotechnology
Genecenter
LMU München
Feodor Lynen-Straße 25
D-81377 München
Tel.: 089-21807-6800
Email: ewolf@lmb.uni-muenchen.de

Immunology Screen

Dr. Thure Adler
Prof. Dr. Dirk Busch
GMC - German Mouse Clinic
Institute for Experimental Genetics
Helmholtz Zentrum München
German Research Center for Environmental Health (GmbH)
Ingolstädter Landstraße 1
D-85764 Neuherberg
Tel.: 089-3187-3656
Fax: 089-3187-3500
Email: thure.adler@helmholtz-muenchen.de

Prof. Dr. Dirk Busch
Institute for Medical Microbiology,
Immunology and Hygiene
Technische Universität München (TUM)
Trogerstr. 9
D-81675 München
Tel.: 089-4140-6191
Fax: 089-4140-4139
Email: dirk.busch@lrz.tum.de

Allergy Screen

Anahita Javaheri, MSc
Antonio Aguilar
Prof. Dr. Markus Ollert
Klinik und Poliklinik für Dermatologie
und Allergologie am Biederstein
Technische Universität München (TUM)
Biedersteinerstraße 29
D-80802 München
Tel.: 089-4140-3551 (M.O.)
Tel.: 089-3187-2554 (A.J.)
Fax: 089-4140-3552
Email: ollert@lrz.tum.de

Steroid Screen

Dr. Cornelia Prehn
Prof. Dr. Jurek Adamski
Institute of Experimental Genetics
Helmholtz Zentrum München
German Research Center for Environmental Health (GmbH)
Ingolstädter Landstraße 1
D-85764 Neuherberg
Tel.: 089-3187-3231
Fax: 089-3187-3500
Email: prehn@helmholtz-muenchen.de

Nociceptive Screen

Dr. Ildikó Rácz
Laboratory of Molecular Neurobiology
Department of Psychiatry
University of Bonn
Sigmund-Freud-Straße 25
D-53105 Bonn
Tel.: 0228-688-5316
Fax: 0228-688-5301
Email: iracz@uni-bonn.de

Prof. Dr. Andreas Zimmer
Laboratory of Molecular Neurobiology
Department of Psychiatry
University of Bonn
Sigmund-Freud-Straße 25
D-53105 Bonn. Germany
Tel.: 0228-688-5303

Lung Function Screen

Dr. Ines Bolle
Prof. Dr. Holger Schulz
Institute for Inhalation Biology
Helmholtz Zentrum München
German Research Center for Environmental Health (GmbH)
Ingolstädter Landstraße 1
D-85764 Neuherberg
Tel.: 089-3187-4119
Fax.: 089-3187-2400
Email: schulz@helmholtz-muenchen.de

Molecular Phenotyping

Dr. Marion Horsch
Dr. Johannes Beckers
Institute of Experimental Genetics
Helmholtz Zentrum München
German Research Center for Environmental Health (GmbH)
Ingolstädter Landstraße 1
D-85764 Neuherberg
Tel.: 089-3187-3513
Fax: 089-3187-4085
Email: horsch@helmholtz-muenchen.de

Metabolic Screen

Dr. Jan Rozman
Nicole Ehrhardt
Institute of Experimental Genetics
GMC - German Mouse Clinic
Metabolic Screen
Helmholtz Zentrum München
German Research Center for Environ-
mental Health (GmbH)
Ingolstädter Landstraße 1
D-85764 Neuherberg
Tel.: 089-3187-3807
Fax: 089-3187-3500
Email: [jan.rozman@helmholtz-
muenchen.de](mailto:jan.rozman@helmholtz-muenchen.de)

Prof. Dr. Martin Klingenspor
Technische Universität München
Nutrition and Food Research Center
Molecular Nutrition
Am Forum 5
D-85350 Freising-Weihenstephan

Cardiovascular Screen

Dr. Anja Schrewe
Institute of Experimental Genetics
GMC - German Mouse Clinic
Cardiovascular Screen
Helmholtz Zentrum München
German Research Center for Environ-
mental Health (GmbH)
Ingolstädter Landstraße 1
D-85764 Neuherberg
Tel.: 089-3187-3646
Fax: 089-3187-3500
Email: [anja.schrewe@helmholtz-
muenchen.de](mailto:anja.schrewe@helmholtz-muenchen.de)

Dr. Boris Ivandic
Prof. Dr. Hugo Katus
Innere Medizin III
Otto-Meyerhof-Zentrum
Im Neuenheimer Feld 350
D-69120 Heidelberg
Tel.: 06221 - 56-1505
Email: [boris_ivandic@med.uni-
heidelberg.de](mailto:boris_ivandic@med.uni-heidelberg.de)

Pathology Screen

Dr. Julia Calzada-Wack
Dr. Gabriele Hölzlwimmer
Dr. Ilona Moßbrugger
PD Dr. Irene Esposito
PD Dr. Leticia Quintanilla-Martinez
Institute of Pathology
Helmholtz Zentrum München
German Research Center for Environ-
mental Health (GmbH)
Ingolstädter Landstraße 1
D-85764 Neuherberg
Tel.: 089-3187-3241
Fax: 089-3187-3360
Email: [irene.esposito@helmholtz-
muenchen.de](mailto:irene.esposito@helmholtz-muenchen.de)